Intramyocellular Lipids and the Progression of Muscular Insulin Resistance

by

Daniel Burkow

A Dissertation Presented in Partial Fulfillment
of the Requirements for the Degree
Doctor of Philosophy

Approved November 2017 by the
Graduate Supervisory Committee:

Carlos Castillo-Chavez, Co-Chair
Jiaxu Li, Co-Chair
Yang Kuang
Susan Holechek

ARIZONA STATE UNIVERSITY

December 2017

ABSTRACT

Diabetes is a disease characterized by reduced insulin action and secretion, leading to elevated blood glucose. In the 1990s, studies showed that intravenous injection of fatty acids led to a sharp negative response in insulin action that subsided hours after the injection. The molecule associated with diminished insulin signalling response was a byproduct of fatty acids, diacylglycerol. This dissertation is focused on the formulation of a model built around the known mechanisms of glucose and fatty acid storage and metabolism within myocytes, as well as downstream effects of diacylglycerol on insulin action. Data from euglycemic-hyperinsulinemic clamp with fatty acid infusion studies are used to validate the qualitative behavior of the model and estimate parameters. The model closely matches clinical data and suggests a new metric to determine quantitative measurements of insulin action downregulation. Analysis and numerical simulation of the long term, piecewise smooth system of ordinary differential equations demonstrates a discontinuous bifurcation implicating nutrient excess as a driver of muscular insulin resistance.

This dissertation is dedicated to my wife, Amy Burkow. You supported me throughout my academic journey, and you showed patience and understanding in even my most stressful times. I owe my entire doctorate degree to your love and support.

To my parents, Richard and Linda Burkow. You instilled in me my desire to question the world and explore it openly.

To my brother, Jonathan Burkow. If not for you, I'd have had no practice being competitive and striving to win. I always did win, of course.

And to my in-laws, the Wetzels – too numerous to count and too wonderful to adequately describe.

Thank you all!

ACKNOWLEDGMENTS

My academic career has been influenced by many people over the years, but my first real step toward applied mathematics was a strong recommendation by Dr. Erika T. Camacho to change majors. She and her husband, Dr. Stephen Wirkus, guided me through my undergraduate degree and introduced me to Dr. Carlos Castillo-Chavez in 2011. Dr. Castillo-Chavez ran a summer research program, the Mathematical and Theoretical Biology Institute (MTBI), which I was a part of for 6 consecutive years, and my respect for his work and program led me to joining his Ph.D. program at Arizona State University. During my time at MTBI, I met Dr. Benjamin Morin, who taught me Matlab and LaTeXprogramming and influenced my fastidious model construction habits. I also met Dr. Susan Holechek in MTBI, who became a mentor of mine in biology and member of my committee. I would like to thank Dr. Yang Kuang for introducing me to Dr. Jiaxu Li while he was visiting Arizona State University on sabbatical and for offering insightful academic and career advice. And I extended a particularly grateful thankfulness to Dr. Jiaxu Li for meeting with me on a weekly basis, even at odd hours, in order to keep me on track and provide me with the help and suggestions necessary to complete my dissertation.

I would also like to thank Dr. Dawn Coletta for her insight in diabetes and obesity related pathophysiology, Dr. David Capco for his thorough lectures on cellular signalling pathways, and the staff at the Simon A. Levin, Mathematical, Computational and Modeling Sciences Center for their infinite support and encouragement (especially Margaret Murphy-Tillis, Sherry Woodley, and Dawn Bies). Finally, I thank Dr. Komi Messan, my officemate, peer, and moral support throughout my time in graduate school.

TABLE OF CONTENTS

CHAPTER Page

LIST OF TABLES

LIST OF FIGURES

Chapter 1

INTRODUCTION

The prevalence of diabetes has increased significantly in the last 50 years with type 2 diabetes mellitus (T2DM) accounting for the majority of diabetes cases (CDC, 2013). The pathogenesis of T2DM is understood to be a result of an orchestra of biochemical responses to environmental stimuli, shaped by genetic predisposition (Association *et al.*, 2006). While genetic components have been discovered, the presence or absence of said genetic components do not turn diabetes on or off, but rather influence the result of lifestyle behavior. More concisely, diabetes is a disease of affluence and civilization – showing up wherever American-style diets exist while staying relatively unseen in communities that eat a more "traditional" diet (Joe, 1994) The symptoms of diabetes have been known for millenia, characterized by sweet urine and unquenchable thirst (King and Rubin, 2003). However, the underlying biological dynamics have only been studied over the last century, as a result of the discovery of insulin (Banting *et al.*, 1922).

The typical metrics of diabetes recorded include elevated blood sugar, elevated insulin, and insulin resistance (Association *et al.*, 2006). Adding to the confusion, it isn't obvious which of these maladies occurs first (Boden, 1997; Ceriello and Motz, 2004). Elevated blood glucose triggers the pancreas to secrete insulin, and the insulin then affects the liver, muscles, and fat tissue to consume and utilize the glucose, removing it from the blood. In a healthy human, this process occurs after each meal and is well regulated in the body (Saltiel and Kahn, 2001). Things take a turn for the worse, however, when insulin is unable to do its job - this is where the insulin

resistance comes in. When insulin is ignored by the tissues it targets, the blood glucose is not consumed and concentrations remain high (Shulman, 2000). The consistently high blood glucose levels force the pancreas to generate and release ever more insulin, eventually leading to β cell dysfunction. So insulin resistance is the key that unlocks the path towards diabetes. Additionally, it seems that insulin resistance may not be the direct effect of elevated insulin or glucose, but a response to excess nutrient consumption and excess fat consumption (Muoio and Newgard, 2008).

Studies in the late 1990's discovered that lipid content within muscle cells were correlated with insulin resistance (Perseghin *et al.*, 1999). Further studies showed that intravenous injection of fatty acids led to a sharp negative response in insulin action that subsided hours after the injection (Boden *et al.*, 2004, 2001; Roden *et al.*, 1996). When patients were fed a high-fat diet for 1-week, a 50% increase in IMCL was seen (Schrauwen-Hinderling *et al.*, 2005). Finally, adipose tissue in the body elevates plasma free fatty acid concentrations and is linked to elevated IMCL (Capurso and Capurso, 2012). Taken together, this implicates dietary choices and visceral adipocity as strong contenders for the cause of insulin resistance. The insulin receptor (IR) in the muscle cells shed light on the biological reason behind the result – the insulin receptor substrate (IRS) was serine phosphorylated on a particular residue which turned the molecule off. When fatty acids accumulate in muscles, a byproduct called diacylglycerol (DAG) is produced and accumulates in the muscle cell membrane which allows PKC-θ to become activated and serine phosphorylate the IRS (Yu *et al.*, 2002). The molecule, DAG, is required for many cellular operations, but when fatty acid concentrations are elevated, the concentration of activated DAG increases (Krebs and Roden, 2005). Additionally, there are other fatty acid byproducts such as ceramides that result in a similar outcome *in vitro*, but not necessarily *in vivo*

(Krebs and Roden, 2005).

Chronic insulin resistance is of more importance, however. The acute affect of a high fat meal subsides 12 hours after ingestion (Weintraub *et al.*, 1987), whereas most people eat meals more frequently. There are multiple hypotheses regarding the long term generation of IMCL induced insulin resistance. One hypothesis is that fat in the blood stream is elevated in overweight and obese individuals due to elevated visceral fat stores which increases the base fatty acid concentration in the blood by releasing non-esterified fatty acids into the portal vein (Klein, 2004). However, other studies have shown that subcutaneous fat and IMCL content independently predict insulin resistance when visceral fat is controlled for, where IMCL concentration has the strongest predictive power (Goodpaster *et al.*, 1997). Hence there may be a common cause for both IMCL level and visceral fat stores.

Ingestion of sucrose is suggested to be a cause of visceral fat accumulation (Matsuzawa *et al.*, 1995). Direct evidence of sucrose on IMCL accumulation hasn't been studied. However, sucrose significantly elevates plasma lipids when compared to an equi-caloric diet with starch in place of sucrose(Reiser *et al.*, 1979) and elevated plasma fatty acid availability is the suggested mechanism behind IMCL accumulation. Overconsumption of fructose (a subunit of sucrose) is additionally correlated to elevated plasma lipids and hepatic insulin resistance (Lê *et al.*, 2009). Additionally, mouse studies suggest that visceral fat and insulin resistance are indissociable under high-fat feeding trials (Kim *et al.*, 2000). However, it was noted that neither visceral fat nor insulin resistance increased when the calories from the high-fat diets were restricted. Hence, excessive calorie consumption may be a necessary condition for insulin resistance. Additionally, insulin sensitive patients with elevated IMCL levels

exhibit elevated lipid oxidation (Perseghin *et al.*, 2002). This is also substantiated by athlete studies that indicate endurance trained athletes have high IMCL levels with accompanying high oxidation (Goodpaster *et al.*, 2001). Finally, some propose that mitochondrial dysfunction is a root cause of IMCL accumulation (Kelley *et al.*, 2002) due to post-hoc measurements, but this view is contested in rat studies that concurrently show insulin resistance and an increase in mitochondrial quantity and activity during high fat feeding (Hancock *et al.*, 2008).

Taken together, it seems that elevated fat or fructose (or sucrose) intake at an excess of daily caloric requirements is sufficient for IMCL accumulation. Since fatty acids take hours ($\sim$12) to be utilized and cleared from the blood stream after a meal, it is not unreasonable to assume that the compounding effect of eating three or more higher fat and calorie meals per day disallows the body to ever reach basal levels of plasma lipid concentrations. So the muscles are constantly encountering higher FFA levels, inflating IMCL concentrations and keeping the IRS turned off. Additionally, inflammatory pathways have been shown to incite insulin resistance (De Luca and Olefsky, 2008)

Glucose is shuttled into muscle cells primarily by glucose transporters (GluT4) that are mobilized and activated when insulin binds to insulin receptors on the membrane of muscle cells. So if the IRS is shut off or insufficiently expressed, GluT4 is not sent to the cell membrane to take in glucose. Increases in IMCL have a direct pathway to disabling the IRS, but inflammatory markers are causally related to decreased IRS activity or expression (De Luca and Olefsky, 2008; Saghizadeh *et al.*, 1996). A particularly common inflammatory marker, TNF-α, is expressed at elevated levels in muscles of patients with insulin resistance (Saghizadeh *et al.*, 1996). The

elevated TNF-α appears to induce serine phosphorylation of the IRS (Hotamisligil *et al.*, 1996). Additionally, a mouse model attenuated the affect of high-fat feeding by replacing 6% of fat intake by omega-3 rich fish oil (Storlien *et al.*, 1987). This is relevant because omega-3 fatty acids are anti-inflammatory in both human and animal trials (Simopoulos, 2002), whereas other fatty acids may be pro-inflammatory (Simopoulos, 2002).

The current biological understanding of these cellular dynamics is at the point that models can be formulated to study caricatures of the cellular environment. The molecular kinetics and pathways are complete enough to generate mathematical models based on observed mechanisms. With such models, *in silico* experiments can be conducted to validate the model and ultimately elucidate potential emergent dynamics. The confusion surrounding what people believe to be the "optimal human diet" and the observed increase in diabetes rates across the world is enough to motivate such studies.

1.1 Biological Background

1.1.1 Cellular Metabolism of Glucose and Fatty Acids

Mitochondria in muscles oxidize glucose and fatty acids to produce adenosine triphosphate (ATP) (Alberts *et al.*, 2008). Glucose is derived from dietary carbohydrate sources directly, or by hepatic gluconeogenesis. The body stores glucose in muscles and in the liver as glycogen which can be quickly converted back into glucose-6-phosphate when necessary for ATP production. Glycogen in the liver can be converted back into glucose and released into the bloodstream in response to insulin levels (Sindelar *et al.*, 1998). Glycogen in the muscles, however, is converted to

glucose-6-phosphate to be metabolized when extracellular sources of glucose are low or during exercise; glycogen in muscles cannot be reconverted to glucose or released back into the bloodstream (Van Schaftingen and Gerin, 2002). The liver also converts proteins into glucose through the gluconeogenesis pathway, which becomes the dominant source of hepatic glucose secretion when liver glycogen is depleted (Tirone and Brunicardi, 2001).

Figure 1.1: Overview of Intramuscular Metabolic and Regulatory Pathways

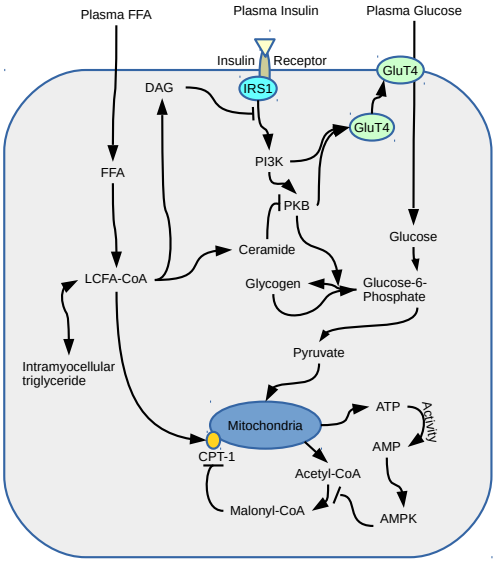

Glucose in the blood needs pores through which to enter muscle and liver cells (among many others) which are opened through a signal cascade in the cell triggered by insulin binding to receptor on the cell membrane. Insulin is a peptide hormone that binds to receptors on many cells to generate behavioral changes. In most situations, insulin's main role is to stimulate the process of glucose uptake and utilization. However, when insulin binds to hepatocytes in the liver, the result is a reduction in liver mediated glucose generation and release in conjunction with an increase in

glucose storage as glycogen. Adipose tissue responds to insulin by slowing down fatty acid release and elevating fat storage as triglycerides. Muscles respond to insulin by storing glucose as glycogen and oxidizing glucose to create energy.

Throughout the pancreas, there are clusters of cells called Islets of Langerhans that contain a variety of cells. The most important are the α and β cells that produce glucagon and insulin, respectively. The β cells constantly release slow, oscillatory bursts of insulin (Simon and Brandenberger, 2002). But when glucose concentrations in the blood rise, the cells secrete large quantities of insulin (Rorsman and Renström, 2003).

Muscles have insulin receptors to which insulin binds that aggregate on the cell membrane, leading to downstream pathways that enable glucose transport into the cells. The insulin receptors activate themselves when insulin binds by auto-phosphorylating their tyrosine residues. Then the insulin receptor substrate (IRS) binds and becomes active, attracting a multitude of other molecules to begin various downstream signals. One of these pathways tells the cell to shuttle glucose transporters (GluT4) to the cell membrane so glucose can be taken up from the bloodstream.

Glucose inside the cell is modified and converted into glucose-6-phosphate (G6P) which either gets converted and stored as glycogen or is sent down the metabolic pathway. The G6P molecules destined to be oxidized in the mitochondria are converted to pyruvate. Pyruvate is either converted to lactic acid for rapid energy production during high intensity exercise, or shuttled into the mitochondria where it is converted into Acetyl-Coenzyme A (A-CoA). The A-CoA enters the krebs cycle which iteratively generates Adenosine triphosphate (ATP) that the muscle uses for energy dependent

activities. Acetyl CoA also can be converted by A-CoA Carboxylase (ACC) to become Malonyl CoA, an important molecule in regulating fatty acid metabolism.

Fatty acids, on the other hand, do not require insulin action to enter muscle cells. As fatty acids are hydrophobic molecules, they can passively diffuse across cellular membranes. There are fatty acid transporters, but mice studies that knock out the gene that codes for these transporters demonstrates that they contribute little to fatty acid infusion under normal conditions. The intracellular fatty acids are lengthened to long chain fatty acids (LCFA) and either stored or converted for other use. When fatty acids are stored, they are converted to triglycerides which consist of three fatty acid tails combined with a glycerol head. Triglycerides in the muscle are called intramyocellular triglycerides (ImcTG) and other intramuscular fatty acids are called intramyocellular lipids (ImcL).

Some of the LCFAs interact with a catalyst on the mitochondrial membrane called the carnitine palmitoyltransferase (CPT), which adds a carnitine molecule to the LCFA allowing it to pass through the mitochondrial membranes. Inside the mitochondria, the carnitine is cleaved off and shuttled back out of the mitochondria while the LCFA is converted to A-CoA. From this point, the A-CoA undergoes the same process as in glucose metabolism.

The fatty acid transfer process into the mitochondria is regulated by M-CoA. Malonyl CoA deactivates CPT, so LCFAs cannot acquire the carnitine "ticket" into the mitochondria. This effectively forces the LCFAs to be stored or converted into other cellular molecules. One of the more important molecules in the context of ImcTG dynamics and insulin resistance is Diacylglycerol (DAG), a fatty acid derived molecule

that resides in the cell membrane.

1.1.2 Intramyocellular Triglyceride and Insulin Resistance

Fatty acids take on multiple forms, namely they can be coarsely divided into saturated and unsaturated categories. While there is nuance in how different kinds of saturated and unsaturated fatty acids interact, the general distinction is adequate for this discussion. Fats are utilized in the body in a number of meaningful and necessary ways, including the production and maintenance of cellular membranes. Every cell has a phospholipid bilayer that protects the cell and allows for an intracellular environment specific to the various molecular interactions cells need to perform. This cell membrane is a fluid mosaic of phospholipids of various kinds along with cholesterol and a host of membrane bound proteins. Fatty acids in the cell are converted into phospholipids through a variety of pathways depending on the resultant phospholipid.

One particular variety of phospholipid is a phosphoinositide, which is a structure with a two strand fatty acid tail with an inositol sugar head. The phosphatidylinositol 4,5-bisphosphate (PI(4,5)P2) is a chemically active phospholipid involved in many signalling pathways, usually involving G-protein coupled receptors. When PI(4,5)P2 is activated, the inositol sugar head is cleaved off releasing inositol 1,4,5 trisphosphate (IP3), which goes on through the cytoplasm to affect downstream pathways (Alberts *et al.*, 2008). However, the key point is that the fatty acid tail is left in the cell membrane which is now called diacylglycerol (DAG). Additionally, when fatty acids are labeled upon ingestion and tracked, unsaturated FA are readily converted into triglyceride whereas saturated FA are converted to phospholipids, some of which allow DAG accumulation (Montell *et al.*, 2001).

The membrane bound DAG is physiologically active, and binds to various forms of protein kinase C (PKC). When PKC binds to DAG, the PKC molecule can be activated by calcium ions. The activated PKC molecule is a serine/threonine activating molecule, and is namely responsible for serine phosphorylating the insulin receptor substrate (IRS), effectively shutting off the downstream insulin signal (Yu *et al.*, 2002). Hence, an accumulation of DAG in the cell membrane allows rapid and constant PKC activation, which in turn regulates IRS activation and mutes the insulin signals pathway.

Another phospholipid of note is sphingomyelin. This molecule begins production in the endoplasmic reticulum (ER) where ceramide is constructed by combining fatty acids with serine. The ER then exports the ceramide into the golgi apparatus where it is given a phosphocholine head to form the final sphingomyelin (Alberts *et al.*, 2008). Again, availability of long chain saturated fatty acids that allow for the start of ceramide synthesis (Summers, 2006), whereas fatty acids incorporated later in the production of ceramide can be either saturated or unsaturated. The mechanism by which ceramide accumulation affects insulin signalling is not clearly understood and could be due to one of multiple potential interruptions in the insulin signalling pathway (Summers, 2006). Some argue that ceramide is independently sufficient for IMCL mediated insulin resistance (Chavez *et al.*, 2003), but since the main mechanism is still under debate, this research will focus on modeling DAG mediated IRS disruption.

1.2 Previous Mathematical Work

Mathematical models have been used to understand biological dynamics since at least the late 18th century, with population growth described by Malthus (Malthus, 1798), resource constrained population growth by Verhulst (Verhulst, 1838) (and subsequently Pearl and Reed (Pearl and Reed, 1920)), and multi-species competition models by Lotka and Volterra (Lotka, 1925; Volterra, 1928). The universe of mathematical biology extends into many subdivisions including epidemiology (Ross, 1911; Kermack and McKendrick, 1927; Brauer *et al.*, 2001), oncology (Wheldon, 1988; Kuang *et al.*, 2016), ecology (Pielou *et al.*, 1969; Levin *et al.*, 2012), bacterial growth and competition (Smith and Waltman, 1995), diabetes (Makroglou *et al.*, 2006; Bergman *et al.*, 1979), and chemical kinetics (Michaelis and Menten, 1913; Hill, 1910) to name only a handful. In the field of cell biology and cell signaling, mathematical models are used to extend what is already known about the cellular dynamics, and simulate details not easily attainable via experiment (Aldridge *et al.*, 2006). Moreover, the theory of metabolic control analysis applies models to describe elasticity of metabolite flux to enzyme activity in metabolic networks (Heinrich and Rapoport, 1974; Fell, 1992), i.e. what the fractional change in a metabolic variable is in response to a fractional change in a parameter (Fell, 1992). The mathematical tools used in metabolic control analysis are important to test the assumed underlying metabolic pathways, but they do not explore the time dependent changes in chemical concentrations as do the tools used in chemical kinetics.

The intracellular kinetics of can be modelled with ordinary differential equations of the general form

$$\frac{dC}{dt} = (\text{generation}) - (\text{consumption})$$

where the generation and consumption terms can be constant, linear, or non-linear terms such as Michaelis-Menten interactions (Eungdamrong and Iyengar, 2004). Constant terms represent a concentration independent interaction, such as a continual drip of bacteria into a chemostat (Smith and Thieme, 2013). An example of such an interaction in a cell might be diffusion of molecule through a semi-porous membrane, such as glucose through a fixed number of transporters on a cell membrane. Linear terms often represent concentration dependent birth or death rates, assuming that these events occur with exponentially distributed waiting times. However, it's the nonlinear dynamics that make these intracellular kinetics interesting.

A common class of cellular kinetics are enzyme dynamics which are commonly modeled with Michaelis-Menten equations (Cornish-Bowden and Cornish-Bowden, 2012). A simple unidirectional enzymatic interaction might be written as

$$A + E \xrightarrow{k} E + B$$

where substrate A binds to enzyme E and becomes substrate B at rate k. However, this skips an intermediate step where the substrate A is bound to the enzyme for a period of time

$$A + E \xrightarrow{k_1} AE \xrightarrow{k_2} B + E$$

where E is the free enzyme and AE is the bound substrate and enzyme pair. Then a system of equations can be constructed to model the interaction

$$\begin{aligned}
\frac{d[A]}{dt} &= -k_1[A][E] \\
\frac{d[E]}{dt} &= -k_1[A][E] + k_2[AE] \\
\frac{d[AE]}{dt} &= k_1[A][E] - k_2[AE] \\
\frac{d[B]}{dt} &= k_2[AE]
\end{aligned}$$

where $[\cdot]$ indicates the concentration. If we call $[E_t] = [E] + [AE]$ the fixed total bound and unbound enzyme, then we can reduce the system to

$$\begin{aligned}\frac{d[A]}{dt} &= -k_1[A][E_t] + k_1[AE] \\ \frac{d[AE]}{dt} &= k_1[A][E_t] - (k_2 + k_1[A])[AE] \\ \frac{d[B]}{dt} &= k_2[AE]\end{aligned}$$

If we assume that $[A] >> [E_t]$, then we can assume a quasi-steady state for $[AE]$. Then $[AE]' = 0$, so we can solve for $[AE]$

$$[AE] = \frac{[E_t][A]}{\frac{k_2}{k_1} + [A]}.$$

If we set $v_{\max} = k_2[E_t]$ and $K_M = \frac{k_2}{k_1}$ then

$$\frac{d[B]}{dt} = \frac{v_{\max}[A]}{K_M + [A]}$$

where K_M is called the Michaelis-Menten constant. As many intracellular interactions are dependent on enzymes, these functional forms are commonly used to model such dynamics. However, there are shortcomings to this quasi-steady state approximation when the low enzyme concentration assumption is not met (Pedersen *et al.*, 2008) and a more robust approximation may be appropriate (i.e. tQSSA (Borghans *et al.*, 1996)). Additionally, in the case of competition between multiple substrates (say A and I) and an enzyme, a modified form of the Michaelis-Menten approximation is used (Yung-Chi and Prusoff, 1973)

$$\frac{v_{\max}[A]}{K_M\left(1 + \frac{[I]}{K_I}\right) + [A]}$$

where I inhibits the binding of A to E. Depending on the complexity of enzyme and inhibitor interactions, various forms of Michaelis-Menten approximations are appro-

priate.

Exact modeling of intracellular dynamics is weighty and the number of equations required to capture each interaction between each important molecule makes for very complicated systems of equations. For example, a mathematical model for sphingolipid metabolism in yeast cells required a 63 variable system of equations with even more parameters (Alvarez-Vasquez *et al.*, 2005). The numerical results validated the model and *in silico* experiments allowed testable predictions about the cellular response in circumstances that could not be tested experimentally. However, due to the unwieldy nature of this "kitchen sink" approach to modeling, it is unlikely to be as useful for cellular dynamics we are less certain about. With this in mind, a simplistic model that is built on the more important verified cellular dynamics is the focus of this research.

Furthermore, the biochemical switching that occurs in regulated cellular pathways brings about a need to consider piecewise smooth differential equations (PWS). A PWS system is defined as a system with disjoint domains on which distinct smooth functions define the dynamics of the system, note that the vector field need not be continuous on the boundaries between domains (such as in Filippov systems (Di Bernardo *et al.*, 2008)). Various aspects of PWS systems have been studied, mainly with respect to their applications in mechanical or electrical systems (Bernardo *et al.*, 2008; Leine and Nijmeijer, 2013). However, the method has been implemented to indicate enzymatic switching in yeast (Simpson *et al.*, 2009), and the basic framework on which molecular interactions can be modeled by PWS smooth systems have been discussed (Noel *et al.*, 2010). However, difficulty in such systems arise when categorizing bifurcations, as PWS systems exhibit bifurcation types that are unseen in

smooth dynamical systems.

Piecewise smooth differential equations are typically described by

$$\dot{\mathbf{x}} = \mathbf{F}_i(\mathbf{x}, \rho; h(\mathbf{x}, \rho)), i = 1, 2, \ldots, m$$

where $\mathbf{x} = (x_1, x_2, \ldots, x_n)$ is the n-dimensional state variable, ρ is the parameter set, $\mathbf{F}_i$ is the function definition of the system on the interior of each of m domains R_i $(i = 1, 2, \ldots, m)$, and $h(\mathbf{x}, \rho)$ is the switching condition. The boundary that separates the domains, R_i, is the set $\Sigma = \{\mathbf{x} | h(\mathbf{x}, \rho) = 0\}$, called the switching manifold. For example, a simple example in $\mathbb{R}$ is

$$\dot{x} = -\text{sign}(x)$$

where $h(x) = x$, $F_1 = -1$ $(x > 0)$, $F_2 \in [-1, 1]$ $(x = 0)$, and $F_3 = 1$ $(x < 0)$. The dynamics on the interior of R_1 $(x > 0)$ and R_2 $(x < 0)$ are simple and easily understood. However, complications arise when attempting to understand dynamics on the switching manifold. Systems of this type exhibit border-collision, grazing, sliding, discontinuous, and discontinuity-induced bifurcations (Bernardo *et al.*, 2008) among others. Often, these bifurcations occur when interior bifurcations pass through or touch the switching manifold. However, research in this field has a lot of open problems concerning specific classes of bifurcations (Colombo *et al.*, 2012).

Full body compartment modelling of glucose-insulin interactions have been studied and used in clinical settings since at least the 1960s (Bolie, 1961). However, the nonlinear model introduced by Bergman *et al.* (1979) which became known as the "minimal model" was used to define an insulin sensitivity index for frequently sampled intravenous glucose tolerance tests that was vetted against other clinical methods

of insulin sensitivity determination (Bergman *et al.*, 1987; Welch *et al.*, 1990). The minimal model was used to create a computational program, MINMOD (Pacini and Bergman, 1986), that determines an insulin sensitivity index from patient data. This began a common trend of using models to determine and compare insulin sensitivity, but others have developed and tested alternative measures of insulin sensitivity to the gold standard, the euglycemic hyperinsulinemic clamp (Gutt *et al.*, 2000). For example, the homeostasis model assessment (HOMA) was developed from work by Turner *et al.* (1979), which became a standard for measuring insulin resistance and β-cell function (Matthews *et al.*, 1985). However, the HOMA estimates are insufficiently precise, and more complicated mathematical models with one or multiple delays provided improvements over the minimal model (Makroglou *et al.*, 2006). For instance, Shi *et al.* (2017), used a system of delayed differential equations to determine an insulin sensitivity index that improved the results over those obtained by the minimal model.

The system of delay, integro-differential equations in De Gaetano and Arino (2000) provided means to improve the insulin release model by requiring insulin release to depend on the concentration of glucose present in the blood over a past interval of time. This system was further improved by Li *et al.* (2001), in which the distributed delay was weighted over the past time interval. This modification resulted in the presence of oscillatory solutions, a characteristic of *in vivo* insulin release that was not captured in (De Gaetano and Arino, 2000). Additionally, multiple delay models (Li *et al.*, 2006, 2012) simulating ultradian oscillations were developed and analyzed the further the mathematical understanding of the glucose-insulin dynamics. These, coupled with partial differential equations Wach *et al.* (1995); Mosekilde *et al.* (1989); Søeborg *et al.* (2009) modeling subcutaneous insulin injection site diffusion (simplified

as ODEs in (Li and Kuang, 2009)) allow for a path toward developing model-based closed-loop control algorithms for the implementation of an artificial pancreas (Huang *et al.*, 2012).

The cellular level dynamics of insulin granule release have been studied by Bertuzzi *et al.* (2007) with a piecewise smooth continuous system of ordinary differential equations. Additionally, a cell population model of insulin release were studied by Palumbo and De Gaetano (2010). It is in these types of mathematical models that we draw inspiration in developing a mathematical tool for understanding the relation between intramyocellular lipids and insulin resistance in muscles. As mathematical tools have proven to be useful in other ways within diabetes research (Nyman *et al.*, 2012), we seek to advance the understanding of skeletal muscle insulin resistance.

Chapter 2

MODEL FORMULATION

The key component of this research would be the construction and vetting of a basic model of IMCL dynamics. Thus the main concern discussed in this proposal will be on the conversion of biological dynamics to ordinary differential equations. Moreover, the inherent complexity of biological dynamics requires a strong set of assumptions to move the model formation forward.

2.0.1 Assumptions

The environment of in the models will be considered the "average" muscle cell across all muscles in the body. This includes smooth and striated muscles, those that are voluntary and involuntary, but other tissues such as fat tissue or organ tissue will not be considered in this average. It is known muscles in various parts of the body metabolize nutrients at different rates and quantities, so this assumption allows for general picture without concern about how a specific muscle in a specific person is known to perform. Thus, model variables such as those for glucose or fatty acids only count the average concentration of said molecule over all the muscles and ignore the blood concentration levels.

Molecules in muscle cells interact as if we are considering homogeneous ideal gas dynamics. The viscosity of cellular cytoplasm and the inevitable interference of organelles and other cellular obstructions are ignored. This assumption is only considered since the muscle cell studied is the abstract "average" and variations in cell size,

shape, and configuration are wide enough to ignore specific cellular configurations and their affect on molecule mobility.

Fatty acids diffuse into muscle cells at a rate proportional to some plasma concentration. There is evidence that fatty acids diffuse passively as well as actively into muscles. However, when the active FFA transport is knocked out in mice studies, fat still enters the muscle cells at nearly the same rate. Thus for simplification, we assume that the transport is passive.

The mitochondrial metabolism of fatty acids and glucose occur at rates proportional to intracellular concentrations. Models of mitochondrial activity become complicated fast due to the complicated nature of the ATP (energy) production cycle (Krebs Cycle) and intricate shuttling of molecules into and out of the dual mitochondrial membrane. We keep track of the concentration of unmetabilized A-CoA that is released and converted into malonyl-CoA.

2.1 Model Construction

We consider a five compartment system of ODEs to model the dynamics between intramyocellular glucose (G), fatty acid (F), glycogen (Y), DAG (D), and M-CoA (M) concentrations. We consider blood concentrations of glucose and fatty acids constant and then assume that both diffuse into the muscle cell at a constant rate (G_{in} and F_{in}, respectively). This is a reasonable assumption during euglycemic-hyperinsulinemic clamp with fatty acid infusion.

The intramyocellular fatty acids and glucose are consumed by the mitochondria

Figure 2.1: Reduced Pathway to Guide Model Formation

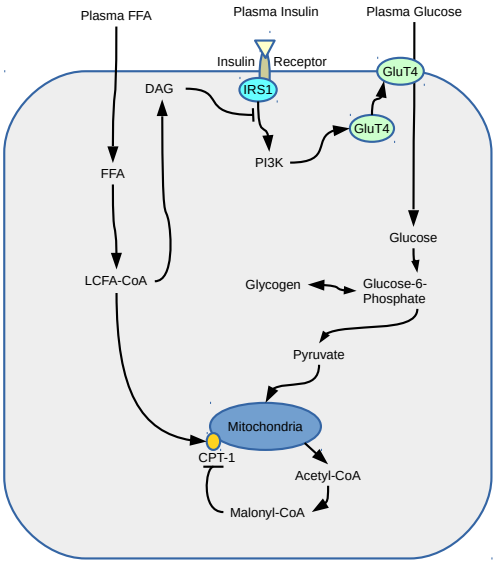

subject to a pair saturable concentration dependent functions. The rate of fatty acid metabolism is negatively affected by both glucose and mitochondria byproduct concentrations. Glucose and fatty acids compete as substrate for the Krebs Cycle, so there is an inherent maximum capacity that the mitochondria can handle. Finally, malonyl-CoA shuts off CPT-1 (Carnitine palmitoyltransferase I) which in turn down regulates a necessary pathway to shuttle fatty acids into the mitochondria for catabolism. Glucose is metabolized at a rate governed by saturable function $f_1(F, G, M)$ which is negatively affected by substrate competition with fatty acids. Fatty acids are metabolized at a rate governed by saturable function $f_2(F, G, M)$. The availability of IMCL to be metabolized is reduced by elevated M-CoA concentration.

Glucose concentration is regulated by conversion to glycogen with general function $f_3(G, M)$. Glycogen can absorb a substantial amount of glucose, and is necessary to

consider since the glucose infusion is high and constant in euglycemic clamp conditions. In the case of low glucose concentrations, glycogen is broken down to be used for energy production. Glycogenolysis converts glycogen to glucose-6-phosphate, but for simplicity we consider this molecule as part of the glucose compartment, G. In the case of clamped fatty acid infusions, glucose is constantly supplied, so little or no glycogen is likely to be converted back into G6P for metabolism.

The fatty acid pool is converted to DAG according to the function $f_4(F, D)$. Then DAG is removed from the system by deactivation or conversion to a downstream molecule at rate μ. Diacylglycerol activates PKC-Θ which leads to inactivation of the IRS by serine phosphorylating a particular residue, so we reduce the glucose inflow of glucose by $0 < f_5(D) \leq 1$ to simulate insulin resistance.

Figure 2.2: Model Flow Chart

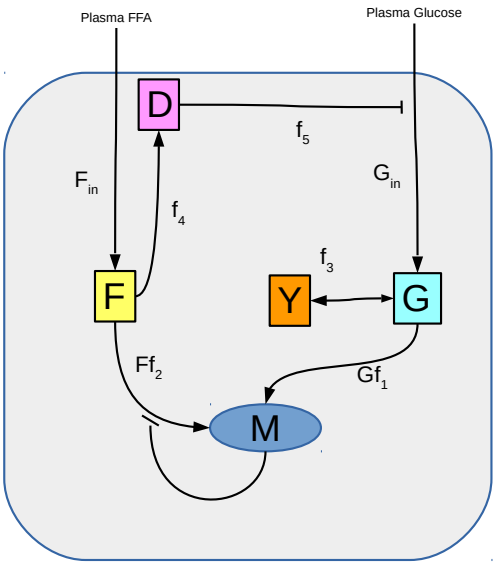

Finally, M-CoA is created at a rate directly proportional to the metabolism of

glucose and fatty acids. The concentration of M decays at rate r.

$$\begin{aligned}
\dot{G} &= G_{in} f_5(D) - G f_1(G,F,M) - f_3(G,Y) \\
\dot{Y} &= f_3(G,Y) \\
\dot{F} &= F_{in} - F f_2(G,F,M) - f_4(F,D) \\
\dot{D} &= c f_4(F,D) - \mu D \\
\dot{M} &= aG f_1(G,F,M) + bF f_2(G,F,M) - rM
\end{aligned} \tag{2.1}$$

2.1.1 Short-term Model: Function Selection

The functions that describe interactions within the model could take many forms. However, certain key considerations are required by biology. The sub-functions drive the dynamics within the muscle cells, and a "correct" choice of function cannot be known until more biological work is conducted. However, validation that certain functional forms replicate the dynamics that we see in clinical trials numerically can give a sense of accuracy. Thus, functional forms will be suggested here and tested numerically against data.

Glucose and Fatty Acid Metabolism, (f_1 and f_2)

Both glucose and fatty acids are metabolized in the mitochondria after being converted to Acetyl-CoA. Glucose undergoes a conversion to Glucose-6-phosphate and then into pyruvate before being shuttled into the mitochondria. Therefore, we only wish to consider the proportion of glucose in a muscle cell that has been converted in pyruvate for metabolism. Similarly, fatty acids need to be tagged with a carnitine

molecule in order to be shuttled into the mitochondria. The CPT1 complex attaches the carnitine to the FA which is removed once the complex is in the mitochondria, and the carnitine then diffuses back out into the cytoplasm. However, CPT1 is shut off by Malonyl-CoA which is a byproduct of metabolism. This works as a regulatory factor to keep FA from being metabolized if the cell has enough energy. Finally, the mitochondria can only process so much A-CoA at a given time and both glucose and fatty acids are converted to the same molecule for processing, so there is competition for substrate.

The biological understanding of mitochondrial metabolism then allows a few rules about the functional forms of f_1 and f_2 to be constructed. Only a proportion of the total concentration of glucose (p_g) and fatty acids (p_f) are available for metabolism. There is a saturable rate of oxidation for glucose and fatty acids: $f_1 \leq m_g,\ f_2 \leq m_f$. Metabolism of one molecule inhibits metabolism of the other by substrate competition: $\frac{\partial}{\partial F}(f_1) < 0,\ \frac{\partial}{\partial G}(f_2) < 0$. Malonyl-CoA concentration reduces the availability of fatty acids to be metabolized, and thus increases glucose metabolism: $\frac{\partial}{\partial M}(f_1) > 0, \frac{\partial}{\partial M}(f_2) < 0$. As glucose or fatty acids increase in concentration, the metabolism rates increase monotonically: $f_1(G+\epsilon,\cdot) - f_1(G,\cdot) > 0$, $f_2(F+\epsilon,\cdot) - f_2(F,\cdot) > 0$. The metabolism functions are non-negative: $f_1, f_2 \geq 0$.

For our initial numerical simulations, we use a simple functional form that satisfies the above requirements:

$$f_1 = \frac{m_g p_g G}{k + p_g G + e^{-qM} p_f F}$$
$$f_2 = \frac{m_f p_f F}{k + p_g G + e^{-qM} p_f F}$$

where e^{-qM} is the reduction of available fatty acids for metabolism.

Glycogen regulation, f_3

Glycogen is produced in an alternate pathway to glucose oxidation from glucose-6-phosphate. When glycogenesis is enabled, such as during times of elevated plasma insulin, G-6-P is converted into glycogen for quick energy storage. When glucose concentration in the muscle cells are lower, glycogen is converted via glycogenolysis back into G-6-P, then into pyruvate and metabolism begins. To avoid a futile cycle, insulin action down regulates glycogenolysis so glycogen remains stored for later use. Then $\frac{\partial}{\partial G}(f_3) \geq 0$ and $\frac{\partial}{\partial Y}(f_3) = 0$ is assumed to avoid a futile cycle. Thus we assume that there is a rate of glucose conversion to glycogen that is saturable with rate p. Additionally, once glycogen is stored, it doesn't leave the compartment since insulin levels remain high.

Then we choose the functional form

$$f_3 = \frac{pG}{C+G}.$$

The concentration of glucose that where glycogen is produced at half its maximal rate is C.

Diacylglycerol Production, f_4

The myocellular lipid stores are converted to DAG when concentrations are high. However the conversion rates leading from myocellular lipids to DAG aren't known, and the functional form ought to be as simple as possible. We assume that $\frac{\partial}{\partial F}(f_4) > 0$ and likely that $\frac{\partial}{\partial D}(f_4) \leq 0$. Thus I chose a production rate, d, that is linearly proportional to the concentration of IMCL, with conversion ratio c:

$$f_4 = dF.$$

Diacylglycerol Inhibition of Glucose Transport, f_5

The elevated concentration of DAG in the cell leads to activation of protein kinase C θ (PKCθ) which phosphorylates a particular residue on the insulin receptor substrate. This phosphorylation shuts off the downstream insulin action pathway, which in turn does not allow intracellular GluT4 to be shuttled to the cell surface. Thus the membrane bound GluT4 is not replaced when they are inactivated, leading to a diminished glucose transport into the myocyte. Therefore, we can deduce that f_5 is a monotonically decreasing function of D, but the shape is unknown. For simplicity, we model this interaction by

$$f5 = \frac{n}{n + D},$$

where n is the concentration of DAG that ends up reducing glucose infusion by one half.

2.1.2 Long-term Model: Function Selection

The key differences between the short-term and long-term model are in the selection of functional forms for the malonyl-CoA induced reduction of fatty acid transport across the mitochondrial membranes and the addition of glycogen returning to the available glucose compartment. Since long term dynamics see intermittent intervals of feeding and fasting, we must account for the reversion of glycogen into readily metabolized byproducts.

Glucose and Fatty Acid Metabolism, (f_1 and f_2)

For algebraic simplicity and to enable simplified analysis, we exchange the M-CoA regulating term with an easier form. In this modification, we substitute $\exp(-qM)$ with $\frac{1}{1+qM}$ to get

$$f_1(G, F, M) = \frac{m_g p_g G}{k + p_g G + \frac{p_f}{1+qM} F}$$

and

$$f_2(G, F, M) = \frac{m_f \frac{p_f}{1+qM} F}{k + p_g G + \frac{p_f}{1+qM} F}.$$

Glycogen regulation, f_3

Glycogen in myocytes supplements the available glucose in times when blood glucose concentration is low, or in times of exercise. Then it is important that lower concentrations of glucose in the cell elicits a glycolysis response to maintain favorable cellular levels of glucose. Additionally, care is taken to prevent a futile cycle in which glucose is being converted to glycogen at the same time that glycogen is converted to glucose. Hence $f_3 < 0$ when glucose is below a threshold g_y and $f_3 > 0$ when glucose is above this threshold. Additionally, glycogen can only be stored and not reverted when no glycogen is present, $f_3|_{Y=0} \geq 0$, and glycogen can only be reverted and not stored when glucose is depleted, $f_3|_{G=0} \leq 0$.

In the cell, glycogen metabolism is regulated by insulin, glucagon, and metabolite concentrations (i.e. AMP and ATP). After a meal, insulin turns off glycogen phosphorylase, a necessary molecule in the metabolism of glycogen, and during times of fasting, glucagon turns it on. Additionally, high concentrations of AMP turn on glycogen phosphorylase in order to produce ATP, and as ATP levels rise, glycogen

phosphorylase is turned off. Hence we construct a piecewise function using glucose concentration in the muscle cell as a rough proxy for the presence of insulin, glucagon, or metabolites.

$$f_3(G,Y) = \begin{cases} \frac{P_f(G-g_y)\left(1-\frac{Y}{m_y}\right)}{C_u+(G-g_y)}, & G \geq g_y, Y < m_y \\ 0, & G \geq g_y, Y \geq m_y \\ \frac{P_r Y(G-g_y)}{C_l+g_y Y}, & G < g_y \end{cases}$$

Then f_3 is continuous, and bounded above by P_f, the maximal forward rate of glycogen storage, and below by $-P_r$, the maximal reversion rate of glycogen to glucose. Both C_u and C_l are shape parameters indicating a half maximal conversion rate.

Finally, we will assume the glycogen compartment has no secondary means of offloading stored glycogen. In reality, consuming so many excess carbohydrates that glycogen stores are continually saturated leads to de novo lipid synthesis. Considering this extreme case in future models may lead to interesting results.

Chapter 3

EUGLYCEMIC-HYPERINSULINEMIC CLAMP MODEL

The short term model is a functionally simple model designed for parameter estimation against biological data. The full model with function substitutions is displayed in (3.1).

$$\begin{aligned}
\dot{G} &= G_{in}\frac{n}{n+D} - \frac{m_g p_g G}{k + p_g G + p_f e^{-qM} F} - \frac{pG}{C+G} \\
\dot{Y} &= \frac{pG}{C+G} \\
\dot{F} &= F_{in} - \frac{m_f p_f e^{-qM} G}{k + p_g G + p_f e^{-qM} F} - dF \\
\dot{D} &= cdF - \mu D \\
\dot{M} &= \frac{a m_g p_g G + b m_f p_f e^{-qM} F}{k + p_g G + p_f e^{-qM} F} - rM
\end{aligned} \tag{3.1}$$

3.0.1 Analysis

Theorem 1 *All solutions of system (3.1) with positive initial conditions remain positive.*

Proof: Consider a trajectory $\Phi(t, X_0)$ with $\Phi(0, X_0) = X_0 \in \mathbb{R}^{5+}_0$, then this trajectory stays positive unless any one of the variables cross to negative. Since the functions are at least $C^1(\mathbb{R}^+)$, the Picard-Lindelöf theorem gives us that solutions exist for some maximal interval and are unique. Suppose there is a time $T > 0$ such that $\Phi(T, X_0) \notin \mathbb{R}^{5+}_0$, then by continuity of the flow and intermediate value theorem, there is a first time $0 < t^* < T$ the trajectory crosses the boundary. Additionally, the variable must cross 0 with negative velocity, and not simply approach 0 asymptotically.

Then we simply need to show that each of the 5 variables cannot be the first to cross this boundary with negative velocity. Suppose then that G is the first to go negative, but $\dot{G}|_{G=0} = G_{in} f_5(D) > 0$ which contradicts our assumptions, then G cannot be the first direction of crossing. Since $f_3 \geq 0$ always holds, Y cannot be the first variable to cross. Suppose F as the first variable to become negative, but $\dot{F}|_{F=0} = F_{in} > 0$ contradicts our assumptions. Then we check D: $\dot{D}|_{D=0} = cf_4(F, 0) \geq 0$ also has non-negative velocity. Finally, we assume that M is the first variable to become negative, but again $\dot{M}|_{M=0} = aGf_1(F, G, 0)+bFf_2(F, G, 0) \geq 0$ gives us our final required contradiction. Therefore, by contradiction, all positive trajectories remain positive. □

Solutions to the system are not guaranteed to be bounded, but glycogen (Y) is a sink. Consider the 4 dimensional system without glycogen,

$$\begin{aligned}
\dot{G} &= G_{in}\frac{n}{n+D} - \frac{m_g p_g G}{k + p_g G + p_f e^{-qM} F} - \frac{pG}{C+G} \\
\dot{F} &= F_{in} - \frac{m_f p_f e^{-qM} G}{k + p_g G + p_f e^{-qM} F} - dF \\
\dot{D} &= cdF - \mu D \\
\dot{M} &= \frac{a m_g p_g G + b m_f p_f e^{-qM} F}{k + p_g G + p_f e^{-qM} F} - rM
\end{aligned} \tag{3.2}$$

Theorem 2 *Define*

$$\hat{G} = \frac{-B + \sqrt{B^2 + 4p_g C G_{in}(m_g + p - G_{in})(k + \frac{p_f F_{in}}{d})}}{2p_g(m_g + p - G_{in})},$$

$$B = p_g C(m_g - G_{in}) + (k + \frac{p_f F_{in}}{d})(p - G_{in}).$$

Let S be a cube in $\mathbb{R}^{4+}_0$ with corners at the origin and $(\hat{G}, \frac{F_{in}}{d}, \frac{cdF_{in}}{d\mu}, \frac{am_g+bm_f}{r})$. The subsystem (3.2) is invariant in S if $m_g + p > G_{in}$.

Proof: The system is bounded below by $\mathbf{0}$, so we need to show it is also bounded above. Let $\Phi(t, X_0)$ be the flow of the system with $\Phi(0, X_0) \in S$. Suppose there is a

time $T > 0$ such that $\Phi(T, X_0) \notin S$, then there must be a first time $0 < t^* < T$ the flow crosses the boundary ∂S. Then we consider each variable as the first direction in which the boundary is crossed, at which time all other variables are assumed to be in the interior of S. If the variable crosses, then it must do so with positive time derivative. Suppose F is the first to cross the upper boundary. Let $F^* \geq \frac{F_{in}}{d}$. Then

$$\dot{F}|_{F^*} = F_{in} - \frac{p_f e^{-qM} F^*}{k + p_g G + p_f e^{-qM} F^*} - dF^* \leq -\frac{p_f e^{-qM} F^*}{k + p_g G + p_f e^{-qM} F^*} < 0.$$

So F must be bounded above by $\frac{F_{in}}{d}$. Suppose $D^* \geq \frac{cdF^*}{\mu}$. Then

$$\dot{D}|_{D^*} = cdF - \mu D^* \leq cd\frac{F_{in}}{d} - \frac{cdF_{in}}{d\mu}\mu = 0.$$

So D is bounded above by $\frac{cdF_{in}}{d\mu}$. Suppose M is the first to cross. Let $M^* \geq \frac{am_g + bm_f}{r}$. Then

$$\dot{M}|_{M^*} = \frac{am_g p_g G + bm_f p_f e^{-qM^*} F}{k + p_g G + p_f e^{-qM^*} F} - rM^* < am_g + bm_f - r\frac{am_g + bm_f}{r} = 0.$$

So M is bounded above by $\frac{am_g + bm_f}{r}$. Lastly, suppose G is the first to cross. Let $G^* \geq \hat{G}$. Then

$$\dot{G}|_{G=G^*} = G_{in}\frac{n}{n + D} - \frac{m_g p_g G^*}{k + p_g G^* + p_f e^{-qM} F} - \frac{pG^*}{C + G^*},$$

and substitute values of other variables, restricted by their upper bound to get

$$\leq G_{in} - \frac{m_g p_g G^*}{k + p_g G^* + p_f \frac{F_{in}}{d}} - \frac{pG^*}{C + G^*}.$$

Combine terms,

$$= \frac{G_{in}(C + G^*)(k + p_g G^* + p_f \frac{F_{in}}{d}) - m_g p_g G^*(C + G^*) - pG^*(k + p_g G^* + p_f \frac{F_{in}}{d})}{(C + G^*)(k + p_g G^* + p_f \frac{F_{in}}{d})},$$

and collect coefficients on powers of G^*,

$$= \frac{-p_g(m_g + p - G_{in})G^{*2} + \left(p_g C(m_g - G_{in}) + (k + \frac{p_f F_{in}}{d})(p - G_{in})\right) G^* + CG_{in}(k + \frac{p_f F_{in}}{k})}{(C + G^*)(k + p_g G^* + p_f \frac{F_{in}}{d})}.$$

Then the numerator is a quadratic with respect to G^*, with a positive constant term and negative leading coefficient (under the presumption that $m_g + p > G_{in}$), hence there is a positive real zero above which the numerator is negative. Let $B = p_g C(m_g - G_{in}) + (k + \frac{p_f F_{in}}{d})(p - G_{in})$ and call $\hat{G}$ the positive solution to the quadratic, then

$$\hat{G} = \frac{-B + \sqrt{B^2 + 4p_g C G_{in}(m_g + p - G_{in})(k + \frac{p_f F_{in}}{d})}}{2p_g(m_g + p - G_{in})}$$

hence $G^* \geq \hat{G}$ gives

$$= \frac{-p_g(m_g + p - G_{in})G^{*2} + \left(p_g C(m_g - G_{in}) + (k + \frac{p_f F_{in}}{d})(p - G_{in})\right) G^* + C G_{in}(k + \frac{p_f F_{in}}{k})}{(C + G^*)(k + p_g G^* + p_f \frac{F_{in}}{d})} \leq 0$$

Thus G^* is bounded above by $\hat{G}$. Therefore, by contradiction, system (3.2) is invariant in S. $\square$

3.0.2 Parameter Estimation

The initial focus of the research is to determine biologically relevant parameters for the model. Data from previous research (Roden *et al.*, 1996) was extracted using DataThief and used for estimation (Fig. 3.1). The research employed euglycemic-hyperinsulinemic clamp methods with fatty acid infusion, and they recorded blood metrics for 6 hours. The glucose infusion rate is adjusted to keep plasma concentrations constant, and the "stable" infusion rate multiplied by .7 to account for muscle uptake is used for G_{in} since about 70% of blood sugar is taken up by muscle. The fatty acid infusion is constant at 1.5ml/min, however the proportion that is taken up by muscles is not given, so we have to estimate this under a constraint that the maximum infusion must be less than 15ml/min. All other parameters are varied and estimated using 6 datasets.

A total of 4 data sets are used to fit the parameters: glucose oxidation rate for

Figure 3.1: Glucose Oxidation Rate and Δ Glycogen for High Fat (Open) and Low Fat (Closed) Infusion. Data Extracted From (Roden *et al.*, 1996).

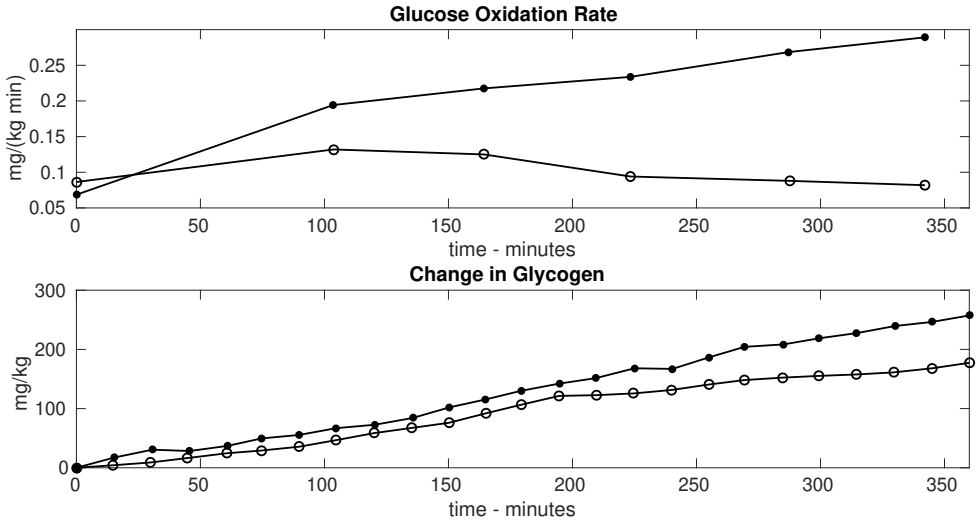

both the high fat and low fat infusion rates and change in glycogen for both high and low fat infusion. We estimated parameters comparing the model simulation to all four datasets simultaneously.

Iterative Latin Hypercube Shrinking Method

A hypercube is constructed of feasible parameter values by selecting a maximum and minimum for each parameter. Thousands of points in the parameter space were selected from an ordered uniform distribution of parameters using Latin Hypercube Sampling. Each set of parameters were used to simulate the system for 360 minutes, and the output was used to calculate the glucose oxidation rate and absolute change in glycogen to compare with the data. The data was normalized to span a range from 0 to 1 by scaling the data with

$$\frac{v_i - v_{min}}{v_{max} - v_{min}}$$

where v_{max} and v_{min} are the largest and smallest data values for dataset $\mathbf{v}$, and v_i is the value of point i. This scaling avoids an issue when fitting the model to multiple datasets with different orders of magnitude. Instead of an absolute squared difference, it is a relative squared difference. The simulation data was similarly scaled with

$$\frac{x_i - v_{min}}{v_{max} - v_{min}}$$

where x_i is the simulated model at the point corresponding to time v_i. The mean squared error for each dataset is then calculated by

$$\frac{\sum_1^n (x_i - v_i)^2}{n(v_{max} - v_{min})^2}$$

and the 4 data sets are summed with weights ω_i, $i = 1, 2, 3, 4$, to control subjective importance of the fit ,i.e. which data set we want to prioritize fit. This avoids falling into local minima that strongly fits more simply "shaped" data but does not match the important dynamics of another dataset.

The point in the parameter space that yielded the lowest mean squared error was selected as a new center value for the hypercube, the max and min bounds for each parameter was shrunk around this new center, and LHS was again used to sample another few thousand points. This continued until the process stabilizes around a local minima. By this, we mean that either the difference between the best fit of multiple subsequent fit attempts is within a predetermined tolerance, or the size of the hypercube is smaller than some tolerance. Since the hypercube is shrunk after each attempt, this yields a predetermined maximum number of possible runs before the size of the hypercube is sufficiently small to consider estimation procedure over. This method allows for exploration over a hypothesized feasible region, and resolution effectively increases as the same number of points are iteratively selected from

smaller regions. Hence, this method balances exploration and fine tuning. The major downfall of this method is the tendency for the system to settle on a local minima and stop exploring the entire feasible region. If exploration is emphasized, then the hypercube is shrunk slowly, and convergence may take a very long time. However, if the hypercube is shrunk too quickly, then the algorithm becomes stuck in an early region of best fit. For this reason, a more robust system was implemented, where each iteration acts as feedback for the next.

Particle Swarm Optimization

The iterative LHS shrinking method is designed to shrink toward a local minima. This unfortunately results in a lack of exploration of the parameter space. For example, if the global minimum exists in a small subset of the parameter space, but the region around the global minimum yields a relatively higher average squared error then another local minimum in the searching region, then there is a chance that the search region will shrink and center around the local minimum, excluding the global minimum from the search region. This scenario is especially prevalent when parameter ranges are chosen to include 0, since parameters that should be on the order of, for example 10^{-3}, could have their global minima excluded from the search region if it shrinks around a local minima sufficiently far from 0. Therefore, a method of parameter estimation that allows for exploration of the parameter space is ideal, especially when information about the order of magnitude of some parameters is unknown. Particle swarm optimization (PSO) evolves a set of mobile points in the parameter space to seek a global minima while still exploring local minima.

The method of PSO defines an initial collection of points in the search region of

the parameter space,

$$p_i(t) = (\rho_1, \rho_2, \ldots, \rho_m),\ i = 1, 2, \ldots, n,$$

where $t \in \mathbb{N}$ is the iteration step, n is the size of the swarm (number of points), $\rho_k,\ k = 1, \ldots, m$ are values of the parameters being estimated, and m is the number of estimated parameters. There are various methods of assigning these points, but we uniformly randomly select points in a designated search region for our algorithm, i.e.

$$\rho_k \in ((\rho_k)_{min}, (\rho_k)_{max}).$$

Each point initializes a random velocity in the direction of every parameter being estimated and it's starting location is recorded as that point's best minimizing location (g_i),

$$v_i(t) = (\delta_1, \delta_2, \ldots, \delta_m), i = 1, \ldots, n,$$

where δ_k is a real number, bounded in magnitude such that $|\delta_k| < ((\rho_k)_{max} - (\rho_k)_{min})/2$, e.g. the particle cannot traverse more than half the initial search region in one step. The velocities in each direction are randomly determined on initialization. Additionally, the swarm of points all know the best minimizing location of the whole swarm,

$$s = \min\{g_i, i = 1, \ldots, n\}.$$

The algorithm then iteratively updates the particles' locations by

$$p_i(t+1) = p_i(t) + v_i(t),$$

and then updates the new velocity,

$$v_i(t+1) = \omega_1 v_i(t) + \omega_2(g_i - p_i(t+1)) + \omega_3(s - p_i(t+1)),$$

where ω_1 is a weight on inertia, ω_2 is a weight on a particles "desire" to move toward its own recorded local minima, and ω_3 is a weight on a particles "desire" to move toward the globally known minima.

A key decision is how to assign the weights $\omega_1, \omega_2, \omega_3$ since these drastically affect the system. First, ω_1 determines the particles' exploration of the parameter space. Values greater than one promote a stubbornness to continue on their current path and look for new minima, whereas values less than one place more emphasis on drifting toward known minima and only searching the local area. Hence ω_1 has an effect on precision, where small values give small but thorough search areas. The weights on moving toward locally known and the globally known minima affect clustering. A strong weight toward the global minima provides a single large cluster and thoroughly searched area around s. On the other hand, a strong weight toward individually known minima potentially leads to multiple clusters or pools of particles searching their own areas. Different landscapes may require different choices of weights, and debate continues on which to use.

Furthermore, weights need not be static. A common modification is to provide a decreasing inertial weight, $\omega_1(t)$, that promotes exploration early in the algorithm, then tends toward a more thorough local exploration. Then the initial weight, function choice, and rate of weight reduction become relevant topics of consideration. For initial results in this project, constant weights are used.

Parameter Estimation Results

The high versus low fatty acid influx to the muscle cells was estimated to be a ratio of 9.5:1 (i.e. $F_{in}^{\text{high}} = 9.5F_{in}^{\text{low}}$) since this was the ratio of high infusion to low infusion in the study. Thus the model is a fit to both high and low triglyceride infusion scenarios with all other parameters fixed.

Table 3.1: Variable and Parameter Descriptions

Variable	**Initial Condition**	**Description**	**Units**
G	$F(0) = 4.9$	Intramuscular Glucose	mg/kg
Y	$Y(0) = 24.1$	Muscle Glycogen	mg/kg
F	$F(0) = 1.2\ 10^{-2}$	Intramuscular fatty acids	mg/kg
D	$D(0) = 4.7\ 10^{-2}$	Diacylglycerol	mg/kg
M	$M(0) = 1.1\ 10^{-1}$	Intramuscular Malonyl-CoA	mg/kg
Parameter	**Value**	**Description**	**Units**
G_{in}	1.4	Glucose infusion rate (Roden *et al.*, 1996)	mg/kg-min
F_{in}	$1.7\ 10^{-3}$	Fatty acid infusion rate	mg/kg-min
a	$8.6\ 10^{-1}$	Glucose to M-CoA Conversion	unitless
b	$1.1\ 10^{-3}$	Fatty acid to M-CoA Conversion	unitless
k	50*	Metabolism Half-Saturation Constant	mg/kg
p_g	$1.1\ 10^{-1}$	Proportion of G Available For Metabolism	unitless
p_f	$8.3\ 10^{-1}$	Proportion of F Available For Metabolism	unitless
m_g	4.6	Maximum Glucose Metabolism Rate	mg/kg-min
m_f	$1.2\ 10^{-1}\ 10^{-1}$	Maximum Fatty Acid Metabolism Rate	mg/kg-min
q	1	M-CoA Induced Fatty Acid Transfer Reduction	kg/mg
r	$4.1\ 10^{-1}$	Decay Rate of M-CoA	1/min
p	1.7	Conversion Rate of Glucose to Glycogen	1/min
C	16.4	Half Saturation for $G \rightarrow Y$ Conversion	mg/kg
d	$2.3\ 10^{-3}$	Production Rate of DAG by FFA	unitless
μ	$1.5\ 10^{-2}$	Decay Rate of DAG	1/min
n	$3.2\ 10^{-1}$	Half Max Reduction of Insulin Action by DAG	mg/kg

*: k is absorbed into p_f and p_g during estimation to reduce redundancy

When comparing results from the table to clinical measurements and approxima-

Figure 3.2: Model Fit to Data

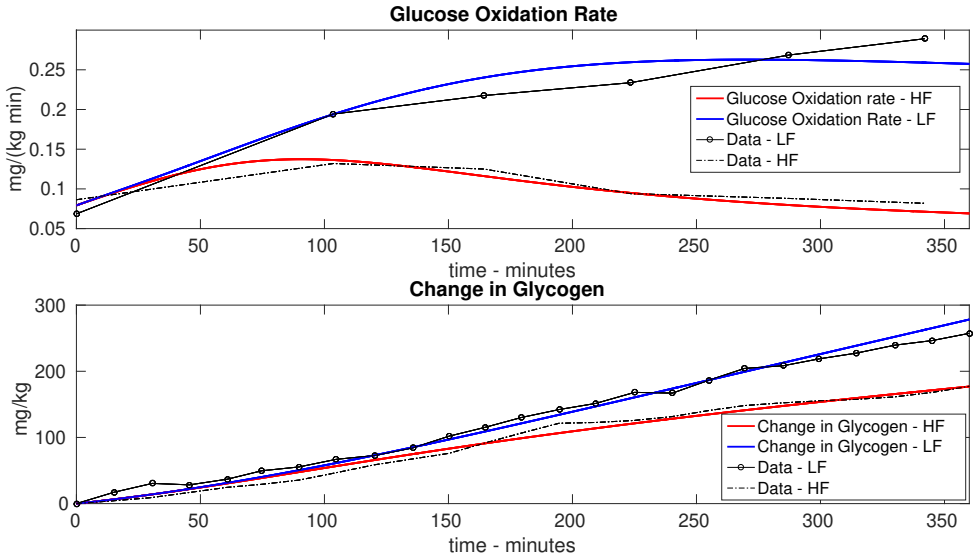

tions, certain conversions need to be taken into account. For example, the maximal fat oxidation rate has been measured to be between 0.27-0.52 g/min (Dandanell *et al.*, 2017) with a resting rate of about 0.15 g/min for patients with a mean fat free mass was between 62 and 70 kg. The estimated skeletal muscle mass is at least half the free fat mass (Kimyagarov *et al.*, 2010), or 31-35kg (this ratio is calculated for elderly individuals). Hence the expected upper limit for m_f is $7.714 - 16.774$ mg/kg-min, while the resting rate should be less than 4.286 mg/kg-min. Both the fit for m_g and m_f match these requirements.

Furthermore, the model fits the dynamics very well for both the high and low fatty acid infusion scenarios (Fig. 3.2). The simulation fits the transient dynamics seen in (Roden *et al.*, 1996), and can be used then to predict the effects of the euglycemic-hyperinsulinemic clamp on other intracellular behaviors (Fig. 3.3). The percent of maximal glucose infusion can be calculated by the predicted DAG concentration as

Figure 3.3: Intracellular Concentrations Predicted for Duration of Clamp Study

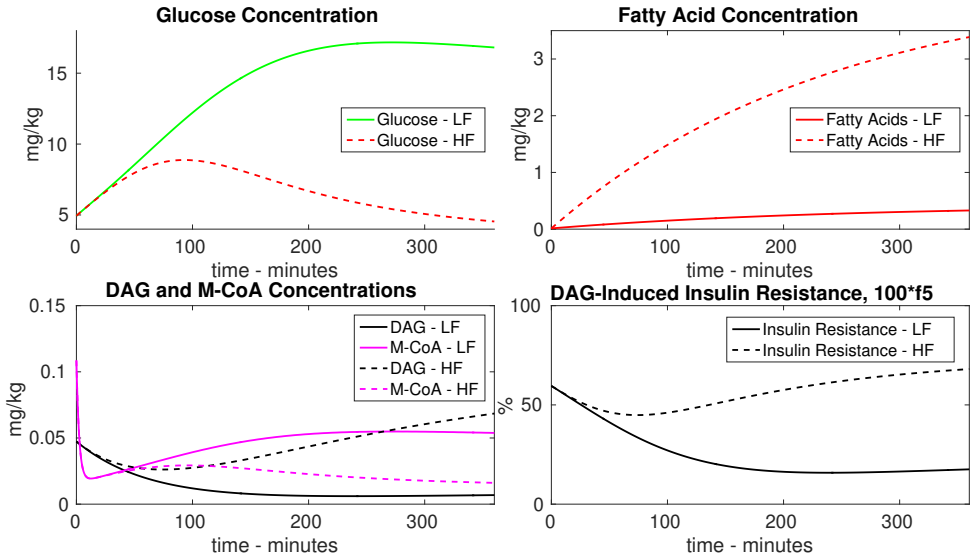

well, which could give insight into how much glucose is being utilized by non-muscle tissues. Additionally, the simulation in Fig. 3.4 demonstrates that under these particular parameters, the longer term dynamics reach equilibria for the subsystem (3.2) while glycogen stores are still submaximal. However, it is likely that once glycogen stores in muscles reach maximum capacity, the patients will become increasingly ill under hyperglycemia. Notably, our short term model does not apply in cases when glycogen is at maximum capacity.

The DAG-induced insulin resistance function, $f_5(D) = \frac{n}{n+D}$, is less than one so long as there is active DAG in the lipid membrane. This condition is biologically feasible, as there is always some concentration of DAG available to activate PKC. Hence the parameter choice for G_{in} is allowed to be greater than our expected glucose infusion rate since the parameter's function in our model is to act as a maximal infusion rate under ideal, non-regulated conditions. In this interpretation, it makes

Figure 3.4: Intracellular Concentrations Predicted Beyond Duration of Clamp Study

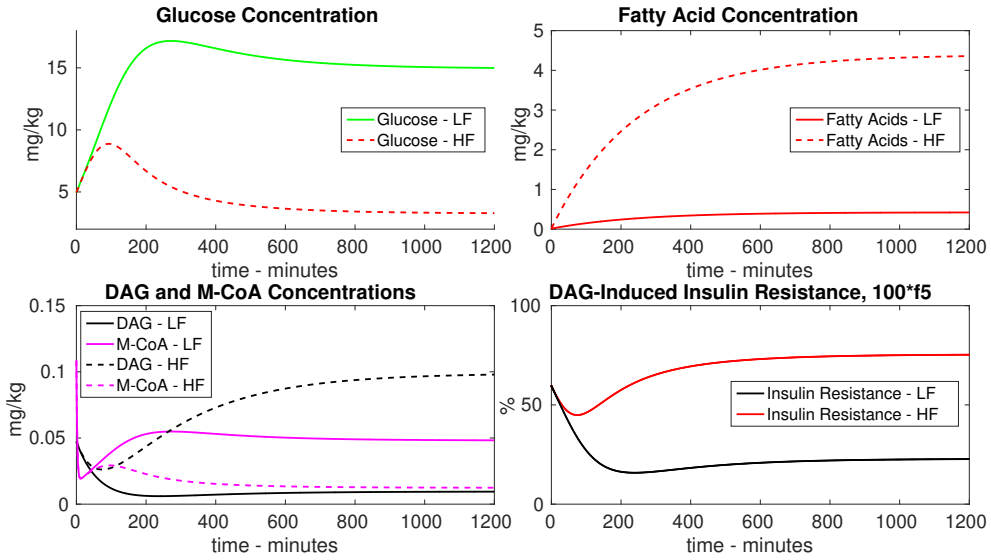

sense that in the low-fat case, Figs. 3.3 and 3.4 show that "insulin resistance" exists but at a lower level than in the high fat case.

3.0.3 Uncertainty Quantification

The parameter estimation algorithm compares outputs for low and high fatty acid inflow simultaneously for glucose oxidation and change in glycogen. Not only is the system highly nonlinear, but it might be unknown what range of values some parameters might take on. Some parameters have a stronger effect on the quality of fit than others, so sensitivity analysis is performed on the sum of squared errors (SSE) for each of the 4 data sets in order to determine how elastic the mean squared error is to parameter perturbations. The elasticity is calculated numerically for the parameter set determined by estimation using a difference quotient. For each parameter (or initial condition), ρ, the elasticity E_ρ of $SSE(\cdot;\rho)$ is calculated as

$$E_\rho = \left|\frac{dSSE}{d\rho}\right| \frac{\rho}{SSE} = \frac{|SSE(\cdot;\rho+\epsilon) - SSE(\cdot;\rho)|}{\epsilon} \frac{\rho}{SSE(\cdot;\rho)}$$

for some $\epsilon > 0$.

The parameter that had the highest effect on the fit of all the models is G_{in}, which is unsurprising since both glucose oxidation and glycogen storage are directly related to glucose availability. It is also obvious that glycogen has no effect on glucose oxidation since the concentration of muscle glucose does not directly affect the dynamics of any other state variable. Besides G_{in}, F_{in} comes in as a parameter for which the fit is rather elastic, which indicates that the concentration of blood fatty acids and their infusion into the cell is an important factor in the dynamics of the system.

Figure 3.5: Uncertainty Quantification for the Squared Error Glucose Oxidation Fit

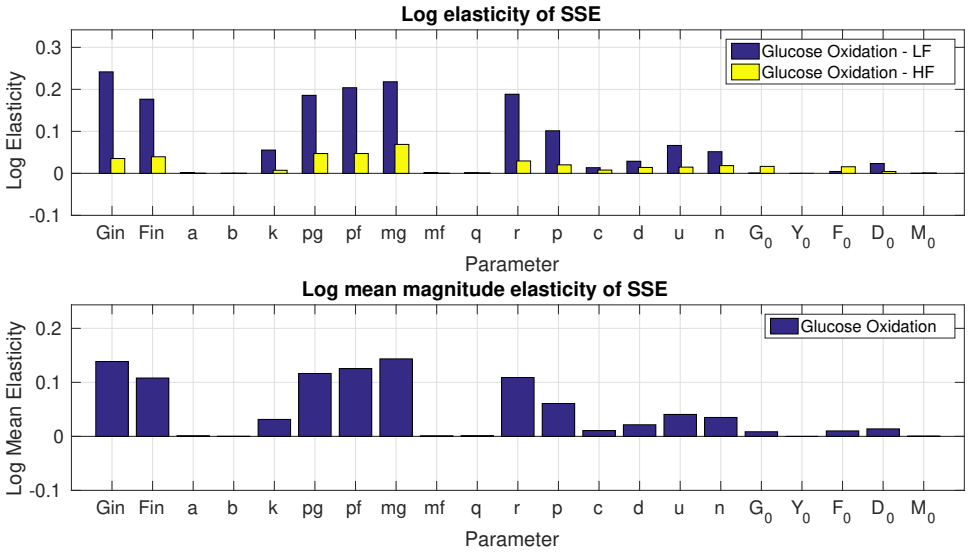

The main difference in elasticity between the fit for the oxidation and Δ glycogen data sets is that oxidation is more elastic to changes in the glucose metabolism

parameters (k, p_g, p_f, and m_g) whereas the glycogen storage is more sensitive to parameters modifying G_{in} (n, d, and C) as well as the glycogen storage rate (p and C). Finally, the parameters controlling concentrations of M-CoA seem to be rather inelastic (a, b, and q), whereas the degradation rate of M-CoA (r) seems to have an unexpectedly high effect on the fit of both datasets. This elasticity of the system to M-CoA degradation may be due to the regulatory effects that it has on keeping the concentration, M, relatively constant. In that way, it's possible that the fit is sensitive to r in the same way it is sensitive to p_f.

Figure 3.6: Uncertainty Quantification for the Squared Error of Δ Glycogen Fit

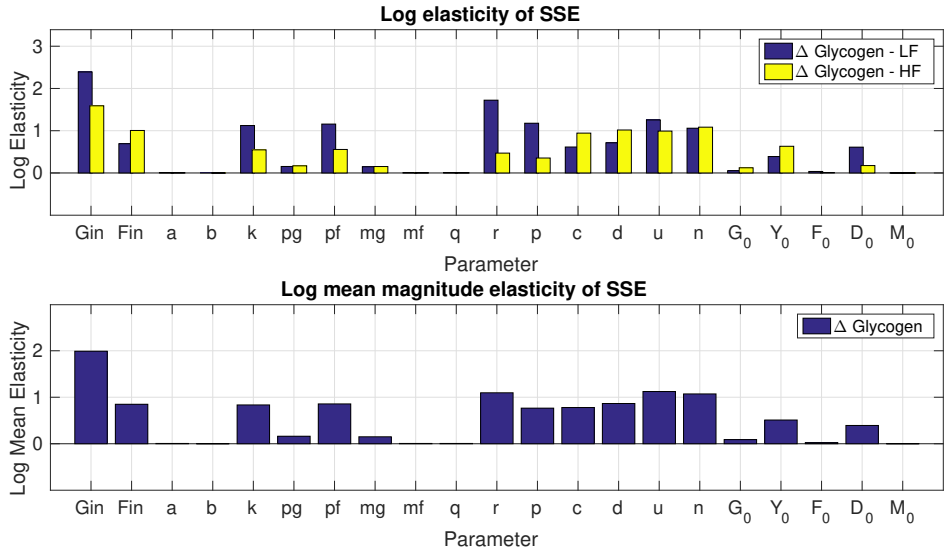

The lack of elasticity on M suggests that the fatty acid regulation dynamics may not play an important role in the system at the concentrations that our parameter estimation results suggest. It is possible that the effect of M on the system would be more poignant if we found another local minima in the parameter space with a similar fit. A more global understanding of the system's feasible parameter regions is needed to make more specific claims.

Chapter 4

LONG TERM CHRONIC INSULIN RESISTANCE MODEL

In chapter 3, the model was designed to fit clinical data over a short period of time during a euglycemic Hyperinsulinemic clamp with fatty acid infusion. As such, the model only admitted flow of glucose into the glycogen compartment, but no flow in the reverse direction. In day to day life, however, glycogen is stored or utilized depending on the cellular environment and energy needs. Hence, it is necessary to consider the conversion of glycogen back to glucose when necessary – namely when available glucose concentrations fall below a threshold.

This additional reversion of glycogen back into glucose allows the system to remain bounded, and long term dynamics to be studied. Additionally, the goal of the long term model is not for parameter estimation or data fitting, but mathematical analysis. To this end, we simplify the functional form by which mitochondrial metabolites (namely malonyl-CoA) affect fatty acid transfer into the mitochondria. The system of equations in (4.1) is the complete long term model with functions as described in chapter 2.

$$
\begin{aligned}
\dot{G} &= \frac{nG_{in}}{n+D} - \frac{m_g p_g G}{k + p_g G + \frac{p_f}{1+qM}F} - \begin{cases} \frac{P_f(G-g_y)\left(1-\frac{Y}{m_y}\right)}{C_u+(G-g_y)}, & G \geq g_y, Y < m_y \\ 0, & G \geq g_y, Y \geq m_y \\ \frac{P_r Y(G-g_y)}{C_l+g_y Y}, & G < g_y \end{cases} \\
\dot{Y} &= \begin{cases} \frac{P_f(G-g_y)\left(1-\frac{Y}{m_y}\right)}{C_u+(G-g_y)}, & G \geq g_y, Y < m_y \\ 0, & G \geq g_y, Y \geq m_y \\ \frac{P_r Y(G-g_y)}{C_l+g_y Y}, & G < g_y \end{cases} \\
\dot{F} &= F_{in} - \frac{m_f \frac{p_f}{1+qM}F}{k + p_g G + \frac{p_f}{1+qM}F} - dF \\
\dot{D} &= cdF - \mu D \\
\dot{M} &= \frac{am_g p_g G + bm_f \frac{p_f}{1+qM}F}{k + p_g G + \frac{p_f}{1+qM}F} - rM
\end{aligned}
\tag{4.1}
$$

Definition 1 *A finite system of ordinary differentiable equations defined on domain* $\mathcal{D} \in \mathbb{R}^n$ *with parameter vector* ρ

$$\dot{X} = F_i(t, X; \rho), X \in R_i$$

is said to be ***Piecewise Smooth*** *if it is smooth on countably many regions,* $R_i \in \mathbb{R}^n$*, with nonempty interior and* $\bigcup \overline{R_i} = \mathcal{D} \in \mathbb{R}^n$*. (Bernardo* et al.*, 2008)*

Definition 2 *Put* $\Sigma_{ij} = \overline{R_i} \cap \overline{R_j}$*,* $i \neq j$*, then* $\Sigma = \bigcup_{i \neq j} \Sigma_{ij}$ *is the* ***switching manifold****. (Bernardo* et al.*, 2008)*

Since the function, f_3 is piecewise continuous, with domains depending on state variables, this system is a piecewise smooth dynamical system. The system can be alternatively represented in PWS notation by

$$\dot{X} = (\dot{G}, \dot{Y}, \dot{F}, \dot{D}, \dot{M})^\top = \mathcal{F}_i(X, h(X, \rho); \rho), i = 1, 2, 3$$

where $h(X,\rho)$ is the switching condition, $\mathcal{F}_i$ is determined by which state the switching condition is in, and ρ is the set of parameters.

We have $\mathcal{F}_1$ defined for $G > g_y, Y < m_y$, $\mathcal{F}_2$ for $G > g_y, Y > m_y$, and $\mathcal{F}_3$ for $G < g_y$. We call the boundary $\Sigma = \{G, Y | G > g_y \text{ and } Y = m_y, \text{ or } G = g_y\}$ the switching manifold. The switching condition takes the value $h(X,\rho) = 0$ for $X \in \Sigma$ and $h(X,\rho) \neq 0$ for $X \notin \Sigma$. Then $\mathcal{F}_i$ is simply the right hand side of system (4.1) for each of the relevant domains in the piecewise function. Hence

$$\mathcal{F}_1 = \begin{pmatrix} \frac{nG_{in}}{n+D} - \frac{m_g p_g G}{k+p_g G+\frac{p_f}{1+qM}F} - \frac{P_f(G-g_y)(1-\frac{Y}{m_y})}{C_u+(G-g_y)} \\ \frac{P_f(G-g_y)(1-\frac{Y}{m_y})}{C_u+(G-g_y)} \\ F_{in} - \frac{m_f \frac{p_f}{1+qM}F}{k+p_g G+\frac{p_f}{1+qM}F} - dF \\ cdF - \mu D \\ \frac{am_g p_g G+bm_f \frac{p_f}{1+qM}F}{k+p_g G+\frac{p_f}{1+qM}F} - rM \end{pmatrix},$$

$$\mathcal{F}_2 = \begin{pmatrix} \frac{nG_{in}}{n+D} - \frac{m_g p_g G}{k+p_g G+\frac{p_f}{1+qM}F} \\ 0 \\ F_{in} - \frac{m_f \frac{p_f}{1+qM}F}{k+p_g G+\frac{p_f}{1+qM}F} - dF \\ cdF - \mu D \\ \frac{am_g p_g G+bm_f \frac{p_f}{1+qM}F}{k+p_g G+\frac{p_f}{1+qM}F} - rM \end{pmatrix}, \quad \mathcal{F}_3 = \begin{pmatrix} \frac{nG_{in}}{n+D} - \frac{m_g p_g G}{k+p_g G+\frac{p_f}{1+qM}F} - \frac{P_r Y(G-g_y)}{C_l+g_y Y} \\ \frac{P_r Y(G-g_y)}{C_l+g_y Y} \\ F_{in} - \frac{m_f \frac{p_f}{1+qM}F}{k+p_g G+\frac{p_f}{1+qM}F} - dF \\ cdF - \mu D \\ \frac{am_g p_g G+bm_f \frac{p_f}{1+qM}F}{k+p_g G+\frac{p_f}{1+qM}F} - rM \end{pmatrix}.$$

The dynamics of the PWS system act as if we glued together each of the three functions. The boundaries along the switching manifold introduce more interesting dynamics.

4.0.1 Preliminary Analysis

Theorem 3 *Solutions to system (4.1) exist and are unique*

Proof: By the Picard-Lindelöf theorem, if $\mathcal{F}_i$ is continuous and Lipschitz then solutions to system (4.1) exist and are unique. Since continuously differentiable and bounded implies Lipschitz, We tackle both by showing the system is $C^1(\mathbb{R}, \mathbb{R}^5)$ on the interior of the regions separated by the switching manifold. The Jacobian of the system is

$G \geq g_y, Y < m_y$:

$$\begin{bmatrix} -\frac{m_g p_g (k+\frac{p_f}{1+qM}F)}{(k+p_g G+\frac{p_f}{1+qM}F)^2} - \frac{C_u P_f (1-\frac{Y}{m_y})}{(C_u+G-g_y)^2} & \frac{P_f(G-g_y)}{m_y(C_u+G-g_y)} & \frac{m_g p_g \frac{p_f}{1+qM}G}{(k+p_g G+\frac{p_f}{1+qM}F)^2} & -\frac{nG_{in}}{(n+D)^2} & -\frac{qm_g p_g \frac{p_f}{1+qM}GF}{(1+qM)(k+p_g G+\frac{p_f}{1+qM}F)^2} \\ \frac{C_u P_f (1-\frac{Y}{m_y})}{(C_u+G-g_y)^2} & -\frac{P_f(G-g_y)}{m_y(C_u+G-g_y)} & 0 & 0 & 0 \\ \frac{p_g m_f \frac{p_f}{1+qM}F}{(k+p_g G+\frac{p_f}{1+qM}F)^2} & 0 & -\frac{m_f \frac{p_f}{1+qM}(k+p_g G)}{(k+p_g G+\frac{p_f}{1+qM}F)^2} - d & 0 & \frac{qm_f \frac{p_f}{1+qM}F(k+p_g G)}{(1+qM)(k+p_g G+\frac{p_f}{1+qM}F)^2} \\ 0 & 0 & cd & -\mu & 0 \\ \frac{p_g(akm_g+(am_g-bm_f)\frac{p_f}{1+qM}F)}{(1+qM)(k+p_g G+\frac{p_f}{1+qM}F)^2} & 0 & \frac{\frac{p_f}{1+qM}(bkm_f-p_g(am_g-bm_f)G)}{(1+qM)(k+p_g G+\frac{p_f}{1+qM}F)^2} & 0 & -\frac{q\frac{p_f}{1+qM}F(bm_f k-p_g(am_g-bm_f)G)}{(1+qM)(k+p_g G+\frac{p_f}{1+qM}F)^2} \end{bmatrix}$$

$G \geq g_y, Y \geq m_y$:

$$\begin{bmatrix} -\frac{m_g p_g (k+\frac{p_f}{1+qM}F)}{(k+p_g G+\frac{p_f}{1+qM}F)^2} & 0 & \frac{m_g p_g \frac{p_f}{1+qM}G}{(k+p_g G+\frac{p_f}{1+qM}F)^2} & -\frac{nG_{in}}{(n+D)^2} & -\frac{qm_g p_g \frac{p_f}{1+qM}GF}{(1+qM)(k+p_g G+\frac{p_f}{1+qM}F)^2} \\ 0 & 0 & 0 & 0 & 0 \\ \frac{p_g m_f \frac{p_f}{1+qM}F}{(k+p_g G+\frac{p_f}{1+qM}F)^2} & 0 & -\frac{m_f \frac{p_f}{1+qM}(k+p_g G)}{(k+p_g G+\frac{p_f}{1+qM}F)^2} - d & 0 & \frac{qm_f \frac{p_f}{1+qM}F(k+p_g G)}{(1+qM)(k+p_g G+\frac{p_f}{1+qM}F)^2} \\ 0 & 0 & cd & -\mu & 0 \\ \frac{p_g(akm_g+(am_g-bm_f)\frac{p_f}{1+qM}F)}{(1+qM)(k+p_g G+\frac{p_f}{1+qM}F)^2} & 0 & \frac{\frac{p_f}{1+qM}(bkm_f-p_g(am_g-bm_f)G)}{(1+qM)(k+p_g G+\frac{p_f}{1+qM}F)^2} & 0 & -\frac{q\frac{p_f}{1+qM}F(bm_f k-p_g(am_g-bm_f)G)}{(1+qM)(k+p_g G+\frac{p_f}{1+qM}F)^2} \end{bmatrix}$$

$G < g_y$:

$$\begin{bmatrix} -\frac{m_g p_g (k+\frac{p_f}{1+qM}F)}{(k+p_g G+\frac{p_f}{1+qM}F)^2} - \frac{P_r Y}{C_l+g_y Y} & -\frac{C_l P_r (G-g_y)}{(C_l+g_y Y)^2} & \frac{m_g p_g \frac{p_f}{1+qM}G}{(k+p_g G+\frac{p_f}{1+qM}F)^2} & -\frac{nG_{in}}{(n+D)^2} & -\frac{qm_g p_g \frac{p_f}{1+qM}GF}{(1+qM)(k+p_g G+\frac{p_f}{1+qM}F)^2} \\ \frac{P_r Y}{C_l+g_y Y} & \frac{C_l P_r (G-g_y)}{(C_l+g_y Y)^2} & 0 & 0 & 0 \\ \frac{p_g m_f \frac{p_f}{1+qM}F}{(k+p_g G+\frac{p_f}{1+qM}F)^2} & 0 & -\frac{m_f \frac{p_f}{1+qM}(k+p_g G)}{(k+p_g G+\frac{p_f}{1+qM}F)^2} - d & 0 & \frac{qm_f \frac{p_f}{1+qM}F(k+p_g G)}{(1+qM)(k+p_g G+\frac{p_f}{1+qM}F)^2} \\ 0 & 0 & cd & -\mu & 0 \\ \frac{p_g(akm_g+(am_g-bm_f)\frac{p_f}{1+qM}F)}{(1+qM)(k+p_g G+\frac{p_f}{1+qM}F)^2} & 0 & \frac{\frac{p_f}{1+qM}(bkm_f-p_g(am_g-bm_f)G)}{(1+qM)(k+p_g G+\frac{p_f}{1+qM}F)^2} & 0 & -\frac{q\frac{p_f}{1+qM}F(bm_f k-p_g(am_g-bm_f)G)}{(1+qM)(k+p_g G+\frac{p_f}{1+qM}F)^2} \end{bmatrix}$$

Each element of the Jacobian matrices is continuous, bounded on their respec-

tive domain, and defined for all positive G, Y, F, D, M. Hence the RHS of system (4.1) is Lipschitz on the interior of each region separated by the switching manifold. Therefore unique solutions to (4.1) are guaranteed to exist for any initial condition that is an interior point of a region separated by the switching manifold, at least on some finite time interval. For initial conditions on the switching manifold, we show that the functions are locally Lipschitz. We test the conditions on the three distinct sections of the switching manifold: $G_0 \geq g_y$ and $Y_0 = m_y$, $G_0 = g_y$ and $Y_0 \geq m_y$, and $G_0 = g_y$ and $Y_0 < m_y$. Since the equations only differ by the value of f_3, we show that f_3 is Lipschitz on the switching manifold, since the sum of finitely many Lipschitz functions is Lipschitz. Put $K = \max\left\{\frac{P_f}{m_y}, \frac{P_r}{g_y}, \frac{P_f}{C_u}\right\}$.

Case 1: $G_0 \geq g_y$ and $Y_0 = m_y$.

Pick $G_0 \geq g_y$ and set $Y_0 = m_y$. Then let $\alpha, \beta > 0$ and consider

$$|f_3(G_0, Y_0 - \alpha) - f_3(G_0, Y_0 + \beta)|.$$

Since $Y_0 - \alpha < m_y$ and $Y_0 + \beta > m_y$, we have

$$f_3(G_0, Y_0 - \alpha) = \frac{P_f(G - g_y)\left(1 - \frac{m_y - \alpha}{m_y}\right)}{C_u + G - g_y}$$

and $f_3(G_0, Y_0 + \beta) = 0$ Hence

$$|f_3(G_0, Y_0 - \alpha) - f_3(G_0, Y_0 + \beta)| = \left|\frac{P_f(G_0 - g_y)\left(1 - \frac{m_y - \alpha}{m_y}\right)}{C_u + G_0 - g_y}\right|$$

$$\leq P_f\left(1 - \frac{m_y - \alpha}{m_y}\right) = \frac{P_f}{m_y}\alpha < \frac{P_f}{m_y}|\alpha + \beta|$$

$$= \frac{P_f}{m_y}|(Y_0 - \alpha) - (Y_0 + \beta)| \leq K|(Y_0 - \alpha) - (Y_0 + \beta)|$$

Since $G_0 \geq g_y, \alpha, \beta$ were chosen arbitrarily, f_3 is Lipschitz on this section of the switching manifold.

Case 2: $G_0 = g_y$ and $Y_0 \geq m_y$.

Pick $Y_0 \geq m_y$ and set $G_0 = g_y$. Then let $\alpha, \beta > 0$ and consider

$$|f_3(G_0 - \alpha, Y_0) - f_3(G_0 + \beta, Y_0)|.$$

Since $G_0 - \alpha < g_y$ and $G_0 + \beta > g_y$, we have

$$f_3(G_0 - \alpha, Y_0) = -\frac{P_r Y_0 \alpha}{C_l + g_y Y_0}$$

and $f_3(G_0 + \beta, Y_0) = 0$. Hence

$$|f_3(G_0 - \alpha, Y_0) - f_3(G_0 + \beta, Y_0)| = \left| \frac{P_r Y_0 \alpha}{C_l + g_y Y_0} \right| \leq \frac{P_r}{g_y} |\alpha + \beta|$$

$$\leq \frac{P_r}{g_y} |(G_0 - \alpha) - (G_0 + \beta)| \leq K |(G_0 - \alpha) - (G_0 + \beta)|..$$

Therefore f_3 is Lipschitz on this section of the switching manifold.

Case 3: $G_0 = g_y$ and $Y_0 < m_y$.

Pick $Y_0 < m_y$ and set $G_0 = g_y$. Then let $\alpha, \beta > 0$ and consider

$$|f_3(G_0 - \alpha, Y_0) - f_3(G_0 + \beta, Y_0)|.$$

Since $G_0 - \alpha < g_y$ and $G_0 + \beta > g_y$, we have

$$f_3(G_0 - \alpha, Y_0) = -\frac{P_r Y_0 \alpha}{C_l + g_y Y_0}$$

and

$$f_3(G_0 + \beta, Y_0) = \frac{\beta P_f (1 - \frac{Y_0}{m_y})}{C_u + \beta}.$$

Hence

$$|f_3(G_0 - \alpha, Y_0) - f_3(G_0 + \beta, Y_0)| = \left| \frac{P_r Y_0 \alpha}{C_l + g_y Y_0} + \frac{\beta P_f (1 - \frac{Y_0}{m_y})}{C_u + \beta} \right|$$

$$\leq \frac{P_r}{g_y} \alpha + \frac{P_f}{C_u} \beta \leq \max \left\{ \frac{P_r}{g_y}, \frac{P_f}{C_u} \right\} |\alpha + \beta|$$

$$\leq K|(G_0 - \alpha) - (G_0 + \beta)|$$

Then f_3 is Lipschitz on this last section of the switching manifold. Therefore, for any $X_0 \in \mathbb{R}_0^{5+}$, solutions to (4.1) exist and are unique. $\square$

Theorem 4 *Let $\Phi_{X_0} \equiv \Phi(t, X_0), t \geq 0$ be a forward flow of system (4.1) with initial conditions*

$$\Phi(0, X_0) = X_0 = (G(0), Y(0), F(0), D(0), M(0)) = (G_0, Y_0, F_0, D_0, M_0) \in \mathbb{R}_0^{5+}$$

Then $\Phi(t, X_0) \in \mathbb{R}_0^{5+}$ for all $t > 0$ on which Φ_{X_0} is defined. Additionally, Φ_{X_0} is bounded above.

Proof: Let $X_0 = (G_0, Y_0, F_0, D_0, M_0) \in \mathbb{R}_0^{5+}$, and let $\Phi(t, X_0)$ be the flow of system (4.1).

Claim 1 (positivity): $\Phi(t, X_0) \in \mathbb{R}_0^{5+} \cup \{\infty\}$ for all $t > 0$ on which Φ_{X_0} is defined.

Since the RHS of (4.1) is continuous, the integral solutions are continuous in time. Then by the intermediate value theorem, if there exists $T > 0$ such that $\Phi(T, X_0) \notin \mathbb{R}_0^{5+}$, then there is a first time $0 < t* < T$ such that $\Phi(t^*, X + 0)e_i = 0$, where $e_i = (0, 0, \ldots, 1, \ldots, 0, 0)$ with 1 in the i^{th} position, $i = 1, \ldots, 5$. Furthermore, in order for the flow to escape $\mathbb{R}_0^{5+}$, we need

$$\frac{d}{dt}\Phi(t, X_0)e_i|_{t=t^*} < 0,$$

i.e. it must cross that boundary with nonzero velocity. Then we simply check each time derivative evaluated on the boundary. Suppose for the sake of contradiction that there exists $T > 0$ such that $\Phi(T, X_0) \notin \mathbb{R}_0^{5+} \cup \{\infty\}$, then there is a first crossing time $t^* > 0$. Moreover, suppose that for $t = t^*$ we have $G(t^*) = 0$. Then the time derivative on the boundary is

$$\dot{G}|_{G=0} = \frac{nG_{in}}{n + D} + \frac{P_r Y g_y}{C_l + g_y Y} > 0$$

assuming $Y, D \geq 0$, which must be true since t^* is the first time $\Phi(t, X_0)$ leaves the positive sector. Continue this for each of the other state variables

$$\dot{Y}|_{Y=0} = \begin{cases} \frac{P_f(G-g_y)}{C_u+(G-g_y)}, & G \geq g_y \\ 0, & G < g_y \end{cases} \geq 0,$$

$$\dot{F}|_{F=0} = F_{in} > 0,$$

$$\dot{D}|_{D=0} = cdF \geq 0,$$

$$\dot{M}|_{M=0} = \frac{am_g p_g G + bm_f p_f F}{k + p_g G + p_f F} > 0.$$

But none of the time derivatives have negative velocity on the boundary, this contradicts the assertion that there is some time $T > 0$ where $\Phi(T, X_0) \notin \mathbb{R}^{5+}_0$. Therefore, $\Phi(t, X_0) \in \mathbb{R}^{5+}_0$ for all $t > 0$ for which Φ_{X_0} is defined.

Claim 2 (boundedness from above):

Let the origin and $\left(\frac{G_{in}(k+\frac{p_f F_{in}}{d})}{p_g(m_g - G_{in})}, \max\{m_y, Y_0\}, \frac{F_{in}}{d}, \frac{cF_{in}}{\mu}, \frac{am_g+bm_f}{r} \right)$ define a hypercube $\mathcal{C} \in \mathbb{R}^5$. We will show that if $X_0 \in C$ then $\Phi(t, X_0) \in C$ for all $t \geq 0$ for which Φ_{X_0} is defined. Let $X_0 \in C$. To show this, it is sufficient to demonstrate that the time derivative is negative for any state variable outside of C. As with positivity, assume there is a first time t^* and first variable to exit C. Hence, we assume that all other variables not being inspected on the boundary ∂C are on the interior of C.

If $F \geq \frac{F_{in}}{d}$, then

$$\dot{F} = F_{in} - \frac{m_f \frac{p_f}{1+qM} F}{k + p_g G + \frac{p_f}{1+qM} F} - dF \leq -\frac{m_f \frac{p_f}{1+qM} F}{k + p_g G + \frac{p_f}{1+qM} F} < 0,$$

hence F is bounded above.

If $D \geq \frac{cF_{in}}{\mu}$, then

$$\dot{D} = cdF - \mu D < cF_{in} - \mu D \leq 0,$$

hence D is bounded above.

If $M \geq \frac{am_g + bm_f}{r}$, then

$$\dot{M} = \frac{am_g p_g G + bm_f \frac{p_f}{1+qM} F}{k + p_g G + \frac{p_f}{1+qM} F} - rM < am_g + bm_f - rM \leq 0,$$

hence M is bounded above.

If $Y > m_y$, then

$$\dot{Y} = \begin{cases} 0, & G \geq g_y \\ \frac{P_r Y(G - g_y)}{C_l + g_y Y}, & G < g_y \end{cases} \leq 0,$$

hence Y is bounded above by m_y if $Y_0 < m_y$ or by Y_0 if $Y_0 \geq m_y$.

Finally, the nature of Y's boundedness requires us to consider 2 cases for G: $G \geq g_y, Y \geq m_y$, and $G \geq g_y, Y < m_y$. Note that if G is bounded in both of these cases, then G is bounded.

Case 1: Begin with

$$\dot{G}|_{G \geq g_y, Y \geq m_y} = \frac{nG_{in}}{n + D} - \frac{m_g p_g G}{k + p_g G + \frac{p_f}{1+qM} F} \leq G_{in} - \frac{m_g p_g G}{k + p_g G + \frac{p_f}{1+qM} F}$$

replacing M with 0 and F with its upper bound

$$\leq G_{in} - \frac{m_g p_g G}{k + p_g G + \frac{p_f F_{in}}{d}} = \frac{G_{in}(k + p_g G + \frac{p_f F_{in}}{d}) - m_g p_g G}{k + p_g G + \frac{p_f F_{in}}{d}}$$

and rearrange

$$\frac{G_{in}(k + \frac{p_f F_{in}}{d}) - p_g(m_g - G_{in})G}{k + p_g G + \frac{p_f F_{in}}{d}} \leq \frac{G_{in}(k + \frac{p_f F_{in}}{d}) - G_{in}(k + \frac{p_f F_{in}}{d})}{k + p_g G + \frac{p_f F_{in}}{d}} = 0$$

Hence $\dot{G}|_{G\geq g_y, Y\geq m_y} \leq 0$.

Case 2:

$$\dot{G}|_{G\geq g_y, Y<m_y} = \frac{nG_{in}}{n+D} - \frac{m_g p_g G}{k + p_g G + \frac{p_f}{1+qM}F} - \frac{P_f(G-g_y)(1-\frac{Y}{m_y})}{C_u + (G-g_y)}$$

But it's clear by the additional negative term that

$$\dot{G}|_{G\geq g_y, Y<m_y} \leq \dot{G}|_{G\geq g_y, Y\geq m_y} \leq 0,$$

so boundedness is automatic. Thence G is bounded.

Therefore, by contradiction, if $X_0 \in C$ then $\Phi(t, X_0) \in C$ for all $t > 0$ for which Φ_{X_0} is defined. □

Beyond the uniqueness, existence, and invariance of solutions of (4.1), we explore how the dynamics of the system changes as we progress from a model of a healthy person, to one with insulin resistance without fatty acid metabolism regulation, and finally to the full model with insulin resistance and fatty acid metabolism regulation.

4.0.2 Sub-models: Ignoring Mitochondrial Metabolites

We analyze sub-models of (4.1) in order to understand how the dynamics evolve from a healthy case without DAG, and with DAG. For these cases, the effect of Malonyl-CoA (M) is ignored due to the highly nonlinear terms that the interaction introduces. Additionally, sensitivity analysis of the parameters involved in the production and function of M-CoA demonstrated that the system is inelastic to their

perturbations. For these reasons, the M compartment is ignored for further study. Hence, we seek mathematically tractable equations to clearly understand the system behavior from the ground up before getting lost in the details analyzing (4.1).

4.0.3 Sub-model: Healthy Individual - No effect of DAG

Suppose that in a healthy individual, the levels of DAG present are too insignificant to influence insulin resistance, then we ignore the compartment and get the system

$$\begin{aligned}
\dot{G} &= G_{in} - \frac{m_g p_g G}{k + p_g G + p_f F} - \begin{cases} \frac{P_f(G-g_y)\left(1-\frac{Y}{m_y}\right)}{C_u+(G-g_y)}, & G \geq g_y, Y < m_y \\ 0, & G \geq g_y, Y \geq m_y \\ \frac{P_r Y(G-g_y)}{C_l+g_y Y}, & G < g_y \end{cases} \\
\dot{Y} &= \begin{cases} \frac{P_f(G-g_y)\left(1-\frac{Y}{m_y}\right)}{C_u+(G-g_y)}, & G \geq g_y, Y < m_y \\ 0, & G \geq g_y, Y \geq m_y \\ \frac{P_r Y(G-g_y)}{C_l+g_y Y}, & G < g_y \end{cases} \\
\dot{F} &= F_{in} - \frac{m_f p_f F}{k + p_g G + p_f F} - dF
\end{aligned} \tag{4.2}$$

Then we have fatty acids still converted to other byproducts, but we don't keep track of DAG if we assume that its concentration is low enough to cause no effect.

Definition 3 *A **discontinuous bifurcation** (or dicontinuity induced bifurcation) occurs when a fixed point of a system passes through the switching manifold. (Bernardo* et al.*, 2008; Simpson* et al.*, 2009)*

Note that stability of an equilibrium lying on a swithcing manifold is an open problem (Bernardo *et al.*, 2008).

Theorem 5 *System (4.2) has a unique equilibrium, (G^*, Y^*, F^*), if $m_g > G_{in}$ for each region. The equilibrium is stable where it exists. The equilibrium is given by*

$$G^* = \frac{A}{p_g}(k + p_f F^*),$$
$$F^* = \frac{(1+A)(p_f F_{in} - dk) - m_f p_f + \sqrt{((1+A)(p_f F_{in} - dk) - m_f p_f)^2 + 4dkp_f F_{in}(1+A)^2}}{2dp_f(1+A)},$$
$$A = \frac{G_{in}}{m_g - G_{in}}.$$

Furthermore, the system presents a discontinuous bifurcation, that is for

$$G^* < g_y,\ Y^* = 0,$$
$$G^* > g_y,\ Y^* = m_y,$$
$$G^* = g_y,\ Y^* \in [0, \infty)$$

The case where $G^* = g_y$ is degenerate and creates a critical line of equilibria.

Proof:

We start by requiring $f_3(G, Y) = 0$, hence we consider 3 cases:

$$\textbf{Case 1}: \quad G^* < g_y, \quad Y^* = 0$$
$$\textbf{Case 2}: \quad G^* > g_y, \quad Y^* = m_y$$
$$\textbf{Case 3}: \quad G^* = g_y, \quad Y^* = Y^* \geq 0$$

The dynamics of the full piecewise-continuous system can be understood by "gluing together" the results of these three cases.

Case 1: $G^* < g_y$

Substituting $Y^* = 0$ and solving $\dot{G} = 0$ for G^* we get

$$0 = G_{in} - \frac{m_g p_g G^*}{k + p_g G^* + p_f F^*},$$

$$m_g p_g G^* = G_{in}(k + p_g G^* + p_f F^*),$$

$$m_g p_g G^* - p_g G_{in} G^* = G_{in}(k + p_f F^*),$$

$$G^* = \frac{G_{in}(k + p_f F^*)}{p_g(m_g - G_{in})}.$$

Then we simplify by substituting

$$A = \frac{G_{in}}{m_g - G_{in}}$$

to get

$$G^* = \frac{A}{p_g}(k + p_f F^*).$$

necessitating $m_g > G_{in}$ for biologically feasible values of G^*.

Similarly, we solve for F^* by setting $\dot{F} = 0$ to get

$$0 = F_{in} - \frac{m_f p_f F^*}{k + p_g G^* + p_f F^*} - dF^*,$$

into which we substitute G^*

$$0 = F_{in} - \frac{m_f p_f F^*}{k + A(k + p_f F^*) + p_f F^*} - dF^*,$$

rearrange

$$m_f p_f F^* + d(k + A(k + p_f F^*) + p_f F^*)F^* = F_{in}(k + A(k + p_f F^*) + p_f F^*),$$

and collect terms on each power of F^*, moving everything to the LHS

$$dp_f(1 + A)F^{*2} + [m_f p_f + (dk - p_f F_{in})(1 + A)]F^* - kF_{in}(1 + A) = 0.$$

Then we find F^* as a solution to $\alpha F^{*2} + \beta F^* + \gamma$ with

$$\alpha = dp_f(1 + A)$$

$$\beta = m_f p_f + (dk - p_f F_{in})(1 + A)$$

$$\gamma = -kF_{in}(1+A)$$

and since $A > 0$ we know there is always exactly one positive real root for F^* by Descartes' rule of signs, since either $\alpha, \beta > 0$, $\gamma < 0$ or $\alpha > 0$,$\beta, \gamma < 0$ yields only one sign change. Solving for F^* we get

$$F^* = \frac{-\beta \pm \sqrt{\beta^2 - 4\alpha\gamma}}{2\alpha}$$

which we can ignore the negative, non-biological equilibrium to get

$$F^* = \frac{(1+A)(p_f F_{in} - dk) - m_f p_f + \sqrt{((1+A)(p_f F_{in} - dk) - m_f p_f)^2 + 4dkp_f F_{in}(1+A)^2}}{2dp_f(1+A)}$$

where the radicand is clearly always positive when $A > 0$.

The Jacobian of the system evaluated at the equilibria takes the form

$$J_1|_{G=G^*,Y=0,F=F^*} = \begin{bmatrix} -\frac{m_g(k+F^*p_f)p_g}{(k+F^*p_f+G^*p_g)^2} & \frac{P_r}{C_l}(g_y - G^*) & \frac{G^*m_g p_f p_g}{(k+F^*p_f+G^*p_g)^2} \\ 0 & -\frac{P_r}{C_l}(g_y - G^*) & 0 \\ \frac{F^*m_f p_f p_g}{(k+F^*p_f+G^*p_g)^2} & 0 & -\frac{m_f p_f(k+G^*p_g)+d(k+F^*p_f+G^*p_g)^2}{(k+F^*p_f+G^*p_g)^2} \end{bmatrix}.$$

The full expressions for G^* and F^* are not substituted so as to ease the digestibility of the analysis. We use the Routh-Hurwitz Criterion to determine stability (Brauer *et al.*, 2001). The Jacobian has a characteristic polynomial determined by setting $\det[\lambda\mathbb{I} - J_1] = 0$ described by $\lambda^3 + a_{1,1}\lambda^2 + a_{1,2}\lambda + a_{1,3} = 0$ with coefficients

$$\begin{aligned}
a_{1,1} =& \frac{P_r}{C_l}(g_y - G^*) + \frac{m_g(k+F^*p_f)p_g}{(k+F^*p_f+G^*p_g)^2} + \frac{m_f p_f(k+G^*p_g)+d(k+F^*p_f+G^*p_g)^2}{(k+F^*p_f+G^*p_g)^2} \\
a_{1,2} =& \left(\frac{m_g(k+F^*p_f)p_g}{(k+F^*p_f+G^*p_g)^2}\right)\left(\frac{m_f p_f(k+G^*p_g)+d(k+F^*p_f+G^*p_g)^2}{(k+F^*p_f+G^*p_g)^2}\right) \\
&+ \left(\frac{G^*m_g p_f p_g}{(k+F^*p_f+G^*p_g)^2}\right)\left(\frac{F^*m_f p_f p_g}{(k+F^*p_f+G^*p_g)^2}\right) \\
&+ \left(\frac{P_r}{C_l}(g_y - G^*)\right)\left(\frac{m_g(k+F^*p_f)p_g}{(k+F^*p_f+G^*p_g)^2} + \frac{m_f p_f(k+G^*p_g)+d(k+F^*p_f+G^*p_g)^2}{(k+F^*p_f+G^*p_g)^2}\right) \\
a_{1,3} =& \left(\frac{P_r}{C_l}(g_y - G^*)\right)\left[\left(\frac{m_g(k+F^*p_f)p_g}{(k+F^*p_f+G^*p_g)^2}\right)\left(\frac{m_f p_f(k+G^*p_g)+d(k+F^*p_f+G^*p_g)^2}{(k+F^*p_f+G^*p_g)^2}\right)\right. \\
&\left. + \left(\frac{P_r}{C_l}(g_y - G^*)\right)\left(\frac{F^*m_f p_f p_g}{(k+F^*p_f+G^*p_g)^2}\right)\right]
\end{aligned} \tag{4.3}$$

The constants, $a_{1,1}$ and $a_{1,3}$ are clearly both positive when $G^* < g_y$ since each term is independently positive. Then we only need to check

$$
\begin{aligned}
a_{1,1}a_{1,2}-a_{1,3} = \\
&\left(\frac{m_g(k+F^*p_f)p_g}{(k+F^*p_f+G^*p_g)^2}+\frac{m_fp_f(k+G^*p_g)+d(k+F^*p_f+G^*p_g)^2}{(k+F^*p_f+G^*p_g)^2}\right)\\
&\times\left[\left(\frac{m_g(k+F^*p_f)p_g}{(k+F^*p_f+G^*p_g)^2}\right)\left(\frac{m_fp_f(k+G^*p_g)+d(k+F^*p_f+G^*p_g)^2}{(k+F^*p_f+G^*p_g)^2}\right)\right.\\
&+\left(\frac{G^*m_gp_fp_g}{(k+F^*p_f+G^*p_g)^2}\right)\left(\frac{F^*m_fp_fp_g}{(k+F^*p_f+G^*p_g)^2}\right)\\
&\left.+\left(\frac{P_r}{C_l}(g_y-G^*)\right)^2\left(\frac{m_g(k+F^*p_f)p_g}{(k+F^*p_f+G^*p_g)^2}+\frac{m_fp_f(k+G^*p_g)+d(k+F^*p_f+G^*p_g)^2}{(k+F^*p_f+G^*p_g)^2}\right)\right]
\end{aligned}
$$

Hence $a_1a_2 - a_3 > 0$. Therefore by the Routh-Hurwitz Criterion, this equilibria is stable when $m_g > G_{in}$ and $G^* < g_y$.

Case 2: $G^* > g_y$

Setting $Y^* = m_y$ and solving for G^* and F^* returns exactly the same results as in case 1,

$$G^* = \frac{A}{p_g}(k + p_fF^*),$$

$$F^* = \frac{(1+A)(p_fF_{in}-dk)-m_fp_f+\sqrt{((1+A)(p_fF_{in}-dk)-m_fp_f)^2+4dkp_fF_{in}(1+A)^2}}{2dp_f(1+A)}$$

$$A = \frac{G_{in}}{m_g - G_{in}}.$$

and the Jacobian of the system is

$$J_2|_{G=G^*,Y=m_y,F=F^*} = \begin{bmatrix} -\frac{m_g(k+F^*p_f)p_g}{(k+F^*p_f+G^*p_g)^2} & \frac{(G^*-g_y)P_f}{(C_u+G^*-g_y)m_y} & \frac{G^*m_gp_fp_g}{(k+F^*p_f+G^*p_g)^2} \\ 0 & -\frac{(G^*-g_y)P_f}{(C_u+G^*-g_y)m_y} & 0 \\ \frac{F^*m_fp_fp_g}{(k+F^*p_f+G^*p_g)^2} & 0 & -\frac{m_fp_f(k+G^*p_g)+d(k+F^*p_f+G^*p_g)^2}{(k+F^*p_f+G^*p_g)^2} \end{bmatrix}.$$

The characteristic polynomial of J_2 takes the form $\lambda^3 + a_{2,1}\lambda^2 + a_{2,2}\lambda + a_{2,3} = 0$ with coefficients

$$\begin{aligned}
a_{2,1} =& \frac{(G^* - g_y)P_f}{(C_u + G^* - g_y)m_y} + \frac{m_g(k + F^*p_f)p_g}{(k + F^*p_f + G^*p_g)^2} + \frac{m_f p_f(k + G^*p_g) + d(k + F^*p_f + G^*p_g)^2}{(k + F^*p_f + G^*p_g)^2} \\
a_{2,2} =& \left(\frac{m_g(k + F^*p_f)p_g}{(k + F^*p_f + G^*p_g)^2}\right)\left(\frac{m_f p_f(k + G^*p_g) + d(k + F^*p_f + G^*p_g)^2}{(k + F^*p_f + G^*p_g)^2}\right) \\
&+ \left(\frac{G^*m_g p_f p_g}{(k + F^*p_f + G^*p_g)^2}\right)\left(\frac{F^*m_f p_f p_g}{(k + F^*p_f + G^*p_g)^2}\right) \\
&+ \left(\frac{(G^* - g_y)P_f}{(C_u + G^* - g_y)m_y}\right)\left(\frac{m_g(k + F^*p_f)p_g}{(k + F^*p_f + G^*p_g)^2} + \frac{m_f p_f(k + G^*p_g) + d(k + F^*p_f + G^*p_g)^2}{(k + F^*p_f + G^*p_g)^2}\right)
\end{aligned} \tag{4.4}$$

$$\begin{aligned}
a_{2,3} =& \left(\frac{(G^* - g_y)P_f}{(C_u + G^* - g_y)m_y}\right)\left[\left(\frac{m_g(k + F^*p_f)p_g}{(k + F^*p_f + G^*p_g)^2}\right)\left(\frac{m_f p_f(k + G^*p_g) + d(k + F^*p_f + G^*p_g)^2}{(k + F^*p_f + G^*p_g)^2}\right)\right. \\
&\left. + \left(\frac{(G^* - g_y)P_f}{(C_u + G^* - g_y)m_y}\right)\left(\frac{F^*m_f p_f p_g}{(k + F^*p_f + G^*p_g)^2}\right)\right]
\end{aligned}$$

Since $G^* > g_y$, it's clear that $a_{2,1} > 0$ and $a_{2,3} > 0$. Then the final condition

$$\begin{aligned}
&a_{2,1}a_{2,2} - a_{2,3} = \\
&\left(\frac{m_g(k + F^*p_f)p_g}{(k + F^*p_f + G^*p_g)^2} + \frac{m_f p_f(k + G^*p_g) + d(k + F^*p_f + G^*p_g)^2}{(k + F^*p_f + G^*p_g)^2}\right) \\
&\times \left[\left(\frac{m_g(k + F^*p_f)p_g}{(k + F^*p_f + G^*p_g)^2}\right)\left(\frac{m_f p_f(k + G^*p_g) + d(k + F^*p_f + G^*p_g)^2}{(k + F^*p_f + G^*p_g)^2}\right)\right. \\
&+ \left(\frac{G^*m_g p_f p_g}{(k + F^*p_f + G^*p_g)^2}\right)\left(\frac{F^*m_f p_f p_g}{(k + F^*p_f + G^*p_g)^2}\right) \\
&\left. + \left(\frac{(G^* - g_y)P_f}{(C_u + G^* - g_y)m_y}\right)^2\left(\frac{m_g(k + F^*p_f)p_g}{(k + F^*p_f + G^*p_g)^2} + \frac{m_f p_f(k + G^*p_g) + d(k + F^*p_f + G^*p_g)^2}{(k + F^*p_f + G^*p_g)^2}\right)\right]
\end{aligned}$$

is also positive. Hence, by the Routh-Hurwitz criterion, the equilibrium is stable.

Case 3: $G^* = g_y$

When $G^* = g_y$, the implication is that sugar is passing into the muscles at exactly the rate required for the muscles glucose concentration to be exactly ideal. Hence, this equilibrium only exists for a specific subset of parameters. Notice above in both of the two cases that $G^* = A(k + p_f F^*)/p_g$. Then, by solving $G^* = g_y$ for F^*, we see

that

$$A(k + p_f F^*)/p_g = g_y$$

gives us

$$F^* = \frac{p_g g_y - Ak}{p_f A}.$$

If we have $p_g g_y - Ak > 0$ then it is possible for the conditions to exist such that $G^* = g_y$. Assume $p_g g_y - Ak > 0$ holds. Then, we can substitute $G^* = g_y$ and $\frac{p_g g_y - Ak}{p_f A}$ into $\dot{F} = 0$

$$\dot{F}^* = F_{in} - \frac{m_f \frac{p_g g_y - Ak}{A}}{k + p_g g_y + \frac{p_g g_y - Ak}{A}} - d\frac{p_g g_y - Ak}{p_f A} = 0$$

rearrange to isolate F_{in}, which we rename to $\hat{F}_{in}$ to denote a special case

$$\hat{F}_{in} = \frac{m_f(p_g g_y - Ak)}{p_g g_y A + p_g g_y} + \frac{d(p_g g_y - Ak)}{p_f A}$$

and substitute $A = \frac{G_{in}}{m_g - G_{in}}$ and simplify the compound fractions

$$\hat{F}_{in} = \frac{m_f(p_g g_y(m_g - G_{in}) - G_{in}k)}{p_g g_y G_{in} + (m_g - G_{in})p_g g_y} + \frac{d(p_g g_y(m_g - G_{in}) - kG_{in})}{p_f G_{in}},$$

$$= \frac{m_f p_f G_{in}(p_g g_y(m_g - G_{in}) - G_{in}k) + dm_g p_g g_y(p_g g_y(m_g - G_{in}) - kG_{in})}{m_g p_g g_y p_f G_{in}},$$

$$= \frac{(p_g g_y(m_g - G_{in}) - G_{in}k)(m_f p_f G_{in} + dm_g p_g g_y)}{m_g p_g g_y p_f G_{in}},$$

$$= \frac{(m_g - G_{in})(p_g g_y - Ak)(m_f p_f A + \frac{dm_g p_g g_y}{m_g - G_{in}})}{m_g p_g g_y p_f A}.$$

This clearly requires the two previous conditions $m_g > G_{in}$ and $p_g g_y > Ak$ in order for a biologically relevant value of $\hat{F}_{in}$.

Moreover, we wish to determine a relationship between F_{in} and G_{in}, so we can expand and combine terms to find

$$\hat{F}_{in}(G_{in}) = -\left(\frac{m_f}{m_g} + \frac{km_f}{g_y m_g p_g}\right) G_{in} + \frac{dg_y m_g p_g}{p_f G_{in}} + \left(m_f - \frac{d}{p_f}(g_y p_g + k)\right),$$

which is continuous for all $G_{in} > 0$,

$$\frac{d\hat{F}_{in}}{dG_{in}}(G_{in}) = -\left(\frac{m_f}{m_g} + \frac{km_f}{g_y m_g p_g}\right) - \frac{dg_y m_g p_g}{p_f G_{in}^2} < 0,$$

and

$$\lim_{G_{in}\to 0} = \infty, \quad \lim_{G_{in}\to\infty} = -\infty.$$

Thus there can only be a single possible value $\hat{F}_{in}$ for any G_{in}. Then this unique value of $\hat{F}_{in}(G_{in})$ is positive when

$$p_g g_y - Ak > 0$$

$$p_g g_y(m_g - G_{in}) - kG_{in} > 0$$

$$G_{in} < \frac{p_g g_y}{p_g g_y + k} m_g < m_g.$$

Hence the conditions for $G^* = g_y$ depend on the parameters, and are not always present.

The expression gives us a single parameter on which we define our bifurcation. In other words, if $F_{in} < \hat{F}_{in}$ then we are in case 1, if $F_{in} > \hat{F}_{in}$ then we are in case 2. The result then when $F_{in} = \hat{F}_{in}$, is that $G^* = g_y$ and $f_3(g_y, Y^*) = 0$ for all values of Y^*, hence $\dot{Y}|_{G^*=g_y} = 0$ implies the equilibrium can exist for any $Y^* \geq 0$. The Jacobian matrix for this set of equilibrium is

$$J_{3,1} = \begin{bmatrix} -\frac{m_g(k+F^*p_f)p_g}{(k+F^*p_f+g_y p_g)^2} - \frac{P_f}{C_u}\left(1 - \frac{Y^*}{m_y}\right) & 0 & \frac{g_y m_g p_f p_g}{(k+F^*p_f+g_y p_g)^2} \\ \frac{P_f}{C_u}\left(1 - \frac{Y^*}{m_y}\right) & 0 & 0 \\ \frac{F^* m_f p_f p_g}{(k+F^*p_f+g_y p_g)^2} & 0 & -\frac{m_f p_f(k+g_y p_g)+d(k+F^*p_f+g_y p_g)^2}{(k+F^*p_f+g_y p_g)^2} \end{bmatrix},$$

$$J_{3,2} = \begin{bmatrix} -\frac{m_g(k+F^*p_f)p_g}{(k+F^*p_f+g_y p_g)^2} & 0 & \frac{g_y m_g p_f p_g}{(k+F^*p_f+g_y p_g)^2} \\ 0 & 0 & 0 \\ \frac{F^* m_f p_f p_g}{(k+F^*p_f+g_y p_g)^2} & 0 & -\frac{m_f p_f(k+g_y p_g)+d(k+F^*p_f+g_y p_g)^2}{(k+F^*p_f+g_y p_g)^2} \end{bmatrix},$$

or

$$J_{3,3} = \begin{bmatrix} -\frac{m_g(k+F^*p_f)p_g}{(k+F^*p_f+g_yp_g)^2} - \frac{P_rY^*}{C_l+g_yY^*} & 0 & \frac{g_ym_gp_fp_g}{(k+F^*p_f+g_yp_g)^2} \\ \frac{P_rY^*}{C_l+g_yY^*} & 0 & 0 \\ \frac{F^*m_fp_fp_g}{(k+F^*p_f+g_yp_g)^2} & 0 & -\frac{m_fp_f(k+g_yp_g)+d(k+F^*p_f+g_yp_g)^2}{(k+F^*p_f+g_yp_g)^2} \end{bmatrix},$$

depending on if we consider the linearization of the system above $G^* = g_y$ when $Y^* < m_y$ (3,1), when $Y^* \geq m_y$ (3,2), or the linearization of the system below $G^* = g_y$ (3,3). For simplicity of notation, we will replace the elements in the Jacobian matrices with j_i, $i = 1, 2, \ldots, 9$ where the i^{th} element is counted across from left to right, top to bottom. Specifically we will use

$$J_{3,\{1,2\}} = \begin{bmatrix} j_1 & 0 & j_3 \\ j_4 & 0 & 0 \\ j_7 & 0 & j_9 \end{bmatrix}.$$

Then the characteristic equation is $\lambda(\lambda^2 - (j_1 + j_9)\lambda + j_1j_9 - j_3j_7) = 0$. So we have a trivial eigenvalue $\lambda_2 = 0$, and the other two eigenvalues (λ_1, λ_3) are solutions to a quadratic expression. Hence, we can expect $\lambda_1, \lambda_3 < 0$ if $j_1 + j_9 < 0$ and $j_1j_9 - j_3j_7 > 0$. Note that the biologically feasible solution space limits $Y \in [0, m_y]$, where m_y is the maximum glycogen storage concentration. Additionally, the forward semi-flow for Y is bounded above by m_y for any $0 \leq Y(t_0) \leq m_y$, so any scenario in which $Y^* > m_y$ will be henceforth neglected.

Immediately, we see $j_1+j_9 < 0$ when $Y^* < m_y$ for Jacobian (3,1), and it is trivially negative for (3,2) and (3,3). The second necessary condition after some simplification is

$$(J_{3,1}): \; j_1j_9 - j_3j_7 = \frac{\left(m_g(k+F^*p_f)p_g + m_fp_fg_yp_g\frac{P_f}{C_u}\left(1-\frac{Y^*}{m_y}\right)\right)(m_fp_fk + d(k+F^*p_f+g_yp_g)^2)}{(k+F^*p_f+g_yp_g)^4} > 0,$$

$$(J_{3,2}): \; j_1j_9 - j_3j_7 = \frac{m_gp_g(k+F^*p_f)(m_fp_fk + d(k+F^*p_f+g_yp_g)^2)}{(k+F^*p_f+g_yp_g)^4} > 0,$$

or

$$(J_{3,3}):\ j_1 j_9 - j_3 j_7 = \frac{\left(m_g(k+F^*p_f)p_g + m_f p_f g_y p_g \frac{P_r Y^*}{C_l + g_y Y^*}\right)(m_f p_f k + d(k+F^*p_f+g_y p_g)^2)}{(k+F^*p_f+g_y p_g)^4} > 0,$$

which holds in all three cases.

Hence, we have $\lambda_1 < 0$, $\lambda_2 = 0$, and $\lambda_3 < 0$. The following analysis is conducted to determine what happens near the critical line $(g_y, Y, \frac{p_g g_y - Ak}{p_f A})$

For ease of handling, the system is non-dimensionalized so we can reduce the number of parameters from 14 to 10. Additionally, we will redefine the system as $\dot{X} = F_i(X; P; h(X))$ where $X = (g, y, f)^\top$, $i = 1$ when $h(X) \geq 0$, $i = 2$ when $h(X) < 0$, and P is our set of parameters as defined in table (4.1).

Table 4.1: Non-dimensionalized Variable and Parameter Substitutions

Parameter	a	b	ρ	m	δ	γ	ξ_1	ξ_2	ζ_1	ζ_2
Substitution	$\frac{G_{in}k}{m_g p_g g_y}$	$\frac{F_{in}p_f}{m_g p_g}$	$\frac{p_g g_y}{k}$	$\frac{m_f p_f}{m_g p_g}$	$\frac{kd}{m_g p_g}$	$\frac{g_y}{m_y}$	$\frac{P_f k}{m_g p_g g_y}$	$\frac{P_r k}{m_g p_g g_y}$	$\frac{C_u}{g_y}$	$\frac{C_l}{g_y m_y}$

$g = \frac{G}{g_y}$	$y = \frac{Y}{m_y}$	$f = \frac{Fp_f}{k}$	$\tau = \frac{t m_g p_g}{k}$

Define

$$h(X) = g - 1$$

Then we have the system

$$\begin{pmatrix} \dot{g} \\ \dot{y} \\ \dot{f} \end{pmatrix} = \begin{cases} F_1 = \begin{pmatrix} a - \frac{g}{1+\rho g+f} - \xi_1 \frac{(g-1)(1-y)}{\zeta_1+g-1} \\ \gamma\xi_1 \frac{(g-1)(1-y)}{\zeta_1+g-1} \\ b - \frac{mf}{1+\rho g+f} - \delta f \end{pmatrix}, & g \geq 1 \\ F_2 = \begin{pmatrix} a - \frac{g}{1+\rho g+f} - \xi_2 \frac{y(g-1)}{\zeta_2+y} \\ \gamma\xi_2 \frac{y(g-1)}{\zeta_2+y} \\ b - \frac{mf}{1+\rho g+f} - \delta f \end{pmatrix}, & g < 1 \end{cases}$$

Hence, the switching manifold is the plane on which $g = 1$.

Notice that $\dot{y} = \gamma f_3$, where $\gamma = g_y/m_g$. This indicates biologically that $\gamma << 1$ since the maximum storage capacity of glycogen in a cell is of much higher magnitude compared to the ideal concentration of active glucose. Hence y changes at a slower pace than g or f. Let the subsystem $(g, f)^\top$ be the fast dynamics, and y the slow dynamics. Then we consider the dynamics of the fast system and slow system separately. Then the linearization for $(g, f)^\top$ gives two negative eigenvalues when $g^* = 1$. Hence the fast system has an asymptotically stable equilibrium. Let $X^* = (g^*, f^*)^\top$ be the equilibrium for the fast system. By the stable manifold theorem (theorem 9.4 in (Teschl, 2012)) there is a neighborhood of X^* such that the flow described by $g(t)$ can be described with $|g(t) - 1| \leq Ce^{-\alpha t}$, where $\alpha < \min\{|\Re(\lambda)||\lambda$ is an eigenvalue of $J, \Re(\lambda) \neq 0\}$, where J is the Jacobian, and $C > 0$ depends on the choice of α.

Suppose $g_0 > 1$. Then we can approximate the flow $g(t) = 1 + (g_0 - 1)e^{-\alpha t}$, where α is chosen as above, and assume that this approximation chooses α such that $C > g_0 - 1 > 0$. Let $y(0) = y_0 \in (0, 1)$. Then we substitute

$$\dot{y} = \gamma\xi_1 \frac{(g_0 - 1)e^{-\alpha t}(1 - y)}{\zeta_1 + (g_0 - 1)e^{-\alpha t}}$$

and integrate,

$$\int \frac{dy}{1-y} = -\gamma\xi_1 \int \frac{(g_0-1)e^{-\alpha t}dt}{\zeta_1 + (g_0-1)e^{-\alpha t}}$$

letting $q = \frac{\gamma\xi_1}{\alpha}$, we get

$$-\ln|1-y| = -q\ln\left|\zeta_1 + (g_0-1)e^{-\alpha t}\right| - C_1$$

rearrange to find

$$C_1 = \ln\left|\frac{1-y}{(\zeta_1 + (g_0-1)e^{-\alpha t})^q}\right|$$

and letting $C = e^{C_1}$, we find by setting $y(0) = y_0$

$$C = \frac{1-y_0}{(\zeta_1 + g_0 - 1)^q}.$$

Hence we have

$$y(t) = 1 - (1-y_0)\left(\frac{\zeta_1 + (g_0-1)e^{-\alpha t}}{\zeta_1 + g_0 - 1}\right)^q. \tag{4.5}$$

Then the final long term behavior of $y(t)$ as $t \to \infty$ indicates that

$$y^* = \lim_{t\to\infty} y(t) = 1 - (1-y_0)\left(\frac{\zeta_1}{\zeta_1 + g_0 - 1}\right)^q.$$

Hence y increases monotonically near the critical line, and the equilibrium value gets closer to 1 the closer y_0 is to 1 or the farther g_0 is from 1. If $y_0 = 1$ then $y(t) = 1$ and $y^* = 1$. If $g_0 = 1$, then $y(t) = y_0$ and $y^* = y_0$, hence if $y_0 = 0$, then we have $y^* = 0$. Choose $y^* \in (0,1)$ and $y_0 \in (0,1)$ Then we can choose g_0 such that

$$g_0 = \zeta_1\left[\left(\frac{1-y_0}{1-y^*}\right)^{1/q} - 1\right] + 1 \geq 1.$$

Since y^* was chosen arbitrarily, any point on the critical line is a potential equilibrium for y when $g_0 \geq 1$.

Similarly, suppose that $g_0 < 1$, then we have the approximation $g(t) = 1 - (1 - g_0)e^{-\alpha t}$. Substituting gives us

$$\dot{y} = -\gamma\xi_2 \frac{y(1-g_o)e^{-\alpha t}}{\zeta_2 + y}$$

and dividing both sides by the terms with y separates the equation to become

$$\dot{y}\frac{\zeta_2 + y}{y} = -\gamma\xi_2(1-g_0)e^{-\alpha t}$$

which we can integrate with respect to time to give

$$\zeta_2 \ln|y| + y = \frac{\gamma\xi_2}{\alpha}(1-g_0)e^{-\alpha t} + C_1.$$

Combine and exponentiate each side letting $C_2 = e^{C_1}$

$$y^{\zeta_2}e^{y} = C_2 e^{\frac{\gamma\xi_2(1-g_0)}{\alpha}e^{-\alpha t}}.$$

Then, we can take the ζ_2 root of both sides and divide both sides by the same to obtain

$$\frac{y}{\zeta_2}e^{y/\zeta_2} = Ce^{\frac{\gamma\xi_2(1-g_0)}{\zeta_2\alpha}e^{-\alpha t}}$$

where $C = C_2^{1/\zeta_2}/\zeta_2$. Here we set $t = 0$ to find

$$C = \frac{y_0}{\zeta_2}e^{y_0/\zeta_2 - \frac{\gamma\xi_2(1-g_0)}{\zeta_2\alpha}}$$

Finally, we can invoke the Lambert-W function to simplify this to

$$y(t) = \zeta_2 W\left(\frac{y_0}{\zeta_2}\exp\left[\frac{y_0}{\zeta_2} + \frac{\gamma\xi_2(1-g_0)}{\zeta_2\alpha}(e^{-\alpha t} - 1)\right]\right). \tag{4.6}$$

This approximation has time derivative

$$y'(t) = -\frac{\gamma\xi_2(1-g_0)e^{-\alpha t}W(\cdot)}{1 + W(\cdot)} < 0$$

Hence $y(t)$ is decreasing monotonically. Taking $t \to \infty$ we find

$$y^* = \lim_{t\to\infty} y(t) = \zeta_2 W\left(\frac{y_0}{\zeta_2}\exp\left[\frac{y_0}{\zeta_2} - \frac{\gamma\xi_2(1-g_0)}{\zeta_2\alpha}\right]\right) = \zeta_2 W(C).$$

Since $C \geq 0$ for all $y_0 \in [0,1], g_0 \in [0,1)$ and $W(C)$ is monotone increasing with $C \geq 0$, the dynamics of y^* can be determined by the dynamics of C. Then we need to know how C varies for different values of y_0 and g_0.

$$\frac{\partial C}{\partial y_0} = \frac{e^{y_0/\zeta_2 - \frac{\gamma\xi_2(1-g_0)}{\zeta_2\alpha}}}{\zeta_2} + \frac{y_0}{\zeta_2^2} e^{y_0/\zeta_2 - \frac{\gamma\xi_2(1-g_0)}{\zeta_2\alpha}} > 0$$

$$\frac{\partial C}{\partial g_0} = \frac{y_0\gamma\xi_2}{\alpha\zeta_2^2} e^{y_0/\zeta_2 - \frac{\gamma\xi_2(1-g_0)}{\zeta_2\alpha}} > 0$$

Hence larger values of y_0 give larger values of y^* and the further g_0 is to the equilibrium $g^* = 1$, the smaller y^* is. Additionally, $W(0) = 0$, so $y^* = 0$ if $C = 0$, which happens precisely when $y_0 = 0$ To check consistency, we determine when $y^* = 1$, or more concisely when

$$W(C) = \frac{1}{\zeta_2}.$$

This, of course, occurs when

$$\frac{1}{\zeta_2} e^{1/\zeta_2} = C = \frac{y_0}{\zeta_2} e^{y_0/\zeta_2 - \frac{\gamma\xi_2(1-g_0)}{\zeta_2\alpha}}$$

hence when $y_0 = 1$ and $g_0 = 1$, as expected.

Finally, suppose that $g_0 \geq 1$ and $y_0 \geq 1$. Then $\dot{y} = 0$ and $y(t) = y_0$. Therefore, depending on the initial conditions, we can obtain any $y^* > 0$ when $g^* = 1$, so the entire critical line is a set of equilibria. □

Numerical Results for the No-DAG System

Since the approximations determined for the degenerate case above are based on theoretical results, it is important to determine how well they match the calculated trajectories for the full system. Parameters in this section are not based on the numerical results determined in the short term model as the focus is on representing a

Figure 4.1: Normal Case: Time Series Plots for System (4.2)

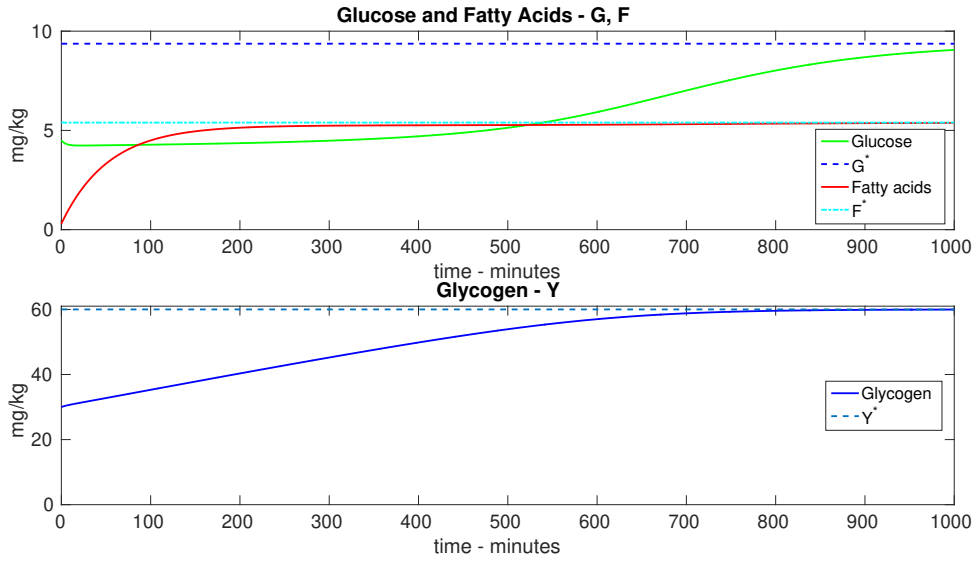

(a)

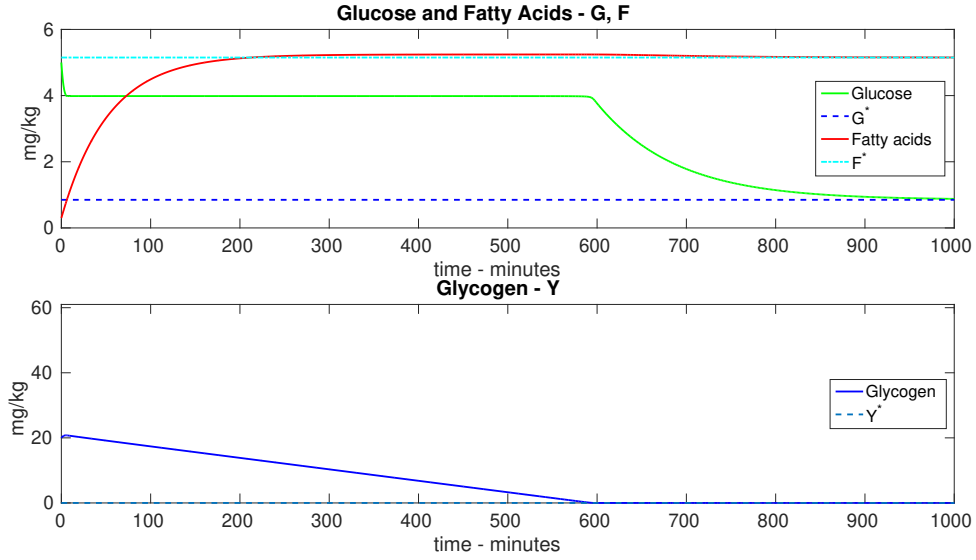

(b)

clear picture of the model dynamics and not on demonstrating an ability to match data.

In the cases where the equilibria does not lie on the switching manifold, the system dynamics evolve as expected (Fig. 4.1). Notice that when glucose infusion (G_{in}) is excessive, the glucose is stored as glycogen and cellular levels of glucose remain around the ideal concentration (g_y, 4 in this case). Additionally, in Fig. 4.1 (b), when the glucose infusion is insufficient, glycogen in depleted in order to maintain cellular glucose at ideal concentrations. Only after glycogen has been filled or depleted do cellular levels of glucose rise or decline and approach equilibrium. Hence this system exhibits the expected response in which glycogen storage buffers the glucose concentration and acts to maintain ideal concentrations of glucose in the cell.

Figure 4.2: 3D Phase Portraits

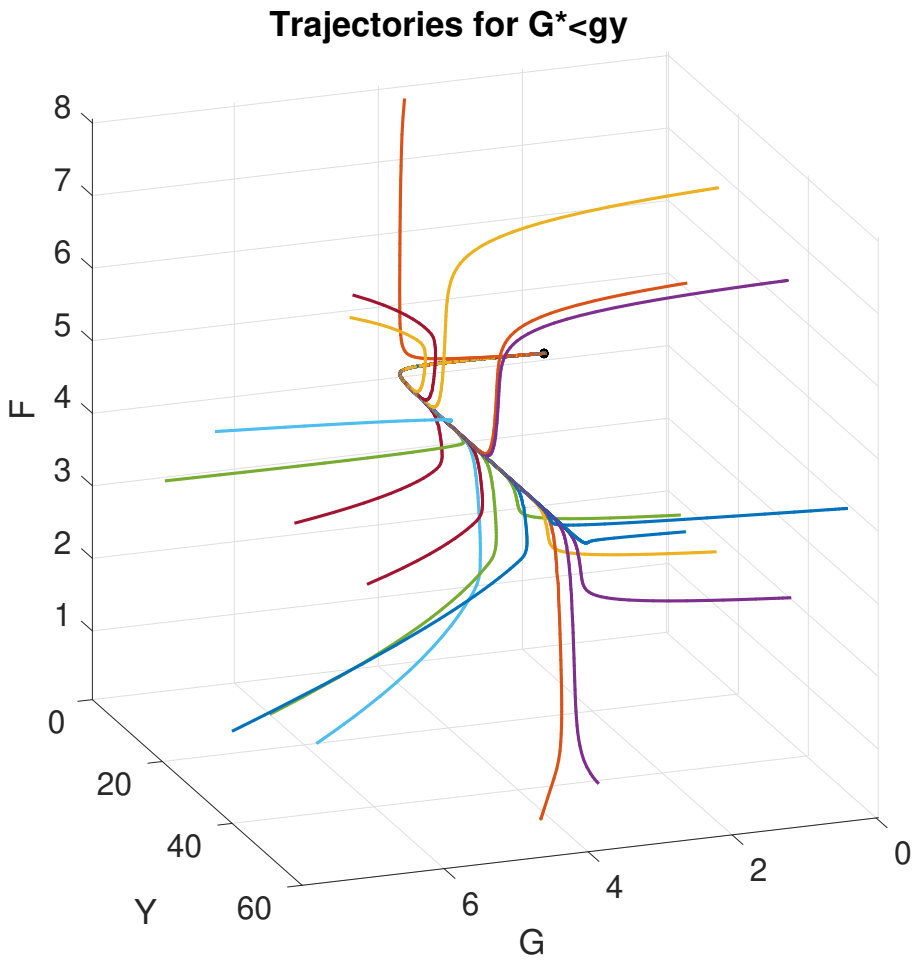

(a)

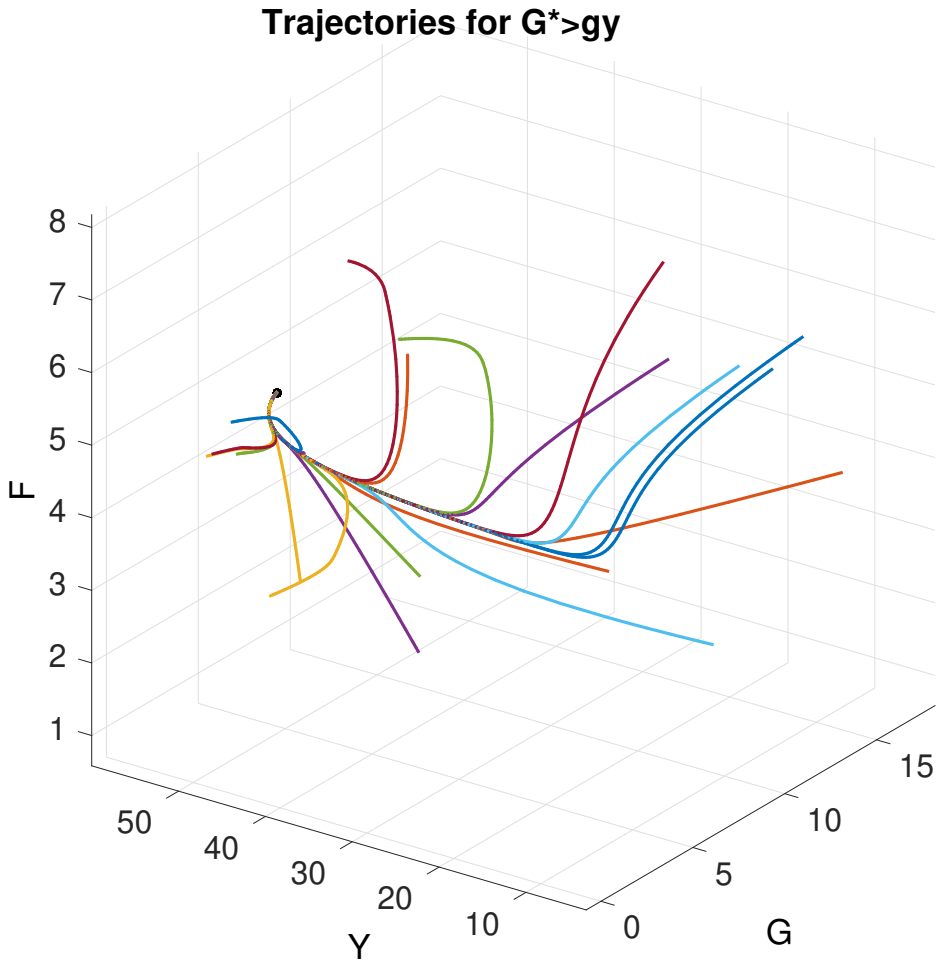

(b)

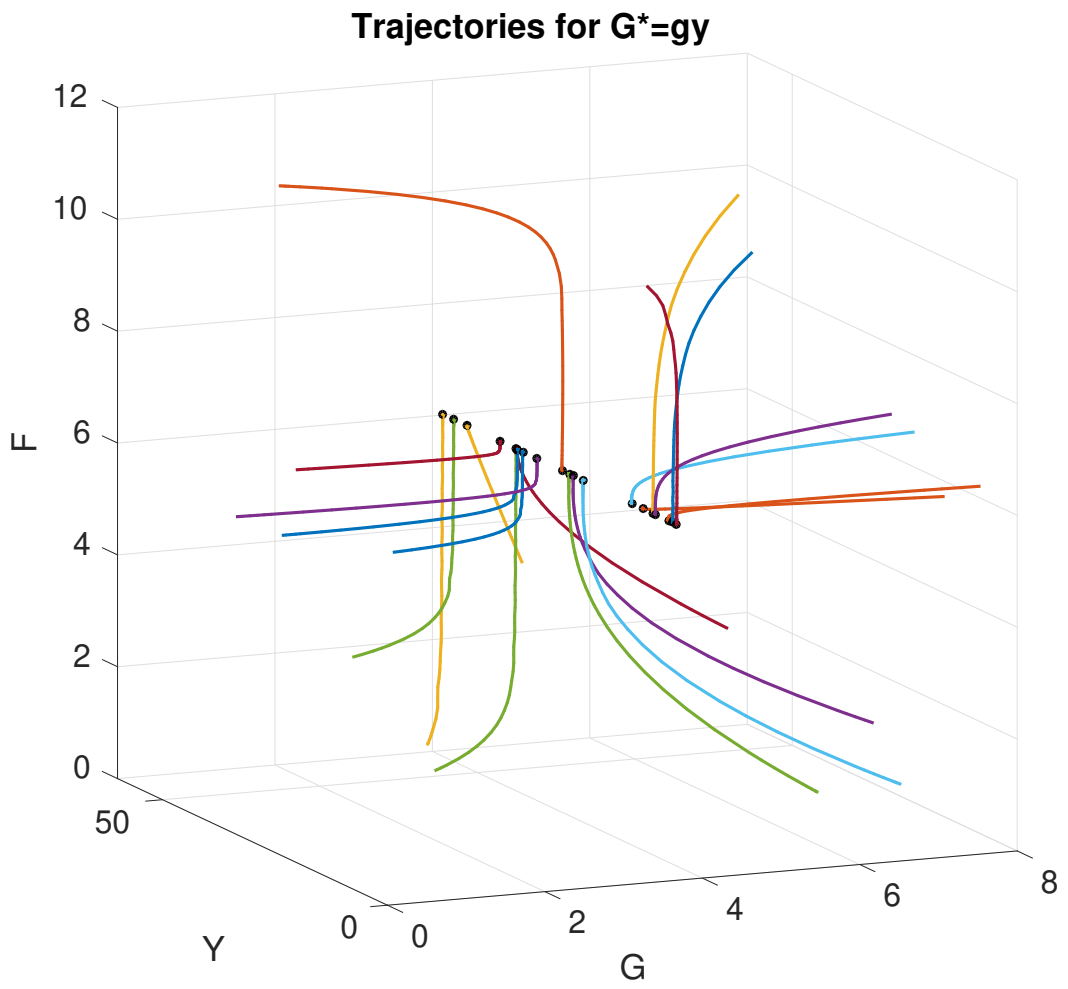

(c)

For each simulation in Fig. 4.2, random initial conditions are selected and the simulations are run until equilibrium. The dynamics of the system when $G^* < g_y$ or $G^* > g_y$ seem to converge onto a stable manifold and move along it toward the equilibrium point (Fig. 4.2 (a),(b)). However, the degenerate case simulations in Fig. 4.2 (c) shows the point at which this stable manifold lies wholly in the switching manifold, and trajectories approach and stick to it tangentially.

The system bifurcates when the levels of glucose infusion and fatty acid infusion

Figure 4.3: Bifurcation Conditions

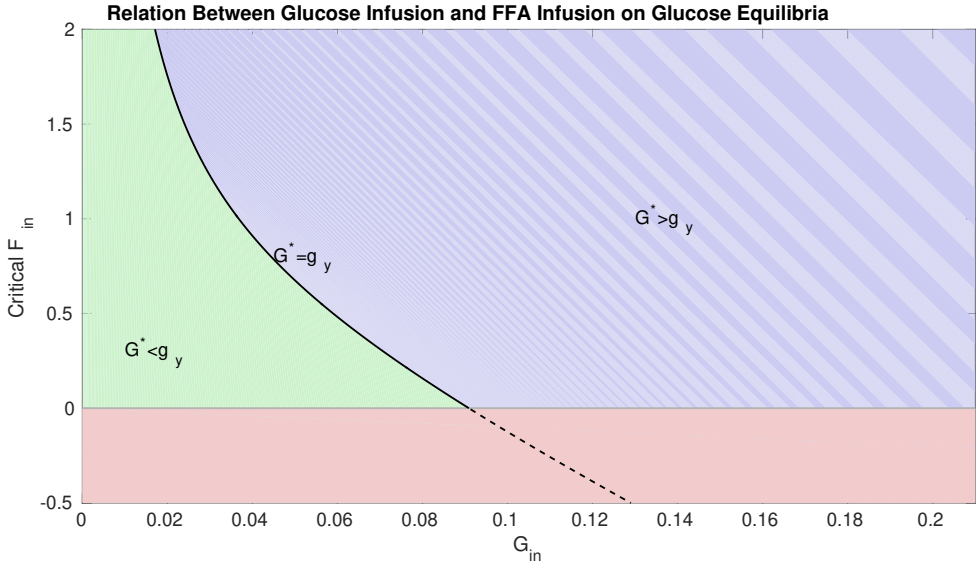

(a)

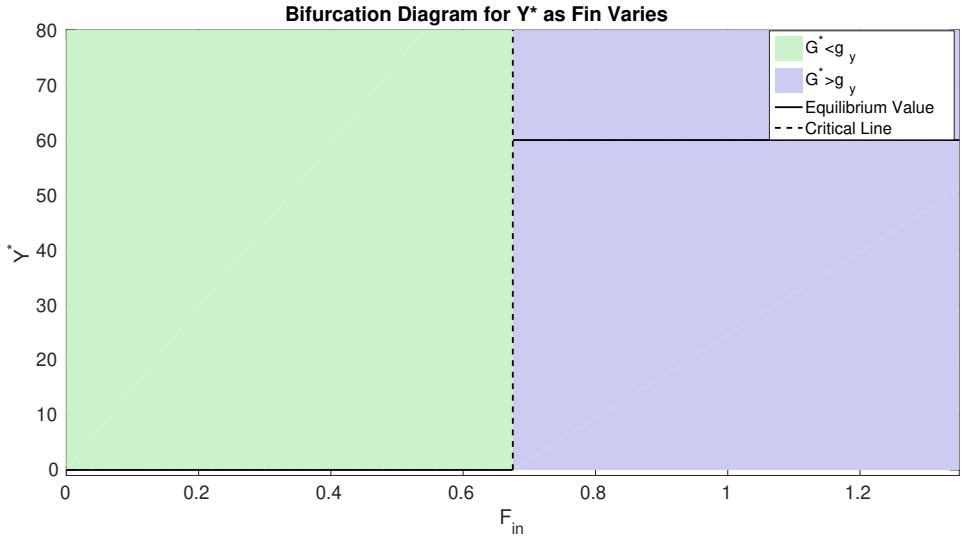

(b)

cross a threshold (Fig. 4.3 (a)). When the level of glucose infusion rises, the bifurcation point for fatty acid infusion becomes closer to 0. This indicates that higher

carbohydrate consumption or endogenous glucose production will induce a high glycogen equilibrium. Since fatty acids compete with glucose for metabolism, if fatty acid infusion is high enough then the system can equilibrate at the high glycogen equilibrium even for a lower rate of glucose infusion. The bifurcation point (Fig. 4.3 (b)) as fatty acid infusion increases for some fixed glucose infusion produces a critical line of equilibria for glycogen. As stated in the previous section, this condition is exactly when $F_{in} = \hat{F}_{in}$. Only along this critical line can we achieve values for Y^* that are not either empty ($Y^* = 0$) or full ($Y^* = m_y$).

This critical line is the degenerate case where $G^* = g_y$. Notably, in the degenerate case, Fig. 4.2 (c) demonstrates that solutions stick to the critical line and do not drift toward either $Y = 0$ or $Y = m_y$. Additionally, trajectories that begin with $G > g_y$ close below the plane $Y = m_y$ approach but never reach m_y. This behavior is predicted by (4.5), which further suggests that only trajectories that begin on $Y = m_y$ ever reach the equilibrium value $Y^* = m_y$ in the degenerate case.

The time evolution of the trajectories can be seen in Fig. 4.5 with initial glucose concentrations below (a) and above (b) the critical line. Notice that the fast-slow estimates for G and Y match closely with the simulated trajectories, but the approximation above (Eqn. 4.5) is more sensitive to deviations of G_0 from the critical line. Figure 4.4 gives a closer inspection of the error induced by the distance between G_0 and g_y, where it can be seen that a small deviation above g_y (a) causes as much error as larger deviations below g_y (b). However, the main result that various initial values for G_0 yield to different equilibria (Y^*) is supported, and the estimations match closely to the numerical simulations.

Figure 4.4: Degenerate Case: Fast-Slow Estimation Error

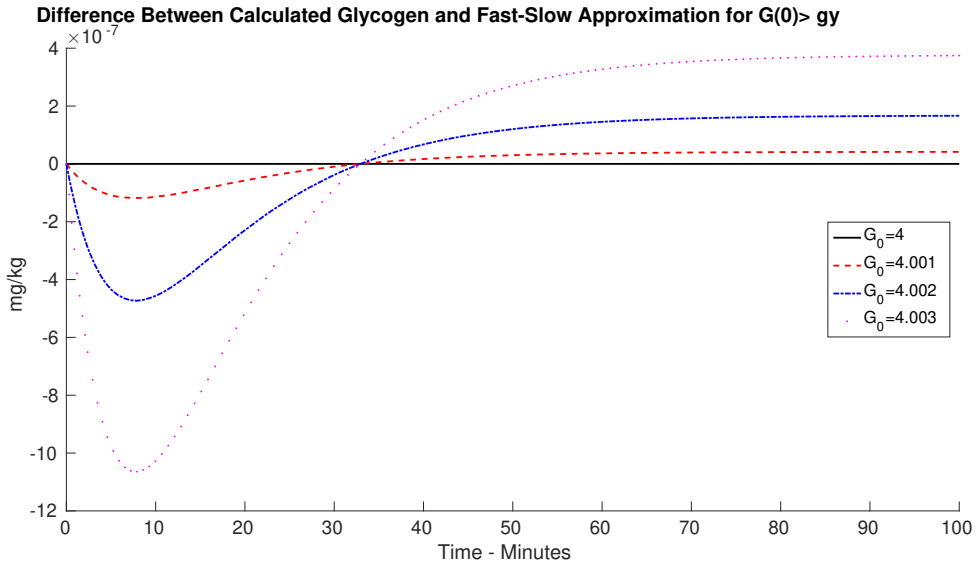

(a)

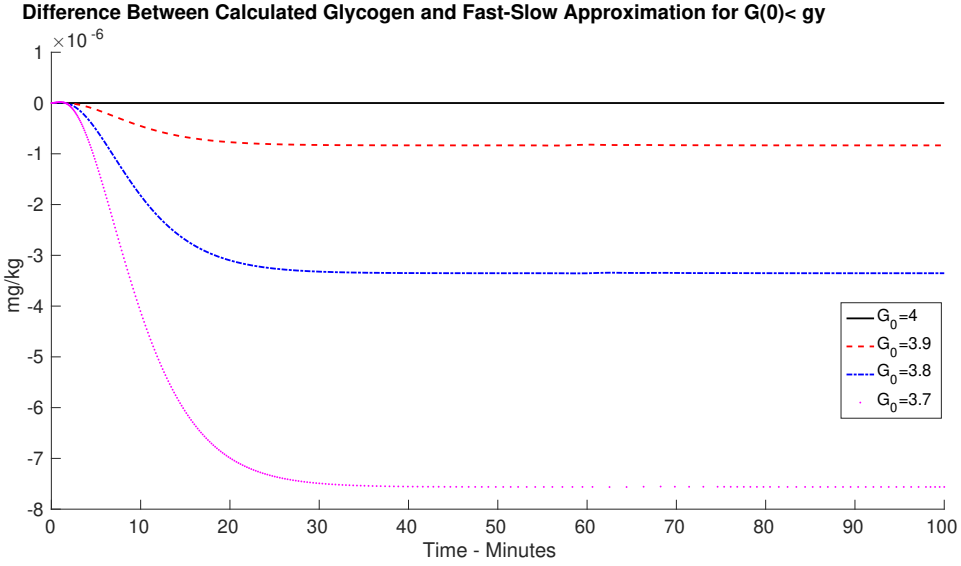

(b)

Figure 4.5: Degenerate Case: Time Series with Fast-Slow Estimation

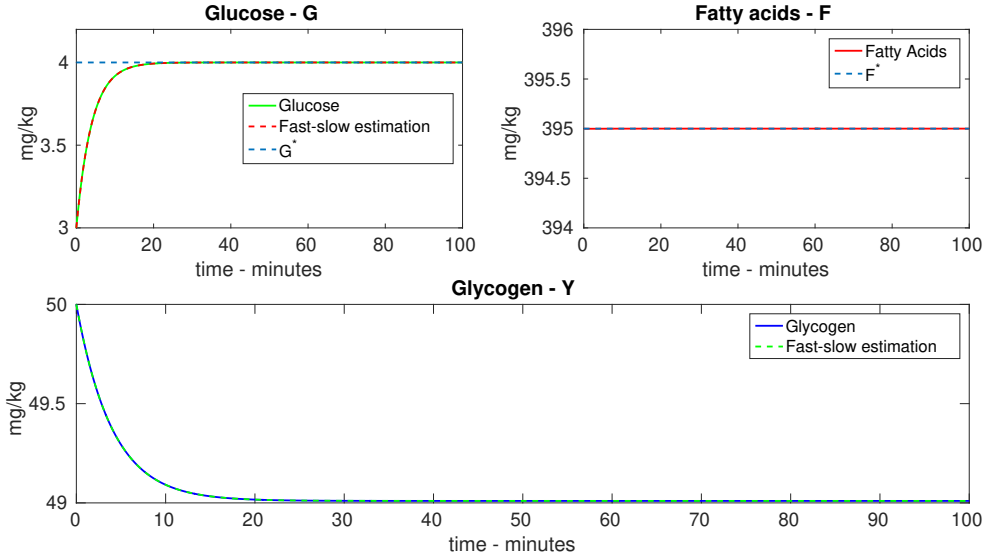

(a)

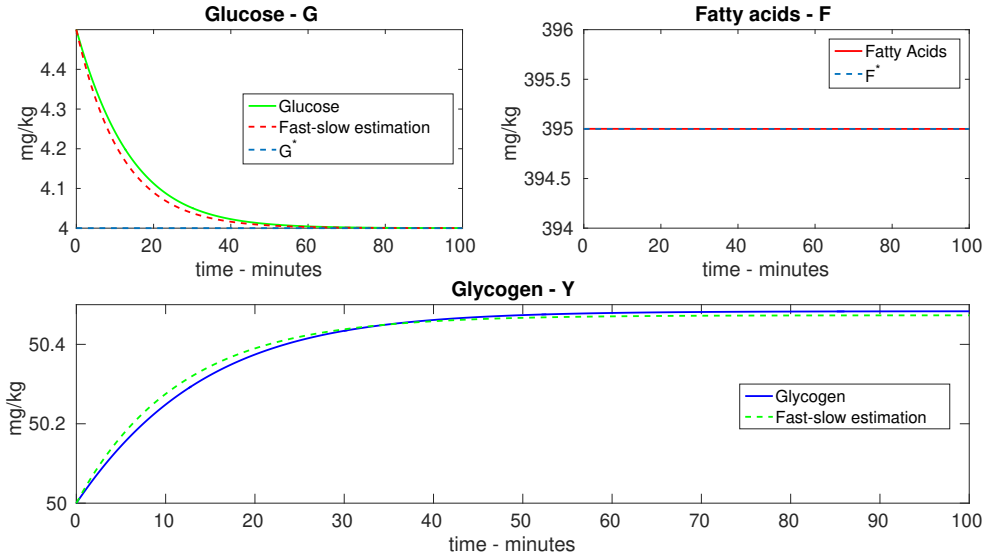

(b)

4.0.4 Insulin Resistant Patient - Including DAG

The case we really wish to study is the one with insulin resistance mediated by DAG accumulation. The previous simple case considered only a healthy individual without excessive myocellular DAG concentration, on this we reintroduce the diminished G_{in} flux via the equation $f_5(D)$. The system we examine (4.7) is 4-dimensional and retains many of the features of the healthy case.

$$\begin{aligned}
\dot{G} &= \frac{nG_{in}}{n+D} - \frac{m_g p_g G}{k + p_g G + p_f F} - \begin{cases} \frac{P_f(G-g_y)\left(1-\frac{Y}{m_y}\right)}{C_u+(G-g_y)}, & G \geq g_y, Y < m_y \\ 0, & G \geq g_y, Y \geq m_y \\ \frac{P_r Y(G-g_y)}{C_l+g_y Y}, & G < g_y \end{cases} \\
\dot{Y} &= \begin{cases} \frac{P_f(G-g_y)\left(1-\frac{Y}{m_y}\right)}{C_u+(G-g_y)}, & G \geq g_y, Y < m_y \\ 0, & G \geq g_y, Y \geq m_y \\ \frac{P_r Y(G-g_y)}{C_l+g_y Y}, & G < g_y \end{cases} \\
\dot{F} &= F_{in} - \frac{m_f p_f F}{k + p_g G + p_f F} - dF \\
\dot{D} &= cdF - \mu D
\end{aligned} \tag{4.7}$$

Theorem 6 *If $m_g > G_{in}$ then system (4.7) has a unique equilibrium, (G^*, Y^*, F^*), given by*

$$\begin{aligned}
G^* &= \frac{\bar{A}}{p_g}(k + p_f F^*), \\
D^* &= \frac{cd}{\mu} F^*, \\
\bar{A} &= \frac{G_{in}}{m_g - G_{in} + \frac{m_g cd}{n\mu} F^*}.
\end{aligned}$$

for a unique $F^* > 0$.

$$\textbf{\textit{Case 1:}} \quad G^* < g_y, \quad Y^* = 0$$

$$\textbf{\textit{Case 2:}} \quad G^* > g_y, \quad Y^* = m_y$$

$$\textbf{\textit{Case 3:}} \quad G^* = g_y, \quad Y^* \in [0, \infty)$$

This system has a discontinuous bifurcation at $G^* = g_y$.

Proof:

Case 1: $G^* < g_y$

To begin, we set $f_3 = 0$ and find that

$$Y^* = 0.$$

Then we look to solve for G^* in $\dot{G}|_{Y=0} = 0$,

$$\dot{G}|_{Y=0} = \frac{nG_{in}}{n + D^*} - \frac{m_g p_g G^*}{k + p_g G^* + p_f F^*} = 0.$$

Multiply both sides by the denominator on the second term, which can never be 0,

$$\frac{nG_{in}}{n + D^*}(k + p_g G^* + p_f F^*) - m_g p_g G^* = 0,$$

then collect terms on G^* and move to the RHS

$$\frac{nG_{in}(k + p_f F^*)}{n + D^*} = p_g \left(m_g - \frac{nG_{in}}{n + D^*} \right) G^*$$

and divide by the coefficient of G^* to isolate

$$G^* = \frac{\bar{A}}{p_g}(k + p_f F^*)$$

$$\bar{A} = \frac{\frac{nG_{in}}{n+D^*}}{m_g - \frac{nG_{in}}{n+D^*}} = \frac{G_{in}}{m_g - G_{in} + \frac{m_g}{n} D^*}.$$

In order to solve for F^*, we must first determine D^*, which is simply

$$D^* = \frac{cd}{\mu}F^*.$$

Then we plug in G^* and D^* to $\dot{F}^* = 0$

$$\dot{F} = F_{in} - \frac{m_f p_f F^*}{k + \frac{G_{in}}{m_g - G_{in} + \frac{m_g cd}{n\mu}F^*}(k + p_f F^*) + p_f F^*} - dF^* = 0.$$

Simplify the compound fraction

$$F_{in} - \frac{m_f p_f (m_g - G_{in} + \frac{m_g cd}{n\mu}F^*)F^*}{k(m_g - G_{in} + \frac{m_g cd}{n\mu}F^*) + G_{in}(k + p_f F^*) + p_f F^*(m_g - G_{in} + \frac{m_g cd}{n\mu}F^*)} - dF^* = 0,$$

and collect common terms on the denominator

$$F_{in} - \frac{m_f p_f (m_g - G_{in} + \frac{m_g cd}{n\mu}F^*)F^*}{m_g(k + p_f F^*)(1 + \frac{cd}{n\mu}F^*)} - dF^* = 0.$$

Next we multiply both sides by the denominator on the second term, which is never 0 valued,

$$m_g F_{in}(k+p_f F^*)(1+\frac{cd}{n\mu}F^*) - m_f p_f (m_g - G_{in} + \frac{m_g cd}{n\mu}F^*)F^* - dm_g(k+p_f F^*)(1+\frac{cd}{n\mu}F^*)F^* = 0$$

and expand, collecting common terms on powers of F^*, and for sake of clarity, multiply the equation by -1 to obtain,

$$\frac{cd^2 m_g p_f}{n\mu}F^{*3} + m_g\left(\frac{cd}{n\mu}\Theta + dp_f\right)F^{*2} + \left(m_g\Theta - \frac{cdkm_g F_{in}}{n\mu} - m_f p_f G_{in}\right)F^* - km_g F_{in}, \tag{4.8}$$

$$\Theta = p_f(m_f - F_{in}) + dk.$$

This cubic polynomial guarantees us at least one positive equilibria because the leading coefficient is positive and the constant is negative, so it must cross the positive axis. We consider two cases: $\Theta > 0$ and $\Theta < 0$ in search for additional possible equilibria.

If we assume $\Theta > 0$, then

$$F_{in} < m_f + \frac{dk}{m_f}$$

and the second order coefficient is positive. Then the first order coefficient

$$m_g\Theta - \frac{cdkm_gF_{in}}{n\mu} - m_f p_f G_{in}$$

could be positive or negative depending on parameter choices, however either case provides a single change in sign. Then Descartes' rule of sign still suggests a single real positive equilibrium.

Suppose then that $\Theta < 0$. Then the first order coefficient is negative and the sign of the second order coefficient does not affect the number of sign changes. Hence, this situation still yields a single real positive equilibrium. Therefore this cubic polynomial always presents a single positive equilibrium, which we will call F^*. The solution of the polynomial is excluded as it too cumbersome to be useful.

Case 2: $G^* > g_y$

In this case, we first solve for $f_3 = 0$ and find that $Y^* = m_y$. Upon substitution into the other equations, the system is identical to that of case 1. Hence we again have

$$G^* = \frac{\bar{A}}{p_g}(k + p_f F^*)$$

$$D^* = \frac{cdF^*}{\mu}$$

$$\bar{A} = \frac{G_{in}}{m_g - G_{in} + \frac{m_g}{n}D^*}$$

where F^* is the positive solution to the cubic expression in equation (4.8).

Case 3: $G^* = g_y$

Given $G^* = g_y$, then $\dot{Y} = 0$ is automatic and independent of the value of Y^*. Hence, when this equilibrium exists, Y^* can be any non-negative value. We have $D^* = \frac{cdF^*}{\mu}$ and substituting $G^* = g_y$ we get

$$G^* = \frac{G_{in}}{p_g(m_g - G_{in} + \frac{cdm_g}{n\mu}F^*)}(k + p_f F^*) = g_y,$$

then

$$G_{in}(k + p_f F^*) = g_y p_g (m_g - G_{in} + \frac{cdm_g}{n\mu}F^*),$$

and solving for F^* yields

$$F^*(p_f G_{in} - \frac{cdg_y m_g p_g}{n\mu}) = g_y p_g (m_g - G_{in}) - kG_{in},$$

then divide

$$F^* = \frac{g_y p_g - k\frac{G_{in}}{m_g - G_{in}}}{p_f \frac{G_{in}}{m_g - G_{in}} - \frac{cdg_y m_g p_g}{n\mu(m_g - G_{in})}},$$

and substituting $A = \frac{G_{in}}{m_g - G_{in}}$,

$$F^* = \frac{g_y p_g - Ak}{p_f A - \frac{cdg_y m_g p_g}{n\mu(m_g - G_{in})}}.$$

Notice that this degenerate case has an additional restriction in addition to those imposed for system (4.2),

$$p_f A > \frac{cdg_y m_g p_g}{n\mu(m_g - G_{in})}$$

or

$$G_{in} > \frac{cd}{n\mu} \cdot \frac{g_y p_g}{p_f} m_g$$

and combined with the necessary condition for the positivity of the numerator

$$\frac{p_g g_y}{p_g g_y + k} m_g > G_{in} > \frac{cd}{n\mu} \cdot \frac{g_y p_g}{p_f} m_g,$$

implies that the degenerate case can only exist if

$$\frac{1}{p_g g_y + k} > \frac{cd}{n\mu}\frac{1}{p_f}$$

which can be interpreted as

$$p_f > \frac{cd}{n\mu}(k + p_g g_y)$$

implying that the proportion of fatty acids available for metabolism has to be sufficiently large. Biologically, the implication is that cellular glucose levels can remain at ideal levels only if the proportion of fatty acids available for oxidations is greater than the average production and lifespan of DAG times the half-maximal metabolism rate of fatty acids at glucose equilibrium, reduced by the half saturation constant for DAG mediated insulin resistance. In other words, the proportion of fatty acids available for metabolism must be greater than the magnitude of effect DAG has on reducing glucose infusion times the concentration of fatty acids necessary for half maximal oxidation.

If fatty acid metabolism saturates quickly (i.e. $k + p_g g_y$ is small), if the half saturation of DAG-induced IR is large (i.e. n is large), or if the production and lifespan of DAG is small (i.e. $\frac{cd}{\mu}$ small) then the glucose equilibrium can remain at ideal levels. This indicates that individuals with efficient fatty acid metabolism or low rates of DAG production can easily find conditions to maintain glucose at ideal cellular concentrations.

Suppose that these conditions are met, we can substitute the conditions into $\dot{F}$ and determine the rate of fatty acid infusion (F_{in}) required to achieve this equilibrium. Call this particular critical value $\bar{F}_{in}$.

$$\dot{F} = \bar{F}_{in} - \frac{m_f p_f \frac{g_y p_g - Ak}{p_f A - \frac{cdg_y m_g p_g}{n\mu(m_g - G_{in})}}}{k + p_g g_y + p_f \frac{g_y p_g - Ak}{p_f A - \frac{cdg_y m_g p_g}{n\mu(m_g - G_{in})}}} - d\frac{g_y p_g - Ak}{p_f A - \frac{cdg_y m_g p_g}{n\mu(m_g - G_{in})}} = 0$$

which can be rearranged to

$$\bar{F}_{in} = \frac{(m_g - G_{in})(p_g g_y - Ak)\left(m_f p_f \left(p_f A - \frac{cdg_y m_g p_g}{n\mu(m_g - G_{in})}\right) + \frac{dg_y m_g p_g}{m_g - G_{in}}\left(p_f - \frac{cd}{n\mu}(k + g_y p_g)\right)\right)}{m_g p_g g_y (p_f A - \frac{cdg_y m_g p_g}{n\mu(m_g - G_{in})})(p_f - \frac{cd}{n\mu}(k + g_y p_g))}.$$

Notice that $\bar{F}_{in}$ is positive if the conditions for $F^* > 0$ are met for $G^* = g_y$. Then $G^* = g_y$ when $F_{in} = \bar{F}_{in}$. □

Suppose we take $c = 0$, then

$$\bar{F}_{in} = \frac{(m_g - G_{in})(p_g g_y - Ak)\left(m_f p_f\,(p_f A) + \frac{dg_y m_g p_g}{m_g - G_{in}}\,(p_f)\right)}{m_g p_g g_y (p_f A)(p_f)}.$$

$$= \frac{(m_g - G_{in})(p_g g_y - Ak)(m_f p_f A + \frac{dm_g p_g g_y}{m_g - G_{in}})}{m_g p_g g_y p_f A} = \hat{F}_{in}$$

So the critical value $\bar{F}_{in}$ agrees with $\hat{F}_{in}$ when the production of DAG (c) is removed. Then

$$\frac{\partial}{\partial c}\bar{F}_{in} = \frac{(m_g - G_{in})(p_g g_y - Ak)}{g_y m_g p_g \left(p_f A - \frac{cdg_y m_g p_g}{n\mu(m_g - G_{in})}\right)^2 \left(p_f - \frac{cd}{n\mu}(k + g_y p_g)\right)^2}$$

$$\times \left[\frac{dm_f p_f}{n\mu}\left(p_f A - \frac{cdg_y m_g p_g}{n\mu(m_g - G_{in})}\right)^2 (k + g_y p_g) + \frac{(dg_y m_g p_g)^2}{n\mu(m_g - G_{in})^2}\left(p_f - \frac{cd}{n\mu}(k + g_y p_g)\right)^2\right]$$

is always positive when the conditions are met. So the production of DAG increases the necessary influx of fatty acids to produce the ideal glucose concentration equilibrium for any given glucose infusion. This result suggests that DAG mediated insulin resistance protects muscles against elevated concentrations of glucose at the expense of other tissues in the body.

Additionally, if you take $c = 0$ in the polynomial (4.8) you get

$$dp_f m_g F^{*2} + (m_g \Theta - m_f p_f G_{in})\, F^* - k m_g F_{in} = 0, \tag{4.9}$$

$$\Theta = p_f(m_f - F_{in}) + dk.$$

which, if multiplied by $\frac{(1+A)}{m_g}$, yields

$$dp_f(1 + A)F^{*2} + \frac{(1 + A)}{m_g}[m_f p_f(m_g - G_{in}) - m_g(dk - p_f F_{in})]F^* - kF_{in}(1 + A) = 0.$$

and since $1 + A = \frac{m_g}{m_g - G_{in}}$, we have

$$dp_f(1 + A)F^{*2} + [m_f p_f + (dk - p_f F_{in})(1 + A)]F^* - kF_{in}(1 + A) = 0,$$

which is the same quadratic that arises from the system (4.2). Then the addition of DAG production in system (4.7) doesn't result in more equilibria, but an altered equilibrium.

Moreover, if you take the polynomial (4.8) and subtract the quadratic (4.9), then you are only left with the terms containing c,

$$\frac{cdm_g}{n\mu}F^*\left(dp_fF^{*2}+\Theta F^*-kF_{in}\right)$$

which is positive for

$$F^*>\frac{-\Theta+\sqrt{\Theta^2+4dkp_fF_{in}}}{2dp_f},$$

and negative for ($F^*<$).

Let $f(F)$ be the cubic polynomial (4.8), $g(F)$ be the quadratic (4.9), F^* be the positive zero such that $f(F^*)=0$, and $\bar{F}$ be the positive zero such that $g(\bar{F})=0$. Put $f_c(F)=f(F)-g(F)$, the terms of $f(F)$ that contain c. Then $f_c(F)>0$ implies that $f(F)>g(F)$, hence $0=f(F^*)>g(F^*)$ implies that the single positive zero of the concave up quadratic $g(F)$ has not occurred yet, hence $F^*<\bar{F}$. On the other hand, if $f_c(F)<0$ then $F^*>\bar{F}$. Hence the addition of c decreases the equilibrium value for F^* if $F^*>\frac{-\Theta+\sqrt{\Theta^2+4dkp_fF_{in}}}{2dp_f}$, but increases it if below that condition. It is not clear if the positive zero for (4.8) could be greater or less than this threshold, as the expression for F^* is algebraically intractable. Understanding the role that DAG production plays on the value of F^* is important since our expressions for G^* and D^* both vary as F^* does. We will explore this numerically.

Numerical Results for the DAG system

The simulations for the 4-dimensional system mirror the dynamics that we see in the 3 dimensional system. The key feature of the simulations is how glycogen stores help to maintain a preferable glucose concentration in the cell. However, once the glycogen is depleted or filled to capacity, the cell cannot maintain ideal levels of glucose and the system hits equilibrium.

Keeping glucose infusion constant, Fig. 4.6 demonstrates the dynamics of the system when fatty acid infusion is high. The DAG concentration in this case lowers the glucose

Figure 4.6: Simulations for System (4.7) with High F_{in}

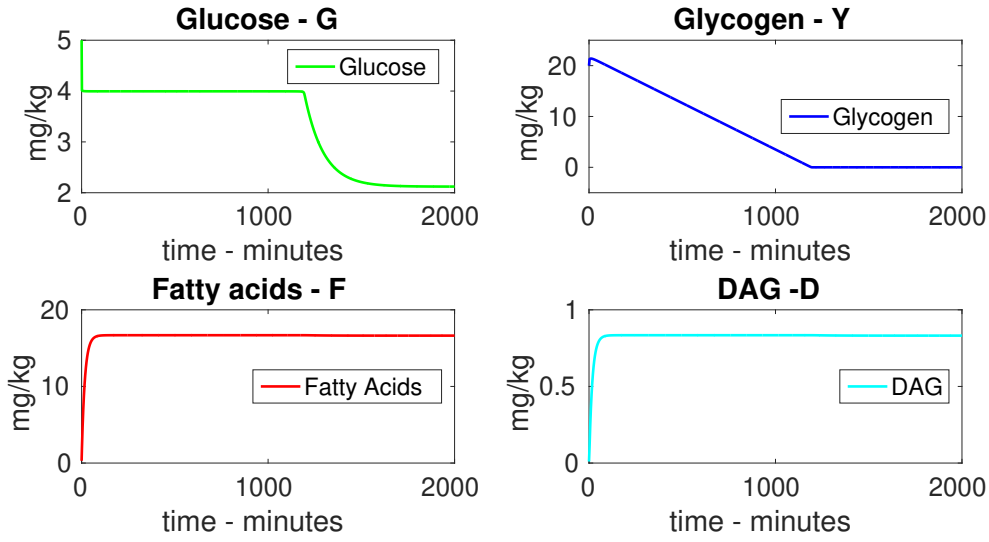

infusion via DAG-mediated insulin resistance, and the steady state concentration of DAG is high enough that glucose levels can only be maintained at ideal levels until the glycogen stores are depleted. After glycogen is depleted, glucose concentrations stabilize at a lower equilibrium. On the other hand, for the same value of G_{in}, Fig. 4.7 shows that the lower concentrations of fatty acids and DAG in the cell allows the cell to maintain constant glucose levels until glycogen fills to capacity.

The relationship between $\bar{F}_{in}$ and G_{in} in Fig. 4.8 demonstrates that as G_{in} increases, the necessary influx of fatty acids necessary to maintain ideal concentrations of intramyocellular glucose increases. Moreover, the vertical dashed grey line is the lower bound threshold for the existence of the degenerate case (i.e. $G_{in} = \frac{cd}{n\mu} \cdot \frac{g_y p_g}{p_f} m_g$). Any glucose infusion below the dashed grey line will result in a glucose equilibrium below the ideal concentration and a depleted glycogen store for any fatty acid infusion. Notice that this is distinctly different than in Fig. 4.3, where there is always some critical value of $\hat{F}_{in}$that would yield the degenerate case for any small G_{in}. Hence the addition of DAG mediated insulin resistance

Figure 4.7: Simulations for System (4.7) with Low F_{in}

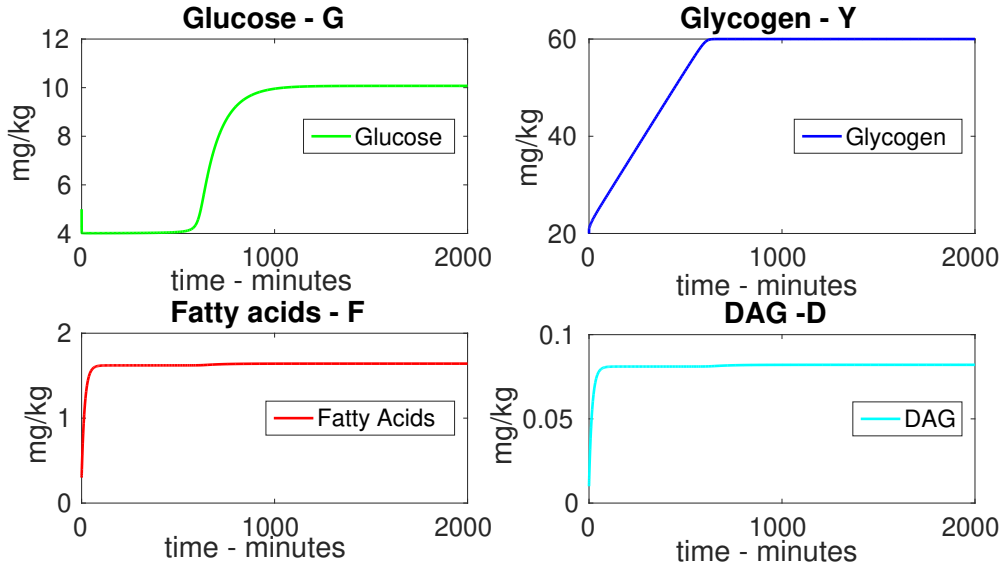

generates a cutoff for glucose infusion, below which you can never fill glycogen stores.

In order to better understand the relation between DAG production (c) and the value of the fatty acid equilibrium (F^*) we look at how F^* varies as c is increased away from 0. The plot in Fig. 4.9 demonstrates that the addition of DAG production in fact reduces the equilibrium value of F^*. Furthermore, while we expect DAG to be fraction of the total byproducts created from IMCL (hence $c < 1$), we can see that the equilibrium, F^* approaches the value of the expression $\frac{-\Theta+\sqrt{\Theta^2+4dkp_f F_{in}}}{2dp_f}$ (Fig. 4.9 (b)). This clearly implies that the terms containing c take over the behavior of (4.8) if we let c get very large. However, this is not biologically feasible, hence we only expect to see some minor decrease in fatty acid concentration such as in Fig. 4.9 (b).

Figure 4.8: Bifurcation Conditions on F_{in} and G_{in}

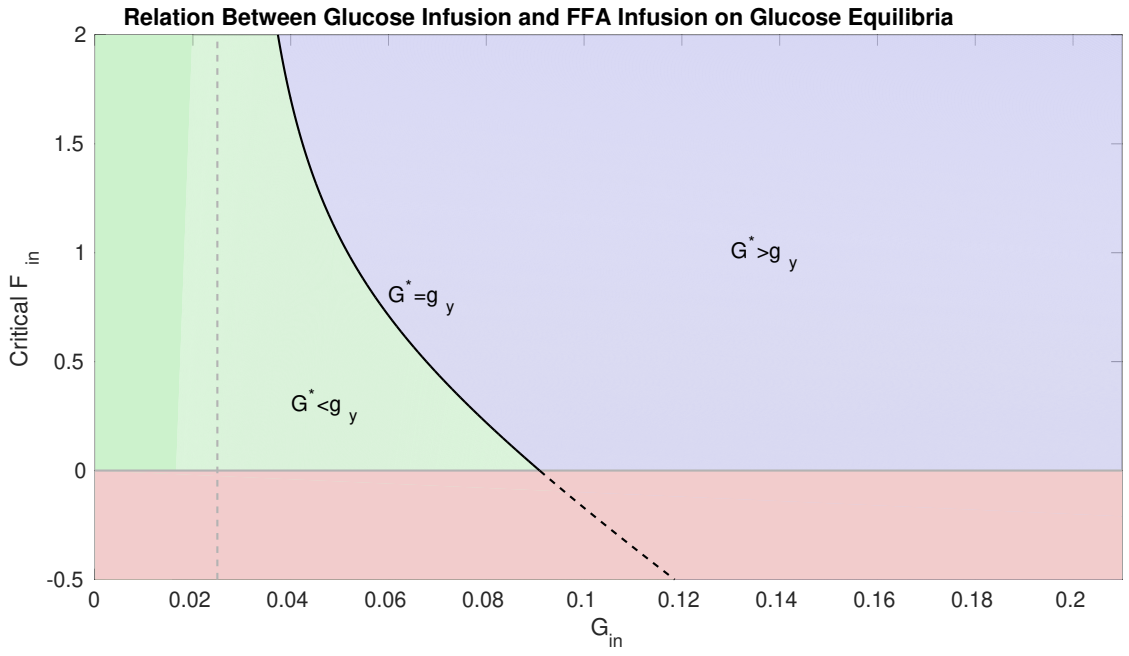

Figure 4.9: Effect of DAG Production on F^*

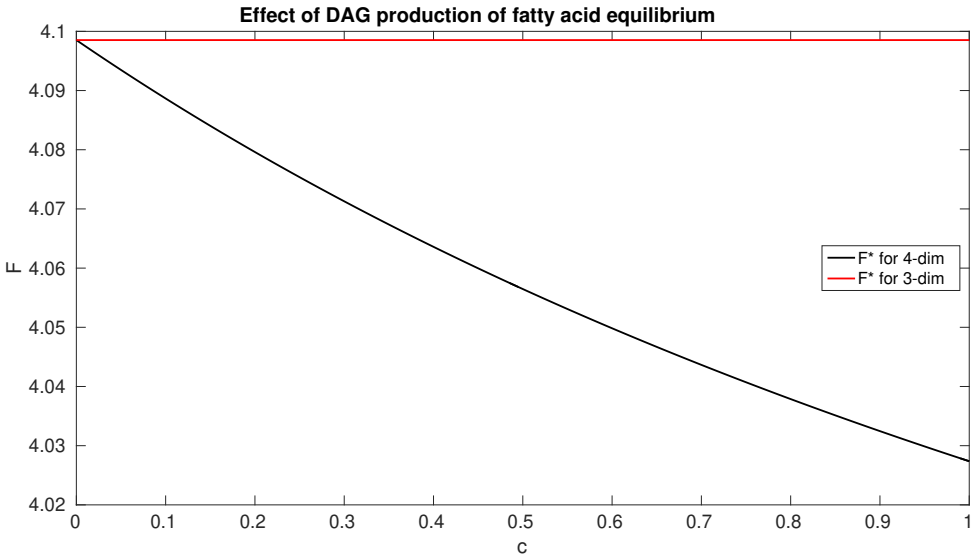

(a)

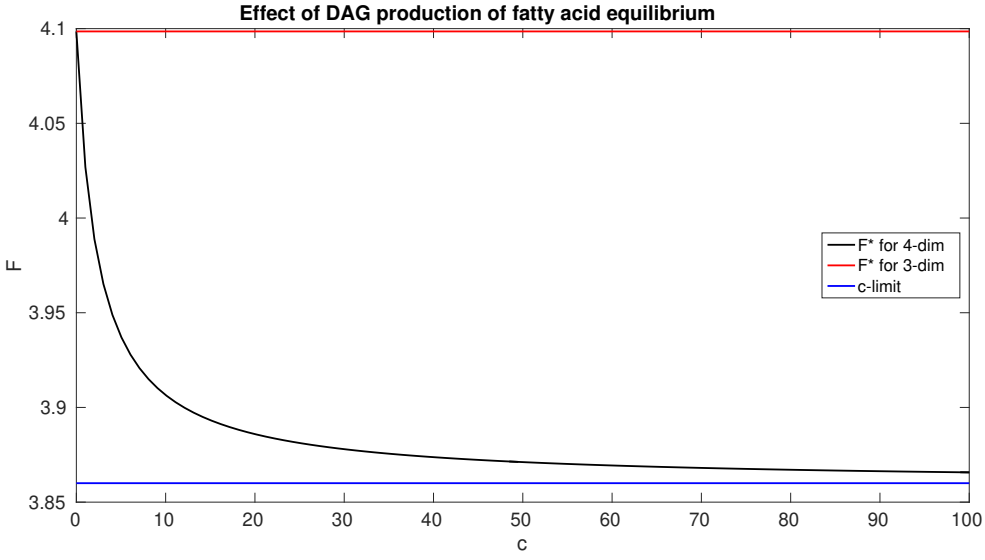

(b)

Chapter 5

DISCUSSION AND FUTURE WORK

5.1 Discussion

Intramyocellular triglyceride, and more generally intramyocellular lipids, play an important role in regulating muscular glucose uptake during a state of high fatty acid influx. This leads to DAG accumulation and glucose transport reduction. The mathematical model proposed is capable of fitting euglycemic-hyperinsulinemic clamp with fatty acid infusion data with reasonable parameter values. Not only does the model replicate data dynamics, it fits 4 related data sets simultaneously with a single set of parameters. This fact indicates that the major mechanisms driving the dynamics seen in (Roden *et al.*, 1996) are represented in this model.

The model's highly nonlinear nature makes it likely that the parameter set found in our estimation is not a global minimum, and uncertainty in our parameter choices could have a large effect on the model's predictive power. Most importantly, the parameters related to glucose and fatty acid infusion into the myocytes change the fit quite dramatically, but those parameters at least have a known feasible range if you have enough information from the clinical procedure. The parameters that govern DAG production and DAG-mediated IR are less well understood and not directly measurable, hence the uncertainty in those values is high. More data is necessary in order to validate the predictive power of this model.

The long term model dynamics demonstrate simple behaviors. Most notably, the glycogen store works as a buffer to maintain cellular levels of glucose at ideal levels, so long as glycogen is available and not at maximal capacity, the muscle cells are able to maintain a fairly constant glucose level. However, the relationship between glucose uptake and fatty

acid infusion suggests certain dietary considerations.

There are four main long term behaviors that our model predicts which may be relevant in understanding insulin resistance. The first is the condition when glucose uptake and fatty acids infusion is low. In this case, the low glucose equilibrium is stable, and glycogen is depleted. Additionally, DAG does not accumulate and insulin resistance is low. Hence an increase in glucose availability will be utilized and stored as glycogen readily.

The second scenario is low fatty acid availability but high glucose. This situation fills the glycogen reserve and intracellular glucose concentrations come to rest at a high equilibrium. In this case, insulin resistance is not present, however the intracellular environment is still hostile due to glucotoxicity from the elevated glucose level. Furthermore, the body responds to situations like these by storing excess glucose as triglycerides in a process called de novo lipogenesis. This often occurs in the liver, but can be found in muscle cells as well. This biological response would increase the pool of intracellular lipids, and would act as a source in addition to passive diffusion from the blood.

The third scenario is interesting, low glucose utilization and high fatty acid availability puts the system into the low glucose equilibrium and depletes glycogen stores. However, without competition from glucose, the fatty acids can be readily metabolized for energy. Additionally, studies on athlete have shown that a high intramyocellular store of triglycerides is not associated with insulin resistance if there is high turn-over, or metabolism. In the case of athletes, the fatty acid infusion is high, but the proportion and maximal rate of β-oxidation lowers the proportion of lipids that are converted into secondary byproducts like DAG. Additionally, this case assumes a low extracellular glucose concentration, so the DAG-mediated IR actually spares glucose by allowing it to continue circulating until it is utilized by other tissues such as nervous tissue. This is a rare case where the insulin resis-

tance may not be detrimental to health.

The final situation is the most common, high glucose availability and high fat availability. The elevated extracellular glucose would come from food consumed, and the elevated fat could be from nutritive sources, or from circulating body fat spilling over from adipose tissue. This case yields the high glucose equilibrium since the critical fatty acid infusion value is actually negative, and biologically infeasible. Thus you have the trifecta, elevated glucose equilibrium, insulin resistance, and a full glycogen store. This case is the most stressful case as it provides glucotoxicity for the muscles, and the insulin resistant cells don't clear glucose from the body, which leads to glucotoxicity for other tissues as well.

The addition of DAG production to the healthy no-DAG model increases the critical fatty acid infusion level required to see the ideal glucose concentration equilibrium. This result suggests that insulin resistance, while detrimental to the body as a whole, can actually be protective for muscles. In other words, insulin resistance in muscles helps keep intramyocellular glucose concentrations lower by reducing the effective influx from the bloodstream. Now, our model says nothing of the effects of glucotoxicity on the body, but if muscles are not utilizing the blood glucose then the glucose levels in plasma will remain higher for longer. However, when fat is present and available for metabolism in the muscle and DAG production is proportionally higher, then glucose is spared for other tissues by means of muscular insulin resistance. Hence a low carbohydrate, high fat diet induces insulin resistance and depletes glycogen stores, but energy production from fat oxidation becomes the main source of energy. We see this exact result in patients on a ketogenic diet (Volek *et al.*, 2015).

However, the other side of the coin implies that intramyocellular lipid availability reduces the efficiency of the muscles' glucose utilization. Hence a diet with higher carbohydrate consumption will benefit from a low fatty acid influx into muscles. If the insulin pathway is not

restricted, then the muscles can efficiently take up and metabolize glucose, clearing it from the blood and alleviating hyperglycemia. Clinical trials implementing a high carbohydrate, very low fat diet demonstrated a significant reduction in IMTG and fat oxidation rates (Coyle *et al.*, 2001), as well as improved insulin action (Barnard *et al.*, 2005). Hence in either extreme, with low-fat-high-sugar or low-sugar-high-fat, the muscles can operate in a healthy way and generate adequate energy. It is only the case of excess sugar and fat, which is likely associated with excess total caloric intake, where we see an insulin resistant and glycogen replete individual. Moreover, the line ($\bar{F}_{in}(G_{in})$) that separates the low and high glycogen equilibria follows an inverse monotone relation with a single positive zero. Hence a healthy balance of glucose and fat availability is only possible up until a maximum calorie intake.

Mathematically, the switching manifold for the long term system brings up interesting questions in a field that is not heavily studied. The discontinuous bifurcation that is induced as the bifurcation crosses the switching manifold creates a dense line of equilibria. However, more work needs to be done in order to prove that the trajectories which approach the line get stuck and do not slide toward either extremum (the trivial or maximal glycogen equilibria).

The 3 dimensional model (system (4.2)) demonstrates these mathematically interesting dynamics, whereas the additional state variables change the conditions necessary for the degenerate case, but do not significantly alter the qualitative behavior. This similarity is demonstrated in numerical simulations, as the 4 and 5 dimensional long term systems were too cumbersome to work with while exploring the bifurcation.

Ultimately, the results suggest that simple relationships between glucose and fatty acid availability drive the long term system dynamics. More questions arise, however when con-

sidering general model. As more information comes to light about how the intramyocellular lipids are utilized and how their byproducts affect insulin resistance, this dissertation acts as a base camp from which new model formulations can be constructed and studied.

5.2 Future Work

The model uses naive assumptions about the functional forms of molecular interactions. Therefore this model can be improved by choosing more accurate interaction terms. Specifically, the production of DAG is linearly proportional to IMCL concentration, and nonlinear saturable functions would likely represent the biological mechanisms more realistically. Another obvious improvement would be the reduction of glucose infusion by DAG concentration. In the cell, DAG does not directly affect GluT4 nor does blocking the IRS activity immediately down regulate glucose transport. Thus a distributed delay for insulin action inhibition would be the most realistic. However, while the long term behaviors may be similar, this addition would likely affect transient dynamics the most.

The main molecule responsible for down regulating insulin activity in euglycemic hyperinsulinemic clamps with fatty acid infusion is DAG. This is due to the fatty acid infusion being unsaturated, and some studies have shown that fatty acid induced insulin resistance occurs without an increase in DAG, but an increase in ceramides. Ceramides can be increased via infusion of saturated fatty acids, but fewer trials of this form have been performed. A comparison between data from typical fatty acid infusions and saturated fatty acid infusions would give insight into fundamental differences between the dynamics and would motivate a more realistic long term dynamics analysis of the model. Additionally, it is possible that DAG and ceramides work together or against each other in some ways that may inspire attaching additional model variables.

This model needs to be tested against more data to determine how robust the chosen parameters are. Given the already complex non-linear nature of the model, the found parameters likely account for one of many parameter sets that locally minimize the difference between simulation and observation. Thus a more thorough vetting of the parameter estimation is needed before this model will be useful in a clinical setting. Additionally, this model can be improved as more biological research elucidates the *in vivo* enzyme interaction dynamics. Parameter estimation will shed light on which model choices make the biggest difference in predictive accuracy. Hence it is important to try different model functions that demonstrate the same qualitative behavior and test them against each other to determine which assumptions best fit the clinical data.

Additionally, the measure of muscular insulin resistance determined by the concentration of DAG provides a novel measure of insulin sensitivity. With the multitude of other insulin sensitivity indices, it would be interesting to determine the differences that this model provides. Moreover, the muscular insulin resistance likely only accounts for a subset of insulin resistance in a diabetic patient, and this new metric may help shed light on what role muscular insulin resistance plays in whole body insulin resistance.

Furthermore, the long term model dynamics need to be studied in more detail. For instance, if there is an enzyme dysfunction (or knockout) that disallows the normal cellular switching from storing to utilizing glycogen, does the system exhibit other types of bifurcations? Perhaps we can discover some other typical bifurcations in the system. Additionally, the switching mechanisms are not, in reality, completely on or off. Hence, some delayed switching time or transition could clarify the cellular dynamics. The results of stability we have already discovered could be strengthened by demonstrating global stability with a Lyaponov function or Dulac critereon tests.

Lastly, this model describes a single clinical protocol that is not only expensive, but short term in scale. The larger application of such a model would be in discovering if these dynamics are a cause of, or result of, chronic insulin resistance. Since the model assumes a constant inflow of glucose and fatty acids, it is currently not guaranteed to be bounded depending on parameter and function choices. Therefore, we need to add self regulation to the system in addition to non-autonomous nutrient infusion rates that depend on external stimuli such as glucose and insulin concentration. Fortunately, glucose-insulin dynamics have been well studied and models of this variety are being used for other predictive application such as closed loop control insulin injection algorithms for type 1 diabetics.

Alberts, B., A. Johnson, J. Lewis, M. Raff, K. Roberts and P. Walter, *Molecular Biology of the Cell* (Garland, 2008).

Aldridge, B. B., J. M. Burke, D. A. Lauffenburger and P. K. Sorger, "Physicochemical modelling of cell signalling pathways", Nature cell biology **8**, 11, 1195–1203 (2006).

Alvarez-Vasquez, F., K. J. Sims, L. A. Cowart, Y. Okamoto, E. O. Voit and Y. A. Hannun, "Simulation and validation of modelled sphingolipid metabolism in saccharomyces cerevisiae", Nature **433**, 7024, 425–430 (2005).

Association, A. D. *et al.*, "Diagnosis and classification of diabetes mellitus", Diabetes care **29**, 1, S43 (2006).

Banting, F., C. Best, J. Collip, J. Macleod and E. Noble, "The effect of pancreatic extract (insulin) on normal rabbits", American Journal of Physiology–Legacy Content **62**, 1, 162–176 (1922).

Barnard, N. D., A. R. Scialli, G. Turner-McGrievy, A. J. Lanou and J. Glass, "The effects of a low-fat, plant-based dietary intervention on body weight, metabolism, and insulin sensitivity", The American journal of medicine **118**, 9, 991–997 (2005).

Bergman, R. N., Y. Z. Ider, C. R. Bowden and C. Cobelli, "Quantitative estimation of insulin sensitivity.", American Journal of Physiology-Endocrinology And Metabolism **236**, 6, E667 (1979).

Bergman, R. N., R. Prager, A. Volund and J. Olefsky, "Equivalence of the insulin sensitivity index in man derived by the minimal model method and the euglycemic glucose clamp.", Journal of Clinical Investigation **79**, 3, 790 (1987).

Bernardo, M., C. Budd, A. R. Champneys and P. Kowalczyk, *Piecewise-smooth dynamical systems: theory and applications*, vol. 163 (Springer Science & Business Media, 2008).

Bertuzzi, A., S. Salinari and G. Mingrone, "Insulin granule trafficking in β-cells: mathematical model of glucose-induced insulin secretion", American Journal of Physiology-Endocrinology and Metabolism **293**, 1, E396–E409 (2007).

Boden, G., "Role of fatty acids in the pathogenesis of insulin resistance and niddm", Diabetes **46**, 1, 3–10 (1997).

Boden, G., X. Chen, J. Ruiz, J. V. White and L. Rossetti, "Mechanisms of fatty acid-induced inhibition of glucose uptake", J. Clin. Invest. **93**, 2438–2446 (2004).

Boden, G., B. Lebed, M. Schatz, C. Homko and S. Lemieux, "Effects of acute changes of plasma free fatty acids on intramyocellular fat content and insulin resistance in healthy subjects", Diabetes **50**, 7, 1612–1617 (2001).

Bolie, V. W., "Coefficients of normal blood glucose regulation", Journal of Applied Physiology **16**, 5, 783–788 (1961).

Borghans, J. M., R. J. De Boer and L. A. Segel, "Extending the quasi-steady state approximation by changing variables", Bulletin of mathematical biology **58**, 1, 43–63 (1996).

Brauer, F., C. Castillo-Chavez and C. Castillo-Chavez, "Mathematical models in population biology and epidemiology", (2001).

Capurso, C. and A. Capurso, "From excess adiposity to insulin resistance: the role of free fatty acids", Vascular pharmacology **57**, 2, 91–97 (2012).

CDC, "Number (in millions) of civilian, noninstitutionalized persons with diagnosed diabetes, united states, 19802011", URL `http://www.cdc.gov/diabetes/statistics/prev/national/figpersons.htm` (2013).

Ceriello, A. and E. Motz, "Is oxidative stress the pathogenic mechanism underlying insulin resistance, diabetes, and cardiovascular disease? the common soil hypothesis revisited", Arteriosclerosis, thrombosis, and vascular biology **24**, 5, 816–823 (2004).

Chavez, J. A., T. A. Knotts, L.-P. Wang, G. Li, R. T. Dobrowsky, G. L. Florant and S. A. Summers, "A role for ceramide, but not diacylglycerol, in the antagonism of insulin signal transduction by saturated fatty acids", Journal of Biological Chemistry **278**, 12, 10297–10303 (2003).

Colombo, A., M. Di Bernardo, S. Hogan and M. Jeffrey, "Bifurcations of piecewise smooth flows: Perspectives, methodologies and open problems", Physica D: Nonlinear Phenomena **241**, 22, 1845–1860 (2012).

Cornish-Bowden, A. and A. Cornish-Bowden, "Fundamentals of enzyme kinetics", (2012).

Coyle, E. F., A. E. Jeukendrup, M. C. Oseto, B. J. Hodgkinson and T. W. Zderic, "Low-fat diet alters intramuscular substrates and reduces lipolysis and fat oxidation during exercise", American Journal of Physiology-Endocrinology And Metabolism **280**, 3, E391–E398 (2001).

Dandanell, S., K. Husted, S. Amdisen, A. Vigelsø, F. Dela, S. Larsen and J. W. Helge, "Influence of maximal fat oxidation on long-term weight loss maintenance in humans", Journal of Applied Physiology pp. jap–00270 (2017).

De Gaetano, A. and O. Arino, "Mathematical modelling of the intravenous glucose tolerance test", Journal of Mathematical Biology **40**, 2, 136–168 (2000).

De Luca, C. and J. M. Olefsky, "Inflammation and insulin resistance", FEBS letters **582**, 1, 97–105 (2008).

Di Bernardo, M., C. J. Budd, A. R. Champneys, P. Kowalczyk, A. B. Nordmark, G. O. Tost and P. T. Piiroinen, "Bifurcations in nonsmooth dynamical systems", SIAM review **50**, 4, 629–701 (2008).

Eungdamrong, N. J. and R. Iyengar, "Modeling cell signaling networks", Biology of the Cell **96**, 5, 355–362 (2004).

Fell, D. A., "Metabolic control analysis: a survey of its theoretical and experimental development.", Biochemical Journal **286**, Pt 2, 313 (1992).

Goodpaster, B. H., J. He, S. Watkins and D. E. Kelley, "Skeletal muscle lipid content and insulin resistance: evidence for a paradox in endurance-trained athletes", The Journal of Clinical Endocrinology & Metabolism **86**, 12, 5755–5761 (2001).

Goodpaster, B. H., F. L. Thaete, J.-A. Simoneau and D. E. Kelley, "Subcutaneous abdominal fat and thigh muscle composition predict insulin sensitivity independently of visceral fat", Diabetes **46**, 10, 1579–1585 (1997).

Gutt, M., C. L. Davis, S. B. Spitzer, M. M. Llabre, M. Kumar, E. M. Czarnecki, N. Schneiderman, J. S. Skyler and J. B. Marks, "Validation of the insulin sensitivity index (isi 0,120): comparison with other measures", Diabetes research and clinical practice **47**, 3, 177–184 (2000).

Hancock, C. R., D.-H. Han, M. Chen, S. Terada, T. Yasuda, D. C. Wright and J. O. Holloszy, "High-fat diets cause insulin resistance despite an increase in muscle mitochondria", Proceedings of the National Academy of Sciences **105**, 22, 7815–7820 (2008).

Heinrich, R. and T. A. Rapoport, "A linear steady-state treatment of enzymatic chains", European Journal of Biochemistry **42**, 1, 97–105 (1974).

Hill, A. V., "The possible effects of the aggregation of the molecules of haemoglobin on its dissociation curves", J Physiol (Lond) **40**, 4–7 (1910).

Hotamisligil, G. S., P. Peraldi, A. Budavari, R. Ellis *et al.*, "Irs-1-mediated inhibition of insulin receptor tyrosine kinase activity in tnf-alpha-and obesity-induced insulin resistance", Science **271**, 5249, 665 (1996).

Huang, M., J. Li, X. Song and H. Guo, "Modeling impulsive injections of insulin: towards artificial pancreas", SIAM Journal on Applied Mathematics **72**, 5, 1524–1548 (2012).

Joe, J. R., *Diabetes as a disease of civilization: the impact of culture change on indigenous peoples*, vol. 50 (Walter de Gruyter, 1994).

Kelley, D. E., J. He, E. V. Menshikova and V. B. Ritov, "Dysfunction of mitochondria in human skeletal muscle in type 2 diabetes", Diabetes **51**, 10, 2944–2950 (2002).

Kermack, W. O. and A. G. McKendrick, "A contribution to the mathematical theory of epidemics", in "Proceedings of the Royal Society of London A: mathematical, physical and engineering sciences", vol. 115, pp. 700–721 (The Royal Society, 1927).

Kim, J.-Y., L. A. Nolte, P. A. Hansen, D.-H. Han, K. Ferguson, P. A. Thompson and J. O. Holloszy, "High-fat diet-induced muscle insulin resistance: relationship to visceral fat mass", American Journal of Physiology-Regulatory, Integrative and Comparative Physiology **279**, 6, R2057–R2065 (2000).

Kimyagarov, S., R. Klid, S. Levenkrohn, Y. Fleissig, B. Kopel, M. Arad and A. Adunsky, "Body mass index (bmi), body composition and mortality of nursing home elderly residents", Archives of gerontology and geriatrics **51**, 2, 227–230 (2010).

King, K. and G. Rubin, "A history of diabetes: from antiquity to discovering insulin.", British journal of nursing **12**, 18 (2003).

Klein, S., "The case of visceral fat: argument for the defense", The Journal of clinical investigation **113**, 11, 1530–1532 (2004).

Krebs, M. and M. Roden, "Molecular mechanisms of lipid-induced insulin resistance in muscle, liver and vasculature", Diabetes, Obesity and Metabolism **7**, 6, 621–632 (2005).

Kuang, Y., J. D. Nagy and S. E. Eikenberry, *Introduction to mathematical oncology*, vol. 59 (CRC Press, 2016).

Lê, K.-A., M. Ith, R. Kreis, D. Faeh, M. Bortolotti, C. Tran, C. Boesch and L. Tappy, "Fructose overconsumption causes dyslipidemia and ectopic lipid deposition in healthy subjects with and without a family history of type 2 diabetes", The American journal of clinical nutrition **89**, 6, 1760–1765 (2009).

Leine, R. I. and H. Nijmeijer, *Dynamics and bifurcations of non-smooth mechanical systems*, vol. 18 (Springer Science & Business Media, 2013).

Levin, S. A., T. G. Hallam and L. J. Gross, *Applied mathematical ecology*, vol. 18 (Springer Science & Business Media, 2012).

Li, J. and Y. Kuang, "Systemically modeling the dynamics of plasma insulin in subcutaneous injection of insulin analogues for type 1 diabetes", Mathematical biosciences and engineering: MBE **6**, 1, 41 (2009).

Li, J., Y. Kuang and B. Li, "Analysis of ivgtt glucose-insulin interaction models with time delay", Discrete and Continuous Dynamical Systems Series B **1**, 1, 103–124 (2001).

Li, J., Y. Kuang and C. C. Mason, "Modeling the glucose–insulin regulatory system and ultradian insulin secretory oscillations with two explicit time delays", Journal of Theoretical Biology **242**, 3, 722–735 (2006).

Li, J., M. Wang, A. D. Gaetano, P. Palumbo and S. Panunzi, "The range of time delay and the global stability of the equilibrium for an ivgtt model", Mathematical biosciences **235**, 2, 128–137 (2012).

Lotka, A., "Elements of physical biology", (1925).

Makroglou, A., J. Li and Y. Kuang, "Mathematical models and software tools for the glucose-insulin regulatory system and diabetes: an overview", Applied Numerical Mathematics **56**, 559–573 (2006).

Malthus, T. R., *An Essay on the Principle of Population, as it Affects the Future Improvement of Society* (1798).

Matsuzawa, Y., T. Nakamura, I. Shimomura and K. Kotani, "Visceral fat accumulation and cardiovascular disease", Obesity research **3**, S5, 645S–647S (1995).

Matthews, D., J. Hosker, A. Rudenski, B. Naylor, D. Treacher and R. Turner, "Homeostasis model assessment: insulin resistance and β-cell function from fasting plasma glucose and insulin concentrations in man", Diabetologia **28**, 7, 412–419 (1985).

Michaelis, L. and M. L. Menten, "Die kinetik der invertinwirkung", Biochem. z **49**, 333-369, 352 (1913).

Montell, E., M. Turini, M. Marotta, M. Roberts, V. Noé, K. Macé, A. M. Gómez-Foix *et al.*, "Dag accumulation from saturated fatty acids desensitizes insulin stimulation of glucose uptake in muscle cells", American Journal of Physiology-Endocrinology And Metabolism **280**, 2, E229–E237 (2001).

Mosekilde, E., K. S. Jensen, C. Binder, S. Pramming and B. Thorsteinsson, "Modeling absorption kinetics of subcutaneous injected soluble insulin", Journal of pharmacokinetics and biopharmaceutics **17**, 1, 67–87 (1989).

Muoio, D. M. and C. B. Newgard, "Molecular and metabolic mechanisms of insulin resistance and β-cell failure in type 2 diabetes", Nature reviews Molecular cell biology **9**, 3, 193–205 (2008).

Noel, V., S. Vakulenko and O. Radulescu, "Piecewise smooth hybrid systems as models for networks in molecular biology", in "Proceedings of JOBIM", (2010).

Nyman, E., G. Cedersund and P. Strålfors, "Insulin signaling–mathematical modeling comes of age", Trends in Endocrinology & Metabolism **23**, 3, 107–115 (2012).

Pacini, G. and R. N. Bergman, "Minmod: a computer program to calculate insulin sensitivity and pancreatic responsivity from the frequently sampled intravenous glucose tolerance test", Computer methods and programs in biomedicine **23**, 2, 113–122 (1986).

Palumbo, P. and A. De Gaetano, "An islet population model of the endocrine pancreas", Journal of mathematical biology **61**, 2, 171–205 (2010).

Pearl, R. and L. J. Reed, "On the rate of growth of the population of the united states since 1790 and its mathematical representation", Proceedings of the National Academy of Sciences **6**, 6, 275–288 (1920).

Pedersen, M. G., A. M. Bersani and E. Bersani, "Quasi steady-state approximations in complex intracellular signal transduction networks–a word of caution", Journal of Mathematical Chemistry **43**, 4, 1318–1344 (2008).

Perseghin, G., P. Scifo, M. Danna, A. Battezzati, S. Benedini, E. Meneghini, A. Del Maschio and L. Luzi, "Normal insulin sensitivity and imcl content in overweight humans are associated with higher fasting lipid oxidation", American Journal of Physiology-Endocrinology And Metabolism **283**, 3, E556–E564 (2002).

Perseghin, G., P. Scifo, F. De Cobelli, E. Pagliato, A. Battezzati, C. Arcelloni, A. Vanzulli, G. Testolin, G. Pozza, A. Del Maschio *et al.*, "Intramyocellular triglyceride content is a determinant of in vivo insulin resistance in humans: a 1h-13c nuclear magnetic resonance spectroscopy assessment in offspring of type 2 diabetic parents.", Diabetes **48**, 8, 1600–1606 (1999).

Pielou, E. C. *et al.*, "An introduction to mathematical ecology.", An introduction to mathematical ecology. (1969).

Reiser, S., J. Hallfrisch, O. E. Michaelis, F. L. Lazar, R. E. Martin, E. S. Prather *et al.*, "Isocaloric exchange of dietary starch and sucrose in humans. i. effects on levels of fasting blood lipids.", The American journal of clinical nutrition **32**, 8, 1659–1669 (1979).

Roden, M., T. B. Price, G. Perseghin, K. F. Petersen, D. L. Rothman, G. W. Cline and G. I. Shulman, "Mechanism of free fatty acid-induced insulin resistance in humans.", Journal of Clinical Investigation **97**, 12, 2859 (1996).

Rorsman, P. and E. Renström, "Insulin granule dynamics in pancreatic beta cells", Diabetologia **46**, 8, 1029–1045 (2003).

Ross, R., *The prevention of malaria* (John Murray; London, 1911).

Saghizadeh, M., J. M. Ong, W. T. Garvey, R. R. Henry and P. A. Kern, "The expression of tnf alpha by human muscle. relationship to insulin resistance.", Journal of Clinical Investigation **97**, 4, 1111 (1996).

Saltiel, A. R. and C. R. Kahn, "Insulin signalling and the regulation of glucose and lipid metabolism", Nature **414**, 6865, 799–806 (2001).

Schrauwen-Hinderling, V. B., M. E. Kooi, M. K. Hesselink, E. Moonen-Kornips, G. Schaart, K. J. Mustard, D. G. Hardie, W. H. Saris, K. Nicolay and P. Schrauwen, "Intramyocellular lipid content and molecular adaptations in response to a 1-week high-fat diet", Obesity research **13**, 12, 2088–2094 (2005).

Shi, X., Y. Kuang, A. Makroglou, S. Mokshagundam and J. Li, "Oscillatory dynamics of an intravenous glucose tolerance test model with delay interval", (2017).

Shulman, G. I., "Cellular mechanisms of insulin resistance", The Journal of clinical investigation **106**, 2, 171–176 (2000).

Simon, C. and G. Brandenberger, "Ultradian oscillations of insulin secretion in humans", Diabetes **51**, suppl 1, S258–S261 (2002).

Simopoulos, A. P., "Omega-3 fatty acids in inflammation and autoimmune diseases", Journal of the American College of Nutrition **21**, 6, 495–505 (2002).

Simpson, D., D. Kompala and J. Meiss, "Discontinuity induced bifurcations in a model of saccharomyces cerevisiae", Mathematical biosciences **218**, 1, 40–49 (2009).

Sindelar, D. K., C. A. Chu, P. Venson, E. P. Donahue, D. W. Neal and A. D. Cherrington, "Basal hepatic glucose production is regulated by the portal vein insulin concentration.", Diabetes **47**, 4, 523–529 (1998).

Smith, H. L. and H. R. Thieme, "Chemostats and epidemics: competition for nutrients/hosts", Math. Biosci. Eng **10**, 5-6 (2013).

Smith, H. L. and P. Waltman, *The theory of the chemostat: dynamics of microbial competition*, vol. 13 (Cambridge university press, 1995).

Søeborg, T., C. H. Rasmussen, E. Mosekilde and M. Colding-Jørgensen, "Absorption kinetics of insulin after subcutaneous administration", European Journal of Pharmaceutical Sciences **36**, 1, 78–90 (2009).

Storlien, L. H., E. W. Kraegen, D. J. Chisholm, G. L. Ford, D. G. Bruce and W. S. Pascoe, "Fish oil prevents insulin resistance induced by high-fat feeding in rats", Science **237**, 4817, 885–888 (1987).

Summers, S. A., "Ceramides in insulin resistance and lipotoxicity", Progress in lipid research **45**, 1, 42–72 (2006).

Teschl, G., *Ordinary differential equations and dynamical systems*, vol. 140 (2012).

Tirone, T. A. and F. C. Brunicardi, "Overview of glucose regulation", World journal of surgery **25**, 4, 461–467 (2001).

Turner, R., R. Holman, D. Matthews, T. Hockaday and J. Peto, "Insulin deficiency and insulin resistance interaction in diabetes: estimation of their relative contribution by feedback analysis from basal plasma insulin and glucose concentrations", Metabolism **28**, 11, 1086–1096 (1979).

Van Schaftingen, E. and I. Gerin, "The glucose-6-phosphatase system", Biochemical Journal **362**, 3, 513–532 (2002).

Verhulst, P.-F., "Notice sur la loi que la population suit dans son accroissement. correspondance mathématique et physique publiée par a", Quetelet **10**, 113–121 (1838).

Volek, J. S., T. Noakes and S. D. Phinney, "Rethinking fat as a fuel for endurance exercise", European journal of sport science **15**, 1, 13–20 (2015).

Volterra, V., "Variations and fluctuations of the number of individuals in animal species living together", J. Cons. Int. Explor. Mer **3**, 1, 3–51 (1928).

Wach, P., Z. Trajanoski, P. Kotanko and F. Skrabal, "Numerical approximation of mathematical model for absorption of subcutaneously injected insulin", Medical and Biological Engineering and Computing **33**, 1, 18–23 (1995).

Weintraub, M. S., S. Eisenberg and J. L. Breslow, "Dietary fat clearance in normal subjects is regulated by genetic variation in apolipoprotein e.", Journal of Clinical Investigation **80**, 6, 1571 (1987).

Welch, S., S. Gebhart, R. Bergman and L. Phillips, "Minimal model analysis of intravenous glucose tolerance test-derived insulin sensitivity in diabetic subjects", The Journal of Clinical Endocrinology & Metabolism **71**, 6, 1508–1518 (1990).

Wheldon, T. E., *Mathematical models in cancer research* (Taylor & Francis, 1988).

Yu, C., Y. Chen, G. W. Cline, D. Zhang, H. Zong, Y. Wang, R. Bergeron, J. K. Kim, S. W. Cushman, G. J. Cooney *et al.*, "Mechanism by which fatty acids inhibit insulin activation of insulin receptor substrate-1 (irs-1)-associated phosphatidylinositol 3-kinase activity in muscle", Journal of Biological Chemistry **277**, 52, 50230–50236 (2002).

Yung-Chi, C. and W. H. Prusoff, "Relationship between the inhibition constant (ki) and the concentration of inhibitor which causes 50 per cent inhibition (i50) of an enzymatic reaction", Biochemical pharmacology **22**, 23, 3099–3108 (1973).